ENVIRONMENTAL ENGINEERING
ASSOCIATION OF THAILAND

THAI ENVIRONMENTAL ENGINEERING JOURNAL

Vol. 38 No. 2 May – August 2024
ISSN (PRINT) : 1686 - 2961
ISSN (ONLINE) : 2673 - 0359

Thai Environmental Engineering Journal

Owner
Environmental Engineering Association of Thailand

Enquiries 122/4 Soi Rawadee, Rama IV Rd., Phayathai, Phayathai, Bangkok 10400

Thai Environmental Engineering Journal

Vol. 38 No. 2 May – August 2024

ISSN (PRINT) : 1686 - 2961
ISSN (ONLINE) : 2673 - 0359

Thai Environmental Engineering Journal Vol. 38 No. 2 (2024) : 1-17
www.eeat.or.th

Sustainable Indicators of Water Resource Development Projects in Conservation Areas, Thailand

Udomsook Suracharttumrongrat*, Chamlong Poboon, Karika Kunta, Chutarat Chompunth and Napong Nophaket

Department of Environmental Management, Faculty of Graduate School of Environmental Development Administration, National Institute of Development Administration, Bangkok 10300, Thailand
*E-mail : Udomsooksu@gmail.com

Article History; *Received: 24 May 2024, Accepted: 17 June 2024, Published: 30 August 2024*

Abstract

Water resources development in Thailand is a very considerable aspect due to high variation of hydrological regime. Responsible agencies have to sufficiently supply in terms of quantity and quality raw water for various needs including water supply, agriculture, as well as industrial and other uses. Development of a water reservoir is one of the efficient measures as for water source, in spite of some limitations. Unfortunately, the appropriate locations of potential reservoirs are mostly located in the natural resources conservation area occupied with the abundantly good ecological system, which might lead to the conflict of interest between the line agencies of water resources development and natural resources conservation. Despite the national laws and policies specify to promote sustainable water resource development, specific guidelines and standards for quantity-based consideration of sustainability together with the balance between resources development and conservation of a potential project have not yet been defined in details.

Consequently, the quantitative criteria to establish the sustainable water resource development indicators, applying the principles of self-sufficiency economy and transitioning from the extreme development of high into moderate impact levels with self-sustaining development, will ensure that the future water resources project development can be carried out successfully and effectively towards sustainability. The study is qualitative research using the Del Phi method. The Del Phi's panel comprised selective 20 experts of various related ields, governmental agencies and independent academia. The research conducted firstly by defining draft relevant dimensions, factors, and indicators drawn from the previous related researches, and from in-depth interviewing 7 experts of the key related fields. Then the additional indicators and their scoring ranges were intensively determined and classified from the data and information of the 30 reservoirs' environmental impact assessment (EIA) reports as well as those referenced from the relevant researches, governmental agencies' regulations and announcements. The draft final indicators and scoring ranges were summarized and proposed to the Del Phi's panel not less than two rounds to obtain their majority conclusion on indicators, weighting factors, scoring ranges and recommendations of sustainability level for the future projects.

The study results indicated that the relative importance weighting of four dimensions to be considered were : engineering (20%), natural resources and environment (35%), social (25%), and economics (20%). This research identified 14 main factors of which 7 factors having high significance, including (1) wildlife, (2) forests, (3) ecology system, (4) number of affected people, (5) quality of life, (6) economic feasibility, and (7) social opposition. These 14 factors comprise a total of 29 key indicators, with 12 highly significant indicators including (1) uniqueness, (2) number of opponents, (3) water quality, (4) annual cultivated area per reservoir capacity, (5) design flood rate per reservoir capacity, (6) environmental economic feasibility, (7) economic feasibility, (8) proportion of beneficiaries on sufferers, (9) conservation area type, (10) Number of evacuated households per unit of reservoir capacity, (11) endangered wildlife, and (12) biodiversity of wildlife.

Keywords : Sustainable indicators of water resource development; Conservation area; Water scarcity indicators; Water resources development necessity indicators

Introduction

Thailand is an agricultural country with a total agricultural area of approximately 56% (178 million rai) and a forested area of approximately 32% (104 million rai) (Department of Land Development (DLD), 2020). However, this vast agricultural area often experiences water scarcity issues, with a need for water in various sectors, including agriculture, domestic consumption for 60 million population, industrial, and other uses. To address these challenges, state agencies responsible for water resource development must secure quality water sources in sufficient quantities to meet the needs of all sectors. Water reservoir development has been an efficient approach. Unfortunately the appropriate location of the reservoir is mostly located in natural resources conservation area where natural resources and the ecosystem is in good condition. Additionally, some potential reservoir sites inundate encroached habitats and agricultural land. In the past, reservoir development has primarily focused on maximizing potentials of topography, hydrology, and economics, rather than adhering to principles of economic self-sufficiency and sustainability in all dimensions, including economic, social, and environmental aspects. Although presently, Thailand has a constitution and development strategies that emphasize sustainability and balance between water resource development and natural resources conservation, but detailed guidelines and criteria for feasible and efficient project planning are lacking. Hence development of key sustainable factors and indicators and their weighting factors as a specific guideline for concerned agencies to develop a balanced sustainable water reservoir project should be established.

From the literature review conducted, it is evident that a substantial amount of research has focused on studying the factors and sustainability indicators for water resource development. Most of these studies have aimed to establish indicators for assessing sustainability at both national and regional levels. These indicators are generally categorized into three main groups: natural resources and environment, water resource development, and water resource management.

The sustainable indicators in the category of natural resources proposed by Piyachana [1] in 2003 consists of three main factors including forest abundance, land use, and water quality. The forestry factor include forest type indicator, timber volume indicator, forest growing rate indicator and ecology system value indicator. The land use factor is proportion of inappropriate land use area in conservation areas. Whereas the water quality factor includes water physical, biological, and chemical parameters, and pesticides indicators.

Poomjamnong [2] in 2017, found that Thailand still lacks clear and specific resource management goals to support sustainable development goal No. 15 (Terrestrial ecosystem). There is also a lack of data and standard criteria for assessing or

weighting forest resource indicators for the regional level. Additionally, the study applied key indicators of the forest resources include the proportion of forested areas, the proportion of conservation areas, and the endangered species of wildlife.

Noywuli, in 2019 [3] studied the carrying capacity of river basins in Indonesia, defining five keys factors: (1) land management, (2) water resource management, (3) socio-economic conditions, (4) public utilities related to water, and (5) watershed utilization. Key indicators included the proportion of green areas, water usage per river runoff, agricultural area per farmer, community area, and the proportion of conservation areas to the total area.

Tong, in 2020 [4] established the key carrying capacity indicators of forestry of which indicators are the proportion of forested areas, biological diversity, timber volume, and forest damage per unit area.

The National Park Research Section, National Park Division, Department of National Park, Wildlife and Plant Conservation (DNP), Thailand, in 2019 [5] studied the prioritization of national parks, utilizing six factors: (1) physical aspects, (2) biodiversity, (3) risk level, (4) global significance, (5) tourism, and (6) management complication. Key indicators included area size, forest type, tree species count, ecology system, population in conservation areas, encroachment area, global significance, tourism diversity, and management complication.

For the research group focusing on the sustainable development indicator for water resources development, Smith, et al, in 2007 [6] proposed the following indicators: impact on water quality, water demand and water resources proportion, water demands, and the risk of extinction of rare plants and wildlife species.

Morris, in 2019 [7] introduced economic indicators, which include productivity or Gross Domestic Product (GDP) per unit of raw water and income indicator or GDP per capita. Additionally, there is the ecological footprint indicator or environmental cost per unit of water. Meanwhile Liang et al. [8] in 2018, proposed a social indicator comprising water use per agricultural area, population growth rate, and sustainability indicators related to resources such as water resources per capita, water demand over water resources ratio, water demand per capita, and environmental indicators including environmental water use, land and water loss, and clean water volume per wastewater volume.

For research group on water resources management, Correa, in 2013 [9] presented a framework to address sustainability challenges in water management, focusing on three aspects: water pollution, forest restoration, and soil conservation. The framework includes 18 indicators categorized into groups related to soil erosion, water quality management, water use and water management, and social aspects. These indicators assess the sustainability of water resource management comprising the length of eroded riverbanks, water quality, agricultural land, and conflicts in the context of water management.

The National Statistical Office of Thailand, 2023 [10] developed the water management indicators (WMI) for the country to aid in decision-making and planning for sustainable water resource management. More than 40 government agencies were involved in this effort, and they identified 59 indicators within 8 dimensions, which include: (1) Water resource storage : e.g. (1) water storage per capita, water storage per river runoff, water quality, (2) domestic water supply management, e.g. water supply serviceable households, (3) water security, e.g. proportion of irrigated area to agricultural area, (4) water balance, e.g. water demand per water resources storage, (5) water quality management, e.g. number of good quality water sources, (6) water-related disasters, e.g. probable flood risk area and drought risk area, (7) forest conservation management, e.g. proportion of forested area and catchment area, forest abundance, and (8) water resource management, e.g. numbers of water management organizations, and numbers of water monitoring systems.

Even previous studies of factors and sustainability indicators concern water resources development and management at the national or regional level, however,

there are several aspects, factors and indicators that can be applied to assess sustainability at the project level. For natural resources aspect, following factors and indicators include (1) forestry factor include biodiversity indicator, forest abundance, (2) wildlife factors include biodiversity indicator, endangered species status. For environmental aspects, including water quality indicator. For economic aspect, including income indicator, environmental cost, whereas social aspects including conflict of interest indicator. These factors and indicators can be valuable for evaluating the sustainability rating of water resource development at project level.

According to The Royal Irrigation Department (RID)'s guidelines of water resources development planning study [11], four key dimensions are applied for project size and location selection comprising (1) geography and engineering, (2) environments (3) social, and (4) economic. They are complied with the guideline of The Office of Natural Resources and Environmental Policy and Planning (ONEP)'s Environment Impact Assessment (EIA) Report Preparation [12]. The geography and engineering dimension is consequently added to three principally sustainable dimensions comprising economic, social, and environments.

In addition, in responsible agencies' practice for considering a water resource development for any requested drought agricultural area, water scarcity level would be assessed to classify the necessity level of the water resource development. Five factors including (1) geography, (2) existence of water resource development, (3) hydrology, (4) water demand, and (5) poverty are considered. Decision of the project development would also take the water scarcity issue into account together with other aspects including socio-economic and environments. Since there has not been researched on the establishment of a sustainable indicators and their appropriate level for water resource development in conservation areas in Thailand at the project based level and different water scarcity status, therefore conducting a study to develop such indicators and sustainable level for different water scarcity level would be valuable guidelines applied for assessing well-balanced sustainability across various dimensions of the water resource development projects. The results could also be applied for relevant agencies responsible in both water resource development and natural resource conservation and environmental quality control to consider project's sustainability and feasibility.

Objectives

1) To study key factors and sustainability indicators of water resource development projects in natural resource conservation areas in Thailand,

2) To develop key factors and indicators to measure the severity of water scarcity problems or necessity of water resources development in the agricultural areas of Thailand, and

3) To establish the sustainability score level for the water resource development projects in natural resource conservation areas.

Methodology

Qualitative research through in-depth interviews with selective 7 qualified experts, along with the Del Phi method using questionnaire surveys of 20 experts in relevant fields related to water resources development, including both government agencies and independent experts.

Design criteria of qualification of all experts were specified in accordance with both related academic background and working experiences as follow;

- Academic : Bachelor's degree or higher degree.
- Work experience : direct or related fields of water resources development projects more than 30 years.
- Occupation : government officers, university lecturers, & organization's professionals, and independent consultants

1) The In-depth interview for questionnaire design group consists of 7 experts from three main aspects,

1.1) Engineering : a senior officer of DWR[1]

1.2) Natural resources : 5 senior officers of RFD[2], &Environments DNP[3], and RID[4], independent consultants in forestry, and wildlife

1.3) Socio & Economic: a senior officer of RID

2) Del Phi's panel group comprising 20 experts from three main aspects,

2.1) Engineering : 4 senior government officers of RID, DWR, ORDPB[5], and ONWR[6]

2.2) Natural resources: 8 senior government and Environments officers each from RFD, DNP, ONWR, DMR[7], RID, watershed committee, and two from ONEP[8] and 4 senior independent consultants in forestry, wildlife, environment, and geologist,

2.3) Socio&economic : 2 senior government officers of RID, NESDC[9], and 2 senior independent consultants in social and economic,

Where,
DWR[1] denotes Department of Water Resource Department,
RFD[2] denotes Royal Forest Department,
DNP[3] denotes Department of National Parks, Wildlife and Plant Conservation,
RID[4] denotes Royal Irrigation Department,
ORDPB[5] denotes Office of the Royal Development Projects Board,
ONWR[6] denotes Office of the National Water Resources,
DMR[7] denotes Department of Mineral Resources,
ONEP[8] denotes Office of Natural Resources and Environmental Policy and Planning, and
NESDC[9] denotes Office of the National Economic and Social Development Council.

Study Procedure

The study procedures is presented in Fig. 1 and described as follows,

1) Data compilation and literature review including researches and studies, concerned agencies' regulations, orders, and announcements, as well as feasibility study (FS) and EIA reports, and in-depth interview with the experts.

2) Study and fact finding of water resources development projects including area problems, stakeholders, constraints and limitation, project potential, and factors and indicators concerned.

3) Screening and defining key indicators and scoring ranges of project's sustainability level, and project's water scarcity level or water resources development necessity level.

4) Questionnaire design covering key dimensions, factors, indicators with scoring ranges, and project sustainability level, additionally factors, indicators with scoring ranges, and project water scarcity level.

5) Summarizing the results of factors and indicators with their weighting ranges (1-100%) and Multi Criteria Analysis (MCA) method by assessing through questionnaires surveys from qualified expertise informants of Del Phi Group at least twice to obtain majority results which equal to or greater than the 75 percentile.

6) Application of the results with data from environmental impact assessment reports of 30 project studies.

7) Summarizing the results of sustainable indicators and corresponding weighting score level and recommendations.

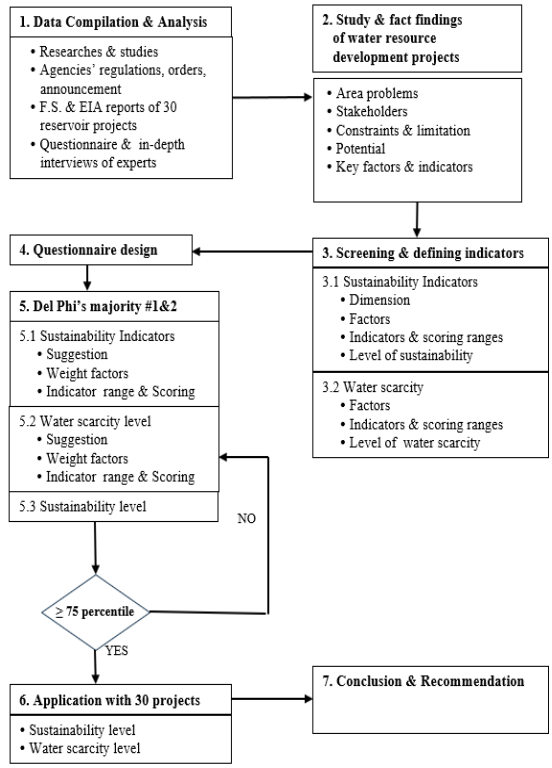

Figure 1 Study Approaches and Procedures

Studying the key indicators of both project's sustainability and water scarcity level were basically determined from literature reviews, in-depth interviews, related agencies' practices and EIA report review, respectively. Additionally, detail indicators were adjusted and modified basing on data accessibility and simplicity of their representing basis for practically applied. Data and information for indicators' ranging scales were manipulated from (1) the FS and EIA reports of water resource development projects, and (2) reference materials from research works, academic papers, regulations, orders, and announcements of relevant government agencies.

Study Data

1) Primary data comprised those from semi structured in-depth interviews together with open-ended questionnaire survey of seven selective expert informants to analyze principals, concepts, and reasons in project defining and prioritizing important dimensions, factors, and indicators that affecting projects sustainability.

2) Secondary data includes data and information documents, statistics of projects from 30 EIA reports of water resource development projects. For the water scarcity assessment, Geographic Information System (GIS) maps of the indicators were referenced from related agencies.

The 30 reservoir projects were selected from different regions of Thailand of which locations presented in Fig 2. 17 projects are located in the northern region (57%), 6 projects are in the eastern region (20%), 3 projects are in the southern region (10%), 3 projects are in the northeastern region (10%), and 1 project is in the central region (3%). These projects have storage capacities ranging from 2 to 295 million cubic meters, covering surface areas ranging from 123 to 16,250 rai. Some of these areas are partially located within conservation areas, including national parks, wildlife sanctuaries area, watershed classification level 1, and conservation zone (Zone C) of national reserved forests excluding wetland and world heritage site.

For Analysis of data, descriptively statistic method, percentile, and MCA are applied, Table 1 presents summary of data collection tools and analysis methods.

Study Results

Results of draft indicators

1. Results from literatures

Even most of literatures are based on regional and national levels, however some indicators are significant for the study which is scoping on project based in conservation areas. 17 from 70 indicators in the four dimensions were screened and modified for first draft key indicators. In the domain of water resources engineering, key indicators encompassed flood discharge, average water volume, and the ratio of water usage per water source. In the aspect of natural resources, it was identified that crucial factors include forest-related aspects with significant indicators such as forest status, proportion of forested areas, biodiversity, vulnerability, and uniqueness. Regarding wildlife, vital factors included biodiversity and the status of endangered species. In terms of environmental quality, the factor of impacted water quality was taken into account. Social aspects involved impacted households and conflict level. On the economic front, considerations included income per capita and ecology cost.

2. Results of in-depth interviews

The remarkable key issues suggested from the in-depth interviews included following items, i.e. consideration of engineering dimension, the importance of the environmental dimension, area uniqueness, recognizing uniqueness in the habitat of endangered wildlife species, reservoir location, natural resource abundance and biodiversity, the status of forest resources, the significance level of conservation area types, project conflicts of interest, and social opposition to the project. These issues were considered and included in the questionnaire design.

Table 1 Summary of data collection, tools, and analysis methods

NO	Objectives	Data Resources /Informants	Tool of data collection	Analysis Methods
1	To study context, concerning factors& indicators, constraints & limitations, and potentials	1) Secondary Data - Study reports of project feasibility and environment impact assessment, researches, agencies' documentations 2) Primary data - In-dept interview questionnaire of experts in engineering, forestry, wildlife, social, economic, environment	1) Secondary Data, Review of study reports of project feasibility and Environment impact assessment, documentations, researches 2) In-depth interview	1) Descriptive Statistics
2	To study dimensions, key factors, indicators and corresponding scoring ranges	1) 20 related expert informants from - Water resources development agencies (RID, WRD, ORDPB) - Natural resources conservation agencies (RFD, DNP, DMR) - Policy and control agencies (ONEP, NESDB, ONWR), Watershed Committee - Related private specialists and consultants	1) Del Phi 's Questionnaire survey	1) Descriptive Statistics 2) Multi Criteria Analysis (MCA) 3) Percentile
3	To apply indicators with 30 projects	1) 30 study reports of project feasibility and environmental impact assessment (EIA)	1) Spreadsheets 2) Geographic Information System (GIS)	1) Descriptive Statistics 2) MCA

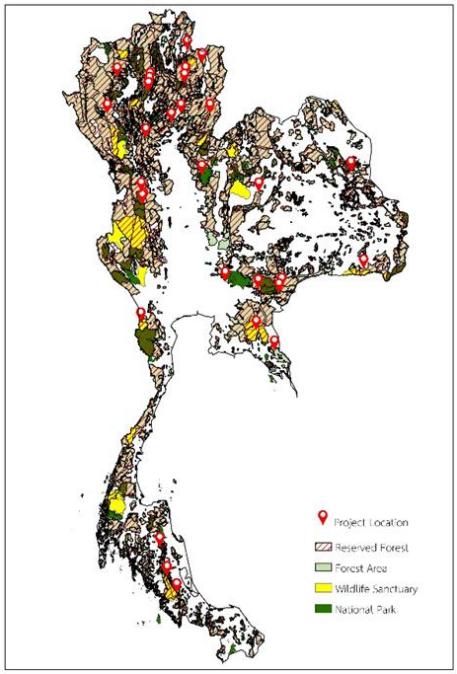

Figure 2 Location of 30 potential reservoirs in the conservation areas

3. Results of agencies' practices and EIA reports

Considering normal practices of most feasible project planning and guidelines of preparing EIA reports, selection of type of water resource development structures, site location and project size would consider following indicators.

For the geography and engineering of which main indicators applied were as follows; i.e. retention area per unit of storage, dam section, geologic conditions, hydrologic conditions, and irrigation area size.

For the environments, indicators mostly applied were size of inundated reservoir area comparable to conservative area, type of conservative areas, abundance or density of trees per area, bio-diversity, status of both forest and wildlife, ecology system, and impacted water quality.

For social dimension, indicators mostly concerned were number of impacted households, encroachment area, and project protestors.

For economic dimension, mostly indicators applied were investment cost per unit of storage volume, and internal rate of return.

These indicators were applied in the second draft indicators proposed in the first Del Phi's questionnaire.

Results of study of the dimensions, factors, and key sustainability indicators from the Del Phi.

1) The main dimensions considered are 4 components consisting of engineering, natural resources and environment, social, and economics.

2) There are 14 significant factors considered for sustainable aspects as follows: (1) engineering dimension comprising 4 factors namely geography, hydrology, geology, and engineering. (2) natural resources and environmental dimension consisting of 4 key factors namely forests, wildlife, water quality, and ecosystem. (3) social dimension concerning 3 core factors namely project opposition, affected stakeholders, and life value or uniqueness. (4) economic dimension comprising 3 factors namely benefits, costs, and feasibility level.

3) The project sustainable indicator comprises 29 indicators as follows: (1) engineering dimension with 6 indicators, (2) natural resources and environmental dimension with 12 indicators, (3) social dimension with 5 indicators, and (4) economic dimension with 6 indicators.

Results of the sustainable indicators

1. Engineering dimension

Engineering dimension consists of 4 key factors:

1.1 Geographic factor consists of two indicators: (1) The dam section per reservoir unit capacity specified from the simplified area of the dam cross section area per reservoir unit capacity, and (2) The reservoir area per reservoir unit capacity.

1.2 Hydrologic factor includes one indicator which is design flood rates per reservoir unit capacity.

1.3 Geologic factor includes two indicators: (1) the seismic indicator, specifying the range of values based on the intensity levels according to the Mercalli intensity scale at the project location, referencing the earthquake risk map by the Department of Mineral Resources (DMR) as shown in Fig.3,

and (2) the permeability indicator, specifying the indicator ranges based on permeability level or the type of bedrock.

1.4 Engineering factor includes one indicator which is the size of the irrigated area per reservoir unit capacity.

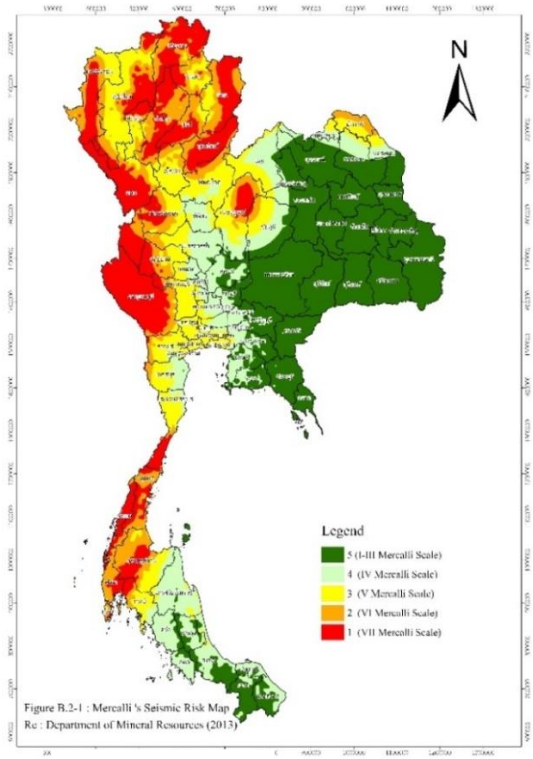

Figure 3 Mercalli's seismic risk map

2. Natural resources and environment dimension

This dimension consists of four factors:

2.1 The forestry factor. It consists of four indicators.

1) The forest abundance indicator is defined by the number of large trees per area of 1 rai in various types of forests, whereas the forest abundance level is applied from the researched figures by the Department of Conservation Science, Faculty of Forestry, Kasetsart University, 2009 [13].

2) The forest bio-diversity indicator is determined by the number of tree species found in high concerned dominated forests type in the reservoir area, whereas the indicator level ranges are referenced to the announcement by the Department of National Parks, Wildlife and Plant Conservation (DNP) regarding the determination of the value of natural resources in protected areas, 2021 [14].

3) The indicator of prohibited tree species is determined based on the number of prohibited tree species found in the reservoir area. The prohibited trees species are referenced to the list in the announcement by the DNP regarding the determination of the value of natural resources in protected areas, 2021.

4) The uniqueness indicator is determined by the presence or absence of unique or outstanding characteristics in the conservation area.

2.2 The wildlife factor. It consists of 4 indicators.

1) The wildlife abundance indicator applies the ratio of number of species of wildlife with low to high population density compared to total species found in the reservoir area.

2) The wildlife bio-diversity indicator is determined by the number of wildlife species found in the reservoir area.

3) The wildlife status indicator is determined by the number of endangered wildlife species, of which status levels are listed as vulnerable (VU), endangered (EN), and critical (CR) by the IUCN Red List, 2015 [15].

4) The uniqueness indicator is determined by the presence or absence of unique national and international wildlife species that cannot be evacuated or translocated.

2.3 The water quality factor

The water quality factor has one indicator which is determined by the level of impact severity on water quality due to project development.

2.4 The ecosystem factor

This factor consists of three indicators,

1) The conservation area type indicator is determined based on the conservation area types impacted by the projects in terms of ecology abundance significance from higher to lower as follows: national park, wildlife sanctuation area, watershed classification 1A, 1B, and national reserved forest area (conservation zone or Zone C), respectively.

2) The impacted conservation area indicator which is the proportion of impacted

conservation area to the total conservation area.

3) The reservoir location indicator is determined by the location of the reservoir within the core area or rim of the conservation area.

3. The social dimension

The social dimension comprises three following factors:

3.1 The project opposition factor

This factor has one indicator which is determined from the number of households opposing the project compared to total households affected by the reservoir.

3.2 The affected stakeholders factor

This factor comprises three indicators:

1) The indicator of the number of affected households in reservoir per unit of reservoir capacity.

2) The indicator of the occupied land in the reservoir area per unit of reservoir capacity.

3) The indicator of the proportion of the benefit area to the reservoir area.

3.3 The factor of quality of life and uniqueness is assessed by the presence of archaeological preserved areas, tourism locations, significant mineral resources, geological conservation areas, and ethnic groups within the reservoir area.

4. The economic dimension

The economic dimension comprises three following factors:

4.1 The factor related to project benefits by applying the indicator of total annual cropping area per unit of reservoir capacity.

4.2 The factor related to project costs by utilizing the indicators of engineering cost, social cost, and environmental cost per unit of reservoir capacity, respectively.

4.3 The factor of project feasibility includes the economic internal rate of return (EIRR) indicator and the environmental economic internal rate of return (EEIRR) indicator.

5. Factors and indicators of water scarcity level

According to related agencies' practices, there are 5 factors consisting of (1) geography, (2) level of development, (3) hydrology, (4) water demand, and (5) society.

5.1 Geography factor

There are 2 indicators including (1) drought risk area, and (2) flood risk area.

5.2 Existence of development factor

The existence of development factor or indicator which is determined the existence of development of water resources and irrigation systems overlapping project area.

5.3 Hydrology factor

There are 2 indicators comprising (1) hydrological variation, and (2) potential of groundwater supply.

5.4 Water demand factor

Water demand factor has one indicator which is determined by cropping types in the benefiting area.

5.5 Social factor

Social factor has one indicator which is determined by the level of poverty.

Weighting factors of sustainability indicators

The results from the Del Phi's 20 specified experts regarding the selected key dimensions, factors, indicators, and their weighting factor values can be summarized as follows:

1. Dimensions

The dimension's weighting factor values among engineering dimension, natural resources and environment dimension, social dimension, and economic dimension are 20 : 35 : 25 : 20, respectively.

2. Factors

1) The physical and engineering dimension. The factors' weighting values among geography, hydrology, geology, and engineering are 25 : 25 : 30 : 20, respectively.

2) The natural resources and environmental dimension. The factors' weighting values among factors of forestry, wildlife, water quality, and ecology are 25 : 30 : 20 : 25, respectively.

3) The social dimension. The factors' weighting values among project opposition, the number of affected households, and the impact on quality of life are 30 : 35 : 35, respectively.

4) The economic dimension. The factors' weighting values among project benefit, project costs, and project feasibility are 30 : 30 : 40, respectively.

3. Indicators

3.1 Indicators of the physical and engineering dimension.

1) The geographical factor includes two indicators: the corresponding weighting values between the dam's cross-section area per unit of reservoir capacity and the reservoir area per unit of reservoir capacity are 45 : 55.

2) The hydrological factor comprises one indicator: that is the design flood peak discharge per unit of reservoir capacity, resulting the weighting value of 100.

3) The geological factor includes two indicators: the weighting values between seismic risk and permeability are 50 : 50.

4) The engineering factor includes only one indicator: it is the irrigation area per unit of reservoir capacity, resulting the weighting value of 100.

3.2 Indicators of the natural resources and environmental dimension

1) The forest factor includes four indicators: the weighting values among abundance, biological diversity, prohibited trees, and uniqueness are 25 : 25 : 20 : 30, respectively.

2) The wildlife factor includes four indicators: the weighting values among abundance, biological diversity, wildlife endanger status, and uniqueness are 30 : 20 : 30 : 20, respectively.

3) The water quality factor includes one indicator: which is the impact on water quality, resulting weighting value of 100.

4) The ecology system factor includes three indicators: the weighting values among the conservation area type indicator, the proportion of impacted area and the conservation area indicator, and the reservoir location indicator are 40 : 35 : 25, respectively.

3.3 Indicators of the social dimension

1) The factor related to project opposition comprises only one indicator which is the proportion of the number of opposition to the total impacted households, resulting the weighting value of 100.

2) The factor related to the impacted sufferers and beneficiaries includes three indicators: the weighting values among the impacted households per unit of reservoir capacity, the encroached area per unit of reservoir capacity, and the proportion of irrigation area and the reservoir area, are 40 : 30 : 30, respectively.

3) The factor related to quality of life concerns one indicator which is the existence of distinctiveness value across either different aspects (archaeologic sites, tourism site, significant minerals resources, geologic conservative site, ethnic groups) resulting the weighting value of 100.

3.4 Indicators of economic dimension

1) The factor related to project benefit includes only one indicator which is the year-round cultivated area per unit of reservoir capacity, resulting the weighting value of 100.

2) The factor related to project costs includes three indicators: the weighting values among engineering costs per unit of reservoir capacity, social replacement costs per unit of reservoir capacity indicator, and environmental mitigation costs per unit of reservoir capacity indicator are 30 : 35 : 35, respectively.

3) The factor related to project feasibility includes two indicators: the weighting values of economic internal rate of return indicator, and environmental economic internal rate of return indicator are 45 : 55.

Consideration of sustainable water resources development project

Any proposed project that be developed should provide overall sustainable point in good level (66-75) or better whereas each dimension point be in moderate level (56-65) or better.

Weighting factors of project's water scarcity level

There are five main factors applied for the assessment of water scarcity level or necessity level of water resource development. They are geography, the existence of water resources and irrigation development, hydrology, water demand, and poverty. The weightage of these factors is distributed as 20 : 15 : 20 : 20 : 25, respectively.

1) The geographic factor consists of two indicators: the drought risk area indicator and the flood risk area indicator. The weightage is distributed as 55 : 45, and the reference maps applied are based on the drought and flood risk level mapping by Geo-Informatics and Space Technology Development Agency (GISTDA) as shown in Fig.4 and Fig.5.

2) The existence of water resources and irrigation development factor consists of a single indicator, resulting a weightage of 100. The reference map is based on the RID's present reservoirs and irrigation areas map as presented in Fig.6.

3) The hydrologic factor includes two indicators: the weighting values of hydrological variation indicator and groundwater recharge indicator, are 65 and 35, respectively. The indicators are based on data from rain gauge stations provided by the RID and the groundwater yield map provided by the Department of Groundwater Resources (DGR) as shown in Fig.7 and Fig.8, respectively.

4) The water demand factor consists of a single indicator which is the agricultural water demand indicator, resulting the weighting value of 100. This indicator is referenced from the land use map provided by the DLD as presented in Fig.9.

5) The poverty factor consists of a single indicator which is the household poverty indicator, resulting the weighting value of 100. This indicator is established from data of the National Electronics and Computer Technology Center (NECTEC) in 2022 as shown in Fig.10.

6) The results from the Del Phi's panel are concluded that a project with a scarcity score or water resources necessity score of less than 33 is considered a low water scarcity level. For scarcity point of a project falling within the range of 34-67, it is considered a moderate level, while a project scoring 68 or higher is considered a significant high water scarcity. In cases where the project has moderate to high water scarcity level, it is advisable to undergo further development. However, if the project has sustainability scores below the moderate threshold (less than 55), it is recommended to revise project size, to alter dam location, or to improve project components to achieve a higher total sustainability rating at least within the moderate range.

Application of sustainability indicators

Tables 2 and 3 show summary of 30 reservoirs' basic data and weighting factors of the project's sustainability indicators, whereas Table 4 presents summary of weighting factors of water scarcity assessment. Results of applying indicators' weighting scores for project sustainability assessment are summarized as follows.

1) Sustainability assessment of engineering dimension, one- third or 11 projects were evaluated as low sustainable level.

2) Sustainability assessment of natural resources and environmental dimension, no projects were assessed as low sustainable level.

3) Sustainability assessment of social dimension, five projects were assessed as low level,

4) Sustainability assessment of economic dimension, eight projects were classified as low level.

5) Overall project sustainability, there were no projects defined as low sustainable level, whereas three projects were assessed as medium level and suggested to be upgraded or improved namely, Nam Yuan, Huai Phet Ja Khor, and Huai Poeng Phark.

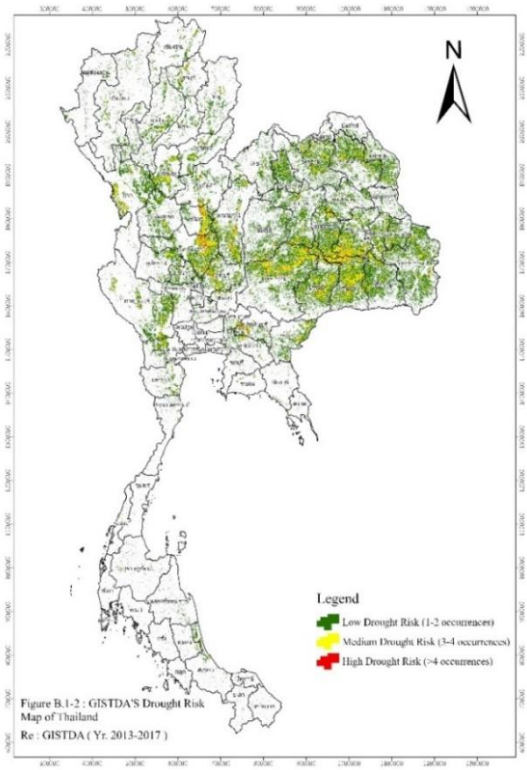

Figure 4 GISTDA's drought risk map

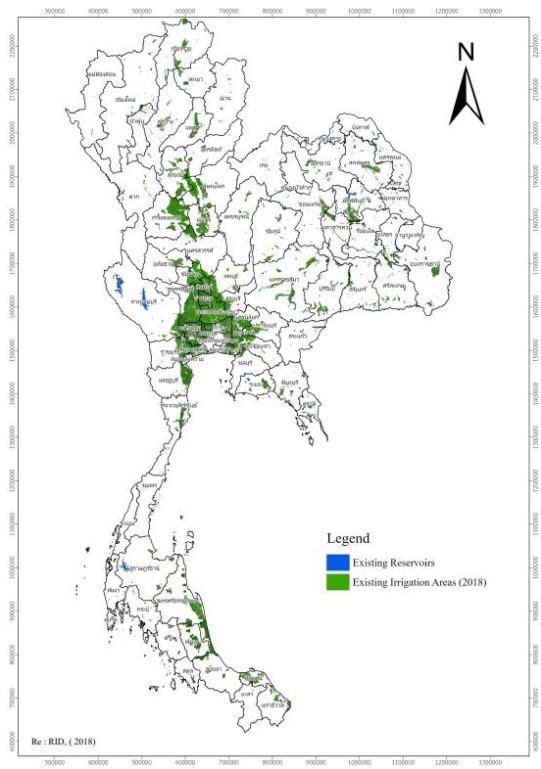

Figure 6 The location map of irrigation areas

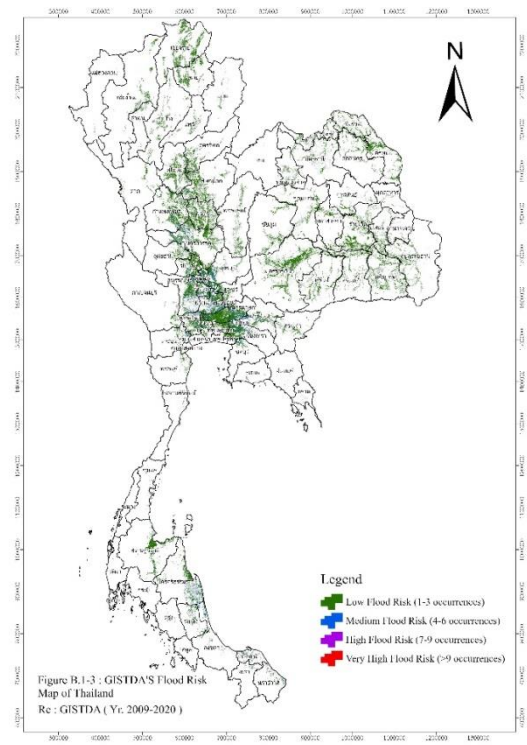

Figure 5 GISTDA's flood risk map

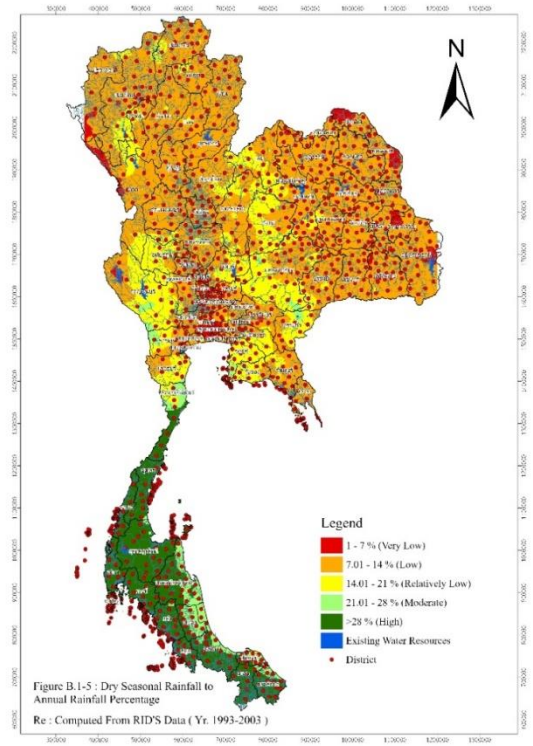

Figure 7 Dry seasonal rainfall to annual rainfall percentage map

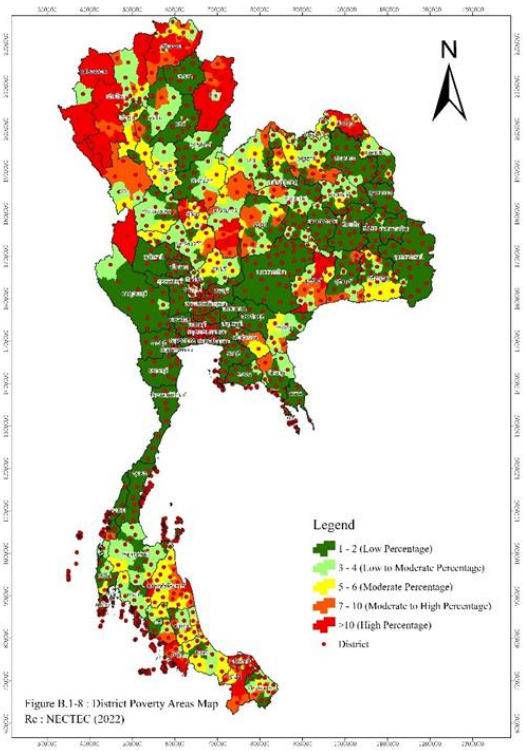

Figure 8 Groundwater potential map

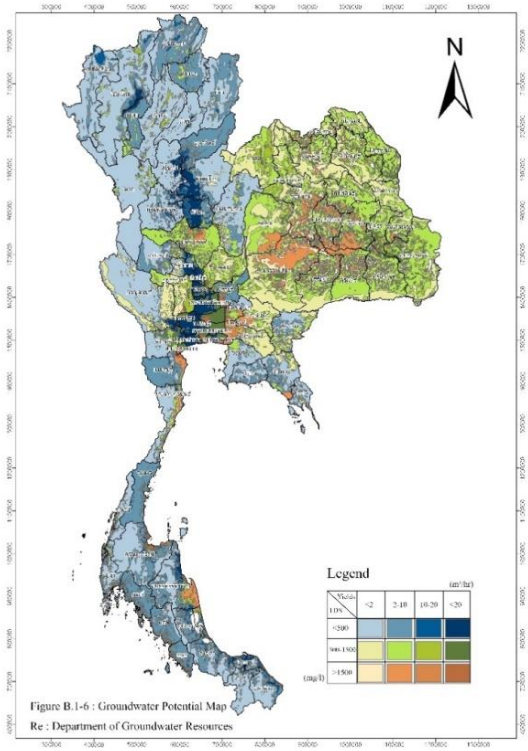

Fig 10 District poverty areas map

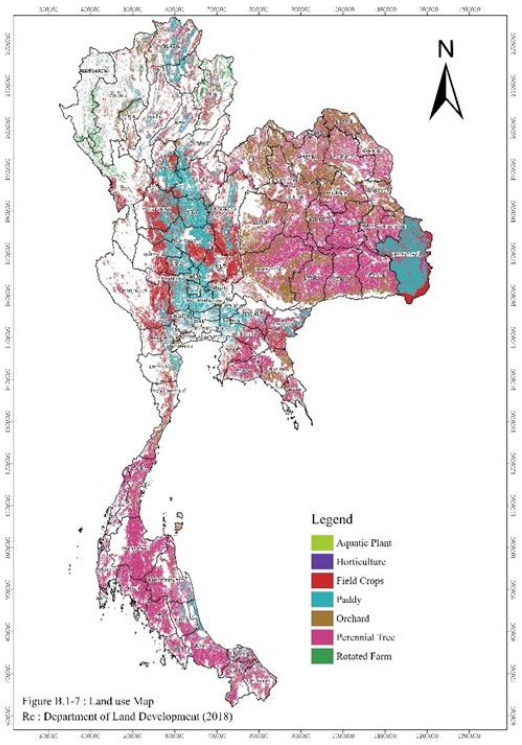

Figure 9 Land use map

6) In term of factor level concerning natural resources and ecology, There were seven projects that were determined low sustainable level namely Klong Yai, Mae Phuak, Huai Satone, Klong Ma Dua, Huai Kha Yung, Khlong Wang Tanode, and Mueng Takua.

7) For project's water scarcity level, only two projects namely Huai Pang Luang and Khlong Chom Phoo were defined as high level whereas the others were middle level.

In summary the established sustainable indicators are applicable complied with the threats and barrier as well as potential and strength of the projects.

Table 2 Summary of basic project components of 30 reservoir projects

Item	Project Features	Unit	Min	Max	Mean
1	Storage Volume	mcm	2.1	295	40.1
2	Retention Area	Rai	87	16,250	2,172
3	Irrigation Area	Rai	1,273	111,300	28,831
4	Dam Crest Length	m.	133	3,000	794
5	Dam Height	m.	11	80	40
6	Construction Cost	MB	149	5,668	1,172
7	Catchment Ares	sq.km	11	677	142
8	Mean Annual Flow	mcm/yr	2.8	266	57
9	Inflow Flood Discharge	mcm/s	35.6	1,428	387

Remark : 1 Rai = 1600 sq.m.

Discussion and Recommendations for Project Enhancement for Sustainability

1) Applying the sufficiency economic concept, comprising moderate scale development together with reasonable outcome and risk management with appropriate impact mitigation plans, would solve unbalance or conflict between economic and environments. Therefore, in case a project's environmental sustainability score is low, modification of project scale, reservoir size, dam relocation will be one of the solution to improve sustainability score level, environmental and social impact, and project feasibility.

2) Reducing the project size by decreasing the storage capacity of the reservoir and the reservoir area in cases where the topography of the reservoir is flat may not significantly affect the sustainability score in the engineering dimension. This is because the indicator value is relative to the unit capacity, and minor changes in engineering size do not have a significant impact on the range of scores in this dimension.

However, the reduction in project size, especially in terms of reservoir capacity or retention area, would result in a better positive impact on natural resources, environments, ecosystem, society, and economic aspects.

3) Nevertheless, in cases where there is no additional revised survey of natural resources due to the reduction in the reservoir area, the sustainability score in the mentioned dimension may not change significantly either, since the scoring interval range of indicators have a wider range of which results are analyzed from wider range of size and varieties of geography, natural resources types and socio-economic characteristics from all regions over the country. Consequently, further studies on scoring range of indicators especially for each region is recommended.

Conclusion

Four dimensions including engineering, natural resources and environment, social and economic are recommended as key dimensions for considering water resource development project's sustainability, whereas the natural resources and environment is the most significant dimension.

There are 14 factors concerning the project sustainability, of which 7 factors that have higher significant weight: wildlife (10.5%), forestry (8.75%), ecology (8.75%), social (8.75%), life value (8.75%), economic feasibility (8%), and opposition (7.5%), respectively.

There are 29 indicators concerning the project sustainability, of which 12 indicators having higher weight: (1) uniqueness, (2) number of opponents per impacted households, (3) water quality, (4) annual cultivated area per unit of reservoir capacity, (5) design flood rate per unit of reservoir capacity, (6) environmental economic feasibility, (7) economic feasibility, (8) proportion of beneficiaries on sufferers (9) conservation area type, (10) Number of compensated households per unit of reservoir capacity (11) endangered wildlife, and (12) biodiversity of wildlife.

There are 5 factors to assess the project's water scarcity level, including geography, existence of irrigation system, hydrology, water demand, and poverty. The poverty, land use, and existence of irrigation system play higher weights. Status of project's water scarcity issue from moderate to high level will be another factor to lessen sustainability level criteria from good to moderate level so that such project could be implemented.

Table 3 Summary of factors and indicators for water scarcity level assessment

Factors / Indicators	Unit	Water Scarcity Level			Gross Weighting Score	Net Weighting Score
		Low (No. of Proj.)	Moderate (No. of Proj.)	High (No. of Proj.)		
1. Geography factor					**100**	**20**
1.1 Drought indicator - Frequency in the past 5 years of droughts.	Years	1-2 (18)	3-4 (8)	≥5 (4)	55	11
1.2 Flooded indicator - Frequency in the past 12 years of floods.	Years	≤4 (26)	5-8 (3)	>8 (1)	45	9
2 Irrigation system existence factor					**100**	**15**
- Irrigation system existence index	-	Partial Irrigated by reservoir. (5)	Partial Irrigated without reservoir. (2)	No Irrigation system. (23)	100	15
3 Hydrology factor					**100**	**20**
3.1 Rainfall variation indicator - Proportion of dry season rainfall to annual rainfall.	%	> 30 (3)	25-30 (5)	< 25 (22)	65	13
3.2 Groundwater potentials indicator					35	7
- Yield	cu.m./hr,	>20 (5)	10-20 (2)	<10 (23)		
- Total Dissolved Solids (TDS)	mg/l	<500 (26)	-	>500 (4)		
4 Water demand factor					**100**	**20**
- Agricultural land use type indicator	Type	Perennial Tree (4)	Field Crops (12)	Orchard/Paddy (14)	100	20
5 Poverty factor					**100**	**25**
- Poverty indicator (Proportion of the poors to district's population.)	%	≤2.5 (15)	2.6-10 (14)	>10 (1)	100	25

Remark : NP = National Park WL = Wildlife Sanctuation Area
1A = Watershed Class. 1A RF = Reserved Forest
1 Rai = 1,600 sq.m.

Acknowledgement

Sincerely thanks to RID, RFD, DNP, DLD, DWR, DMR, DGR, GISDA, NSTDA, NESDC, ONWR, ONEP, ORDPB, and all academic experts, who kindly supported all valuable data, and information, especially the Bureau of Project Management of RID and DNP who supported updated essential data, and concerned reports. In addition, highly appreciate to Del Phi's experts who kindly shared valuable opinions and suggestions.

References

[1] Piyachana, A. 2013. The State of Natural Resources and Environment at Phu Phan National Park and Surrounding Areas. Sripatum Review of Humanities and Social Sciences.

[2] Poomjamnong, N. and Charoenwong, U. 2017. The project to survey the status of sustainable development goals in the context of Thailand and options for economic, social, and legal measures. Goal 15. Final Report, Mahidol University.

[3] Noywuli, N. Sapei, A. Pandjaitan, H. N. and Eriyatno, E. 2006. Assessment of Watershed Carrying Capacity for the Aesesa Flores Watershed Management, East Nusa Tenggara Province of Indonesia. Environment and natural resources Journal. 17(3). (2019) Jul-Sep.

[4] Tong, X. Guan, X. Lu, S. Qin, F. Liu, X. and Zhang, D. 2020. Examining the spatiotemporal change of forest resource carrying capacity of the Yangtze River Economic Belt in China. Environmental Science and Pollution Research. 27: 21213-21230. (2020).

[5] National Park Research Section, Nation Park Division, Department of National Park, Wildlife and Plant Conservation. 2019. Prioritization of the National Parks in Thailand.

[6] Smith, T. E. and Zhang, X. H. 2007. Evolution of Sustainable Water Resource Indicators. Water Environment Federation. 2624-2649.

[7] Morris, J. 2019. Developing and exploring indicators of water sustainable development. Heliyon. 5(5). May 2019. https://doi.org/10.1016/j.heliyon.2019. e01778.

[8] Liang, X. Zhang, R. Liu, C. and Liu, H. 2018. Quantitative Measurement of the Sustainable Water Resource Development System in China Inspired by Dissipative Structure Theory. Sustainability. 2018. 10(11): 3996. https://doi.org/10.3390/su10113996.

[9] Corrêa, M.A. and Teixeira, B.A. 1905. Developing Sustainability Indicators For Water Resources Management In TIETÊ-JACARÉ BASIN, BRAZIL. Journal of Urban and Environmental Engineering. 7(1). (January to June 2013): 8-14. ISSN 1982-3932 doi: 10.4090/juee.2013.v7n1.008014.

[10] The National Statistical Office of Thailand. 2023. Establishment of the water management indicator (WMI) in Thailand. Bangkok.

[11] Bureau of Project Management of The Royal Irrigation Department. 2014. Study guideline of water resource development planning. Bangkok. Royal Irrigation Department. Retrieved from https://www.dmr.go.th

[12] Office of Natural Resources and Environmental Policy and Planning. 2023. Guidelines for preparing environmental impact assessment reports for water development projects. Bangkok. Office of Natural Resources and Environmental Policy and Planning.

[13] Department of Conservation Science. 2009. Final Report Watershed Analysis of Huai Isar, and Huai Rang River Uthai Thani Province. Faculty of Forestry, Kasetsart University. Bangkok.

[14] Department of National Parks, Wildlife and Plant Conservation (DNP). 2021. The announcement regarding the determination of the value of natural resources in National Park, Park, Forest park, and Arboretum 2021. Ratchakitcha. Vol 138, Part 301.

[15] IUCN. 2015. The IUCN Red List of threatened species. Version 2015.4. http://www.iucnredlist.org. Assessed. August 2016.

Thai Environmental Engineering Journal Vol. 38 No. 2 (2024) : 19-33
www.eeat.or.th

Investigating the Impact of Aeration and Leachate Recirculation for Biodrying of Food and Vegetable Waste from the Market

Ye Nyi Nyi Lwin[1,2], Abhisit Bhatsada[1,2], Sirintornthep Towprayoon[1,2], Suthum Patumsawad[3], Noppharit Sutthasil[4] and Komsilp Wangyao[1,2*]

[1]The Joint Graduate School of Energy and Environment (JGSEE), King Mongkut's University of Technology Thonburi, Bangkok 10140, Thailand
[2]Center of Excellence on Energy Technology and Environment (CEE), Ministry of Higher Education Science, Research and Innovation (MHESI), Bangkok 10400, Thailand
[3]Department Mechanical and Aerospace Engineering, Faculty of Engineering, King Mongkut's University of Technology North Bangkok, Bangkok 10800, Thailand
[4]Department of Environmental Health, School of Health Science, Mae Fah Luang University, Chiang Rai 57100, Thailand
[*]E-mail : komsilp.wan@kmutt.ac.th

Article History; *Received: 20 June 2024, Accepted: 20 June 2024, Published: 30 August 2024*

Abstract

The increasing production of waste from the market presents significant challenges for waste management, necessitating efficient treatment methods like biodrying. This study examines optimizing biodrying methodologies for the treatment of fruit and vegetable waste collected from market sources, emphasizing the nuanced impact of leachate recirculation within zero discharge systems. Aimed at bolstering the efficiency of converting market refuse into a biodried product suitable for integration into the waste-to-energy framework, our research meticulously assessed the performance of three lysimeters, arranged in parallel, under distinct aeration rates: Lysimeter 1 with an aeration rate of 0.2 m^3/kg/day, followed by Lysimeters 2 and 3 with 0.4 m^3/kg/day and 0.6 m^3/kg/day respectively. Lysimeter 1 emerged as the front-runner, showcasing better performance metrics across CO_2 concentration, weight reduction, leachate volume, and temperature profiles. Notably, it achieved a remarkable 5.97% moisture content (MC) reduction at the lowest aeration rate of 0.2 m^3/kg/day. The controlled aeration strategy employed in Lysimeter 1 facilitated significant organic content transformation and led to an impressive 317% boost in heating value, surpassing the results of Lysimeters 2 and 3, which recorded MC losses of 7.97% and 2.47%, respectively. These findings highlight the critical importance of optimizing aeration rates and the detrimental effects of leachate recirculation on the biodrying process. They advocate for future research endeavors to refine aeration rates further and exclude leachate recirculation, aiming to produce a biodried product that meets the moisture loss and heating value requirements for the cement industry's RDF standards. This study contributes valuable insights towards enhancing biodrying efficiency, with significant implications for waste management and energy recovery practices.

Keywords : Biodried Product; Waste-to-Energy; Biodrying Efficiency; Controlled Aeration; Leachate Return

Introduction

Municipal solid waste (MSW) production is increasing due to urbanization as well as the complexation of MSW composition, which remains one of the key challenges [1-3]. MSW is typically disposed of in sanitary landfills or open dumps, particularly in low- and middle-income nations, for convenient and economic reasons [4]. On the other hand, poor waste management at these locations has resulted in several environmental issues, including the emission of greenhouse gases (GHGs) and pollution of water and soil [5]. GHG emissions from MSW are relatively low, with landfills being the primary source due to the anaerobic decomposition of organic waste, which produces methane (CH_4). Aerobic decomposition of organic waste emits carbon dioxide (CO_2) but to a lesser extent than methane from anaerobic processes. Market waste, including food and non-food-related waste [6], presents significant challenges to waste management, characterized by high waste mass but low density, and rapid decomposition, which can lead to environmental and sanitary problems, i.e., infestation of insects, odor, and leachate spilling on the surrounding [7]. Centralized wholesale marketplaces in developing nations generate segregated organic waste, hindering efficient waste treatment [8]. By 2050, food and green waste will account for over 50% of all waste in low- and middle-income nations [9]. Many countries continue to generate a considerable amount of mismanaged organic waste, particularly in those where agriculture is the primary source of revenue [10].

In Thailand, waste is categorized into four types: municipal, industrial, household hazardous waste, and hazardous waste [11]. However, there are no separate collection and treatment systems for market waste, further creating environmental threats [12]. Thailand employs three main waste disposal methods, incorporating composting, combustion, and disposal on land, while the solid waste problem is still considered a prime environmental concern [13, 14]. Thailand's waste management system is currently facing issues such as garbage overflow in landfills due to increased waste generation with population growth and subsequent improper disposal [15-18]. Innovative waste management technologies are needed to efficiently handle market waste, such as food waste in Vietnam and Thailand, reducing moisture content (MC) for efficient disposal and energy recovery from solid waste [19, 20]. Refuse-derived fuel (RDF) synthesis eliminates MC and non-combustible elements, resulting in a cost-effective and safe burning product for cement kilns or biomass boilers. Alternative fuels are crucial for reducing fuel prices and enhancing GHG emission reduction. [21, 22]. In Thailand, most cement plants use the local RDF-3 standard, which sets a minimum threshold of 4,500 kcal/kg [23]. In waste-to-energy plants, lower heating values are feasible to meet combustion chamber requirements; thus, alternative fuels from MSW are continuously used [24]. MSW's high MC and organic proportion can result in low energy gain during thermal conversion [25].

Mechanical biological treatment (MBT) processes, including composting, biostabilization, and biodrying, are widely used to manage, convert, and transform MSW [26-28]. Due to the continuous increase in solid waste generation, which shortens landfill lifespans, treating solid waste through methods such as composting and biodrying can significantly reduce the volume of waste destined for sanitary landfills, thereby extending their lifespan [29]. Biodrying is a promising solution for treating organic waste efficiently, reducing volume, MC, and GHG emissions. It ensures environmental sustainability by reducing landfill waste and mitigating leachate leakage. Biodried products can recover energy from high calorific values, but aeration rate is crucial [30].

Biodrying reactors are based on a combination of physical and biochemical processes and are designed as open tunnel halls or rotating drums. On the biochemical side, aerobic biodegradation of easily decomposable organic materials occurs. Aeration is used to remove convective moisture effectively. Although the reactor architecture and biochemical process are similar to composting, the specific operation differs greatly [30]. Lysimeters are increasingly used to investigate the effects of climate change on land and water resources. Lysimeter experiments provide more

accurate leaching test results than static leaching tests [31]. Thus, lysimeters are commonly used in biodrying experiments because they can accurately measure moisture content and other parameters critical to biodrying.

Moisture in MSW significantly affects biodrying, with high moisture levels preventing oxygen (O_2) transmission and low moisture levels preventing microbial activity [32]. Organic waste decomposition is hindered by O_2 shortage, necessitating biodrying, and natural aeration. Positive or negative forced aeration ensures O_2 availability, with negative aeration causing more extensive water loss-to-volatile solids ratios [33, 34]. Positive aeration in an open-top lysimeter arrangement can improve moisture evaporation and reduce leachate generation; nevertheless, this can cause non-homogeneous moisture distribution due to condensation and, given the compacted waste, insufficient air movement through the waste matrix. Biodrying evaporates water from biological waste, but leachate can form, requiring careful control before discharge into aquatic bodies [35]. Leachate recirculation enhances biodrying efficiency by maintaining moisture levels, promoting biological decomposition, and enhancing heat generation while managing rates and frequency for optimal process conditions [36]. Zhang et al. (2009) found that pH-neutralized leachate recirculation enhances total water removal and organics degradation in a hydrolytic-aerobic bio-pretreatment for MSW [37].

For this study, 'market waste' refers to food and vegetable waste collected from market sources. Despite advances in waste management technologies, there is still a significant gap in our understanding of biodrying processes, mainly when applied to market waste. With its high organic content, market waste poses particular challenges and potential for biodrying procedures. However, current research focuses primarily on generic organic waste streams, ignoring the complexities of market waste biodrying. The effect of leachate recirculation on a biodrying process is quite limited, as the quantity of leachate and the minimal MC for biodrying operations that inhibit biodegradation have not been widely identified. On the other hand, if the water concentration is too high, it plugs the waste pores, making the process anaerobic [38]. With high MC, market waste generates large quantities of leachate during biodrying. Recirculating leachate containing nutrients and organic matter can improve organic material degradation, generate metabolic heat for efficient moisture removal, and reduce the need for external management and treatment. This study aims to (1) determine the optimal aeration rate for biodrying market waste, (2) assess the impact of leachate recirculation on microbial activity and heat generation, and (3) evaluate the overall efficiency of different aeration rates and leachate recirculation practices. This study introduces a novel approach by integrating different aeration rates and leachate recirculation practices in a zero-discharge system. The expected impact includes enhanced biodrying efficiency and improved waste management practices, contributing to sustainable environmental management.

Materials and Methods

Feedstock preparation

Market waste, including mainly vegetable and fruit residues, was collected from Eastern Energy Plus Co., Ltd. in Samut Prakan province, Thailand, as part of the feedstock preparation process. The trials in this study were conducted from November 3rd to November 18th, 2023, with an average relative humidity of 30-50% and a temperature range of 25-33°C. The market waste utilized as feedstock was typically similar in composition. Plastic bags comprised 6.84% of the non-biodegradable components, while packaging and plastic tubes comprised 0.54%. Organic waste included up to 91.25% of the degradable materials, with milk cartons and paper waste accounting for 1.37%. The market waste stockpile was homogenized using the ASTM D5231-92 standard's quartering process, a straightforward method that involves splitting, mixing, and repeating until a representative sample is obtained. A total of 18.5 kg of market waste was collected and analyzed before biodrying, including two 1.5 kg samples of market waste and one 0.5 kg sample of organic waste. The MC, volatile solid (VS), and ash were measured using an ASTM D7582

thermogravimetric analyzer (TGA801; LECO Corporation, St. Joseph, MI, USA). The high heating value (HHV) was determined using an ASTM D240 bomb calorimeter (AC-500 calorimeter, LECO®, USA), then converted to LHV. The organic material included carbon (C), hydrogen (H), oxygen (O), nitrogen (N), chlorine (Cl), sulfur (S), and ash content studies. The feedstock's physical and chemical properties – weight, and bulk density, which were measured before each experiment – the MC, Ash content, low heating value (LHV), and MC were 90.23% (by wt), 1.07% (by wt), 47.5 kcal/kg, and 0.03% (by wt), respectively. The characteristics of feedstock were similar to those of Hanrinth and Polprasert. (2016) regarding MC and organic content: MC 89.36% and 88.46% w/w of organic matter for vegetable residue, fruit peel, and food debris derived from the fresh-food market [39].

Experimental design

The feedstock quantity in each lysimeter varied 45.35, 62.98, and 66.65 kg for Lysimeters 1,2 and 3 with waste densities of 151.16, 209.92, 222.16 kg/m^3 at a feedstock elevation of 1.2 m. The aeration rate was set as 0.2, 0.4, and 0.6 kg/m^3 with the associated proportion of feedstock's mass and cross-sectional area of ventilation pipes, transforming the air flow rates to be 0.05, 0.14, and 0.23 m/s, respectively. Recirculation of leachate was carried out from day 1-6. All the experiments lasted 15 days.

The purpose of the leachate recirculation on the decomposition of market waste in the biodrying process can be the stage that Lysimeter 1 was the low aeration and density conditions that are close to anaerobic digestion similar to landfill conditions [40] – leachate recirculation helps to provide leachate volume reduction and leachate dilution; Lysimeters 2 and 3 were the sufficient aeration consistent with stoichiometric value – leachate recirculation supports the acceleration of degradation processes associated with high oxidizable organic matter from recirculated leachate, minimize pollutants by provide a stabilized leachate generation. To prevent the low oxidizable organic matter from returning to the digestion process, the recirculation period was limited to day 6 [41].

Operating mode

This experiment used a 1.5-meter-high lysimeter for biodrying processes, incorporating leachate recirculation. A metal plate stabilized the raw material, while ventilation pipes, condensation pipes, and blowers created airflow. Leachate was collected using a U-trap pipe, and interior gas was measured using 20mm diameter perforated pipes. This apparatus was created using data from a study by Bhatsada et al. (2023). Figure 1 illustrates the lysimeter's schematic design in more detail.

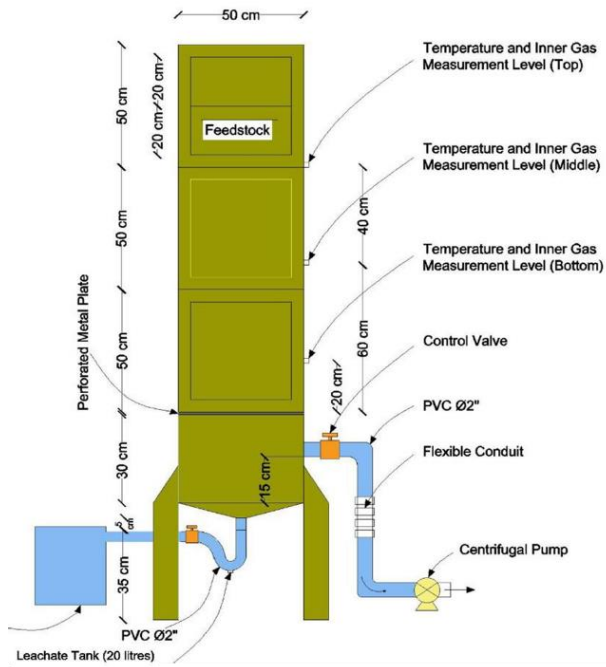

Figure 1 Schematic of lysimeter design [42, 43]

Monitoring parameters and performance indicators

Temperatures were measured at 20, 60, and 100 cm heights using type-K thermocouples (temperature range: -270 °C to 1,327 °C). Another sensor was inserted outside the lysimeter to detect the ambient temperature. A data logger (Graphtec GL200A Midi Data Logger; DATAQ Instruments, Akron, OH, USA) was used to record the temperature hourly. The concentration of O_2, CO_2, CH_4, hydrogen sulfide (H_2S), and Nitrogen (N_2) at three levels within the lysimeters, in the ambient air, and the exhaust were measured daily with a Biogas 5000 gas analyzer (Geotechnical Instruments International,

Ltd., Berlin, UK). In addition, the ambient air was concentrated in 0%, 0%, 20.9%, 0 ppm, and 79.1% of CH_4, CO_2, O_2, H_2S, and N_2, respectively. The feedstock height inside the lysimeter was measured vertically with a tape measure. The daily control of aeration rates in each lysimeter (m^3/kg/day) were measured in air velocity through the 1 × 3 cm hole perforated pipe using an airflow meter.

Temperature integration (TI) index was used to calculate the accumulated daily difference between the matrix and ambient temperatures.

$$TI = \sum_{i=1}^{n}(T_m - T_a).\Delta t \quad (1)$$

where T_m and T_a are the matrices and ambient temperatures at day I, Δt is the time element [37].

The aeration and leachate flow were in the same direction that was introduced at the top to the bottom of the lysimeter. However, the end location was different following Figure 1. The all-leachate generation in the collected system was daily upward, and some of them were accumulated in the lysimeter. To determine the leachate recirculation pattern, the accumulation of leachate within the process can also be considered.

$$L.A_n = L.\,Gen_n + L.Re_{n-1} \quad (2)$$

where $L.A_n$ is leachate accumulation in n days, and $L.Gen_n$ and L. Ren-1 are leachate generation and recirculation.

The settlement rate within the waste pile can be determined with changes in elevation during biodrying. The elevation change can be calculated using daily measurements of the waste height.

$$\text{Elevation Change (\%)} = (H_{n-1} - H_n / H_{n-1}) \times 100 \quad (3)$$

where H_n is the waste height (m) in n days, and H_{n-1} is the waste height (m) from the previous day's measurement.

Statistical analysis

The significant difference in three trials was performed with 95% confidence using one-factor variance analysis (ANOVA) in Excel 2010 to assess the temperature differences between the layers and the ambient environment with a significance level (cutoff p-value) of 0.05 [33].

Results and Discussion

Leachate recirculation

The biodrying of market waste using a zero-discharge system involved collecting and returning leachate from each lysimeter daily from day 1 to day 6 as shown in Figure 2. The amount of leachate accumulation was equal to that of generation on day 7 and afterward. Lysimeter 1 started producing on day 2, while Lysimeters 2 and 3 had significantly higher leachate generation and return amounts. This phenomenon indicates that although the leachate generation experienced

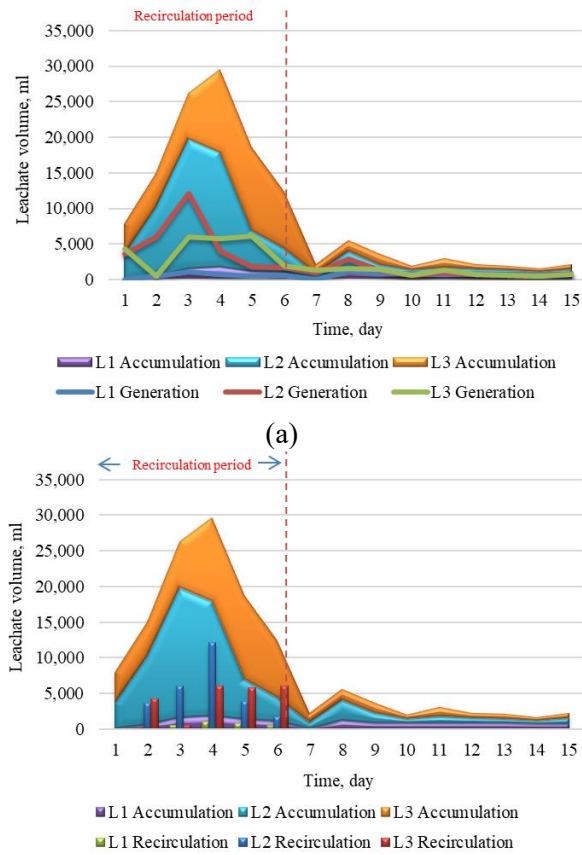

Figure 2 (a) Leachate accumulation vs generation and (b) Leachate accumulation vs recirculation during biodrying (L1 = lysimeter 1, L2 = lysimeter 2, L3 = lysimeter 3)

a declining trend due to high-temperature formation within the waste matrix, much higher volumes were accumulated due to recirculation. During the non-recirculation period, leachate generation decreased steadily to a stable generation quantity. Bilgili et al. (2012) investigated the effect of leachate recirculation in four landfill test cells. The quantity of leachate decreased by 29.7%, 37.8%, and 22.5% in three recirculated cells, while there were no changes in the quantity of the control cell. The more significant decrease in leachate quantity can be explained by the effect of evaporation of the waste temperature and the effect of air-drying the waste [44].

The accumulated leachate volume was superior to other feedstocks since market waste mainly comprises organics with high MC. Sutthasil et al. (2022) discovered that waste with high initial MC levels of 70-80% showed abnormal leachate formation and evaporation. This could be due to the high water content of the waste, which created an overflow of leachate outflow and impaired drying effectiveness [45]. According to Awasthi et al. (2018) and Wijerathna et al. (2024), moisture levels exceeding 80% can cause anaerobic respiration, limit compost porosity, and produce leachate and unpleasant odors [46, 47]. Ma et al. (2021) reported that the larger amount of leachate recirculation increased the waste MC and thus was suitable for microorganism growth in semi-aerobic reactors [48]. Ma's study supports the present study that sufficient aeration stimulates the decomposition (high leachate generation) by Lysimeters 2 and 3. Luo et al. (2019) varied the concentration of leachate recirculation effects on solid waste degradation by observing that the organic reduction increased gradually with increasing water replacement [49]. The study found that leachate generation increased due to high accumulation and recirculation but decreased after day 3 and continued until day 6. This correlation mirrors Calabrò et al.'s (2018) study, suggesting that leachate recovery mirrors generation as long as it remains at the landfill bottom [50]. Consequently, the present study decreased the belatedness trend of leachate recirculation due to some leachate accumulating in the bottom waste.

Temperature evolution during biodrying

Temperature evolution is divided into three stages: heating, high-temperature maintenance, and cooling. Heating rapidly raises the temperature, while high-temperature maintenance is steady, affecting water evaporation and organic deterioration [51, 52]. During the process of biodrying market waste, the temperature evolution was quite different from a typical biodrying system, when the heating phase was reached within days 1-2, followed by the declining phase (days 3-5) and the stable phase (days 6-15) (See Figure 3). This phenomenon can be explained by the recirculation of leachate into the lysimeters from day 1 to day 6. Moreover, temperature patterns separate the different stages of its evolution; mesophilic is characterized by bacterial bioactivity and temperatures starting from ambient temperature and a gradual rise to between 35 °C to 40 °C; transitions into the thermophilic phase where waste achieves maximum evolution at temperatures of 55 °C to 70 °C [52]. While microbial activity can enhance the decomposition of organic matter [53], providing a condition suitable for thermophilic microorganisms' growth could accelerate the thermophilic phase's start, leading to an increase in the biodegradation of organic matter [54]. Lysimeter 1 reached the thermophilic stage on day 2 in an experiment due to a lower aeration rate and leachate influence, unlike other lysimeters. The results indicated a high biodegradation process from substantial microorganism metabolism, and stability was achieved in the mesophilic phase after day 5. The study's findings were consistent with Zaman, B. et al. (2021). This indicated a temperature rise from around 43 °C on the second day, followed by a drop to 39 °C on the third day, utilizing a low airflow of 2.88 m^3/kg/day [38, 55]. The middle layer of Lysimeter 1 has optimal conditions for microbial activity, moisture reduction, and organic matter decomposition, leading to increased heat production during biodrying. The top and middle layers have higher temperatures and larger waste weights, while the bottom layer collects water, indicating insufficient microbial activity for biological stability. This is consistent with the findings of Jalil et al. (2016), who used

solid waste samples such as food scraps, papers, plastics, and wood. This denotes a lack of sufficiently large microbial activity required to achieve circumstance biological stability following the biodrying procedure [54]. Lysimeter 3's top and middle layers were cooler due to increased ambient heat transfer, while the intermediate layer's maximum aeration rate of 0.6 m^3/kg/day enhances dry air and heat dissipation.

The temperature fluctuations in layers were explained by the recirculation of large amounts of leachate at a high aeration rate during the heating phase. Sutthasil et al. (2022) investigated the biodrying process of domestic waste in tropical Asian climatic conditions by adding 135 ml/day of water for 15 days. The study observed that the temperature increased from days 1-2 and remained at approximately 30 °C until day 7. Then, the temperature ascended again on day 8, shifting suddenly to the declining phase [45]. Temperatures in all lysimeters dropped until day 5, stabilizing, indicating a certain equilibrium in the biodrying process, possibly suggesting the completion or stabilization of specific stages. Kumar et al. (2008) investigated the impact of leachate recirculation in waste in a bioreactor. They observed that the starting temperature recorded at various depths lowers with leachate recirculation, demonstrating the cooling effect of leachate recirculation [56]. Biodrying increases microbial activity due to high temperatures and rich organic materials. As substrates decrease and microbial populations saturate, decomposition rates stabilize, leading to thermal equilibrium. The optimum temperature range for biodrying in this experiment was found to be 45-60°C, enhancing moisture evaporation and stabilizing organic matter. Temperatures below this range may prolong the process, while temperatures above it can cause excessive heat generation. Based on the results, we can conclude that the experiment can be terminated after day 10 instead of going until day 15.

The temperature differences between waste layers were analyzed in terms of the homogeneous temperature layers. A p-value > 0.05 implies acceptance of the null hypothesis, suggesting equality in mean temperatures among the layers. However, a p-value of ≤ 0.05

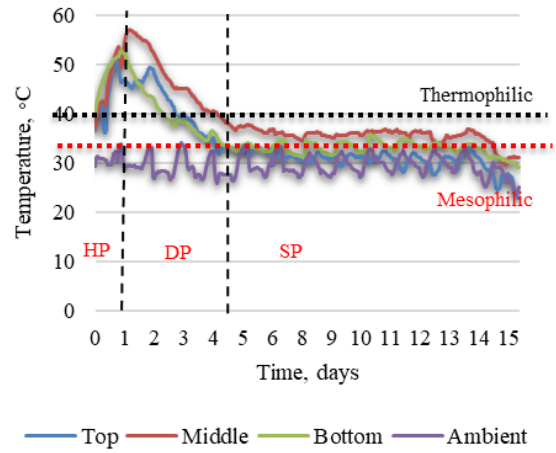

(a)

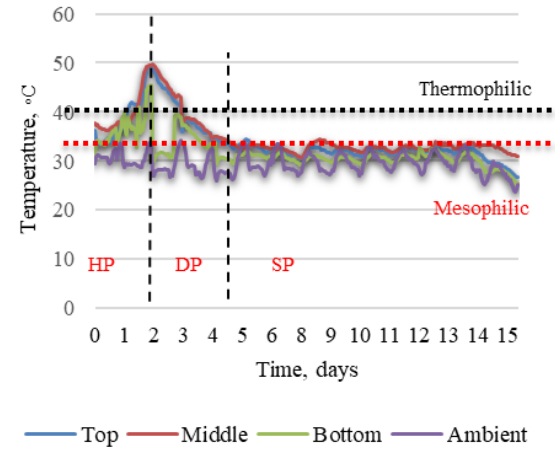

(b)

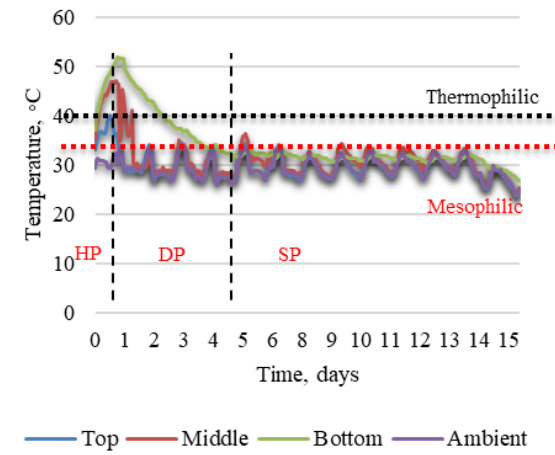

(c)

Figure 3 Temperature evolution during the biodrying process for (a) lysimeter 1, (b) lysimeter 2, and (c) lysimeter 3 (HP, Heating Phase, DP, Declining Phase, SP, Stable Phase)

indicates substantial variations in mean temperatures among the layers. For Lysimeter 1, the temperature differences between the top and bottom layers ($p < 0.05$) were found to be statistically significant in the heating phase. At the same time, there were no differences in the top-middle and middle-bottom layers, showing homogeneity. During the declining phase, the top and bottom layers showed similar temperature distributions ($p = 0.349$). In Lysimeter 2, the temperature between the top and middle layers showed similar temperatures in the heating and declining phases, while statistically significant temperature differences were observed in other layers. However, in Lysimeter 3, there were similar temperatures only in the middle and bottom layers for the heating phase and the top and bottom layers for the stable phase. Regarding the overall phase, the three layers in all lysimeters had p-values lower than 0.05, showing significant temperature differences.

Payomthip P. et al. (2022) found that excessive aeration increases heat dispersion in waste materials' top and middle layers. Meanwhile, continuous aeration achieves effective heat dispersion, resulting in high-temperature uniformity during biodrying. The same scenario can be seen in Lysimeter 3, indicating excessive aeration, while the other lysimeters had uniform temperature distribution.

Temperature integration index

The TI indicates heat accumulation values during the biodrying process were estimated and shown separated in recirculation and non-recirculation periods based on temperatures at the bottom layer because of minimal displacement due to volume reduction. Figure 4 (a) shows the TI value in the recirculation period that Lysimeter 1 had the greatest TI value (2,063 °C), followed by Lysimeters 3 and 2, which had 1,580 °C and 797 °C values, respectively. The TI values were significantly lower than those reported in previous research, with higher TI values associated with longer biodrying periods. Payomthip P. et al. (2022) obtained TI values of 365.6 °C, 346.2 °C, and 318.0 °C after seven days of biodrying, but Shao et al. (2012) reported TI values ranging from 432.0 to 542.0 °C after 14 days of processing [28]. Waste materials can self-heat due to microorganisms and biodrying treatment duration, resulting in lower non-recirculation periods and lower daily temperature evolution.

The TI phase of the three biodrying phases is compared in Figure 4(b). The study revealed that Lysimeter 1 had higher TI values during the heating phase, while Lysimeter 1 and 3 had similar values during the heating and declining phases. The findings of the study associated with the work of Bhatsada et al. (2023) when the highest TI values were found in the declining phase and a lower aeration rate having a higher TI due to the airflow rate conducive to heat accumulation [42]. The higher airflow rate increased heat loss to the exhaust air through ventilation.

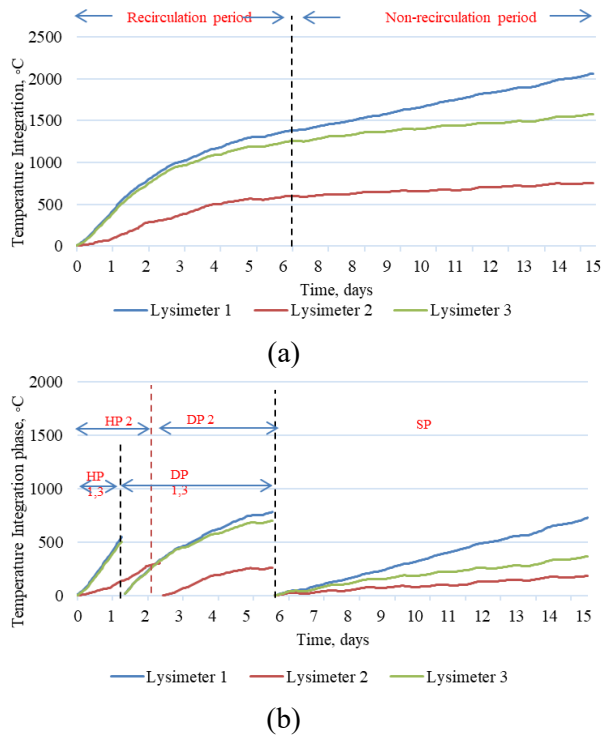

Figure 4 (a)Temperature integration index (b) temperature integration index by phase during the biodrying process (HP, Heating Phase, DP, Declining Phase, SP, Stable Phase, 1= Lysimeter 1, 2= Lysimeter 2, 3= Lysimeter 3)

Gas generation and concentration

Various factors, including waste properties and operating parameters, cause this variation in gas generation. CH_4 and CO_2 are the significant gases produced during anaerobic breakdown. In contrast, aerobic decomposition, which

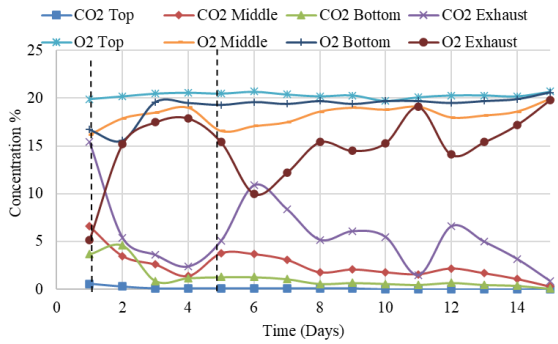

(a)

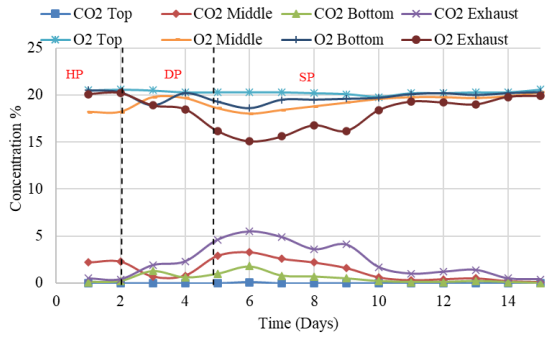

(b)

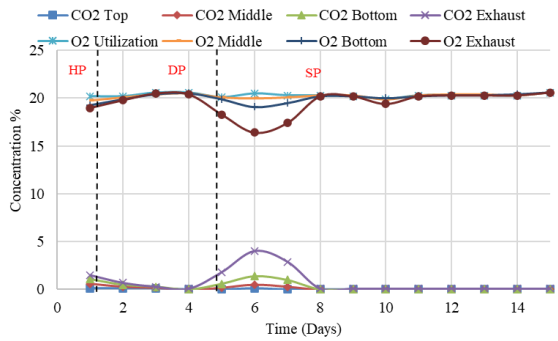

(c)

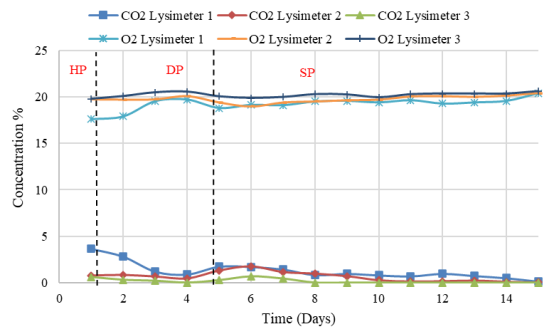

(d)

Figure 5 CO_2 and O_2 concentration during the biodrying process for (a) Lysimeter 1, (b) Lysimeter 2, (c) Lysimeter 3, and (d) their average concentration (HP, Heating Phase, DP, Declining Phase, SP, Stable Phase)

requires O_2, produces primarily CO_2 [57]. The optimum O_2 concentration for aerobic breakdown is between 15% and 20% [51]. Lower O_2 concentrations would result in inefficient, anaerobic conditions; however, the quantities utilized in this study guaranteed that microorganisms had a steady O_2 supply to continue metabolic activity. Figure 5 shows the gas generation and concentration at all lysimeters' top, middle, and bottom levels.

The 15-day experiment in Lysimeter 1 revealed unique CO_2 concentration patterns across vertical layers. The top and middle layers had comparable CO_2 levels, but the lower layer showed a diverging pattern, starting higher on day 1 and decreasing until the end. This scenario is similarly similar to the work by Sutthasil et al., (2022), in which facultative biodegradation was developed at the start of the operation with a sudden increase in CO_2 from day 2-5 during the biodrying process with water addition [45]. The experiment showed low CO_2 levels in Lysimeters 2 and 3, significantly increasing the lower layer. Lysimeter 3 had the lowest CO_2 levels, indicating lesser microbial activity. The overall CO_2 concentration trend showed high levels in the bottom layer for the first two days, but activity remained low when leachate was returned. The recirculation of leachate led to a jump in CO_2 concentrations, progressively falling until the experiment ended. The content of exhaust CO_2 was significantly higher than the ambient CO_2, which is only about 400 ppm. This significant difference indicates that ambient CO_2 has no substantial impact on the results of this study.

Anaerobic breakdown of organic materials produces CO_2, H_2S, and CH_4 gases. Lysimeters show fluctuating CH_4 levels, with Lysimeter 1 having the highest levels, as shown in Figure 6. Low aeration and leachate recirculation increase CH_4 levels. Leachate recirculation resulted in higher degradation of the original C content in the solid waste and increased C emissions in the form of CH_4 [58]. The study confirms Francois et al. (2007) 's findings, revealing increased CH_4 and CO_2 production in columns undergoing leachate recirculation, suggesting accelerating degradation processes [59]. Top et al. (2019) found that leachate recirculation and aeration in

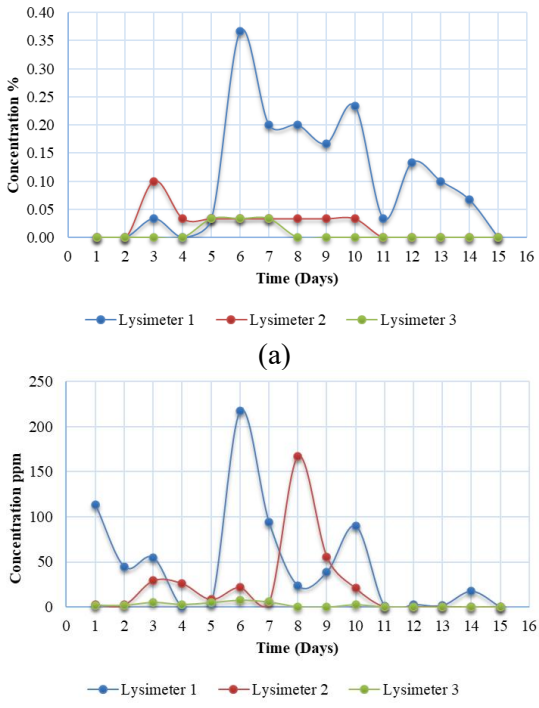

Figure 6 (a) CH_4 and (b) H_2S concentrations during the biodrying process

landfill cells improve gas generation, reduce volume, enhance waste breakdown, and enhance leachate quality [60]. Tran et al. (2014) studied MBT techniques. Recycling of leachates and extra aeration are known to reduce emissions to standard levels in a reasonable amount of time [61]. Anaerobic digestion leachate recycling techniques were investigated by Kusch et al. (2012). The results indicate that intermittent return was not superior to continuous flow, implying that if methanogenesis is the rate-limiting phase, continuous leachate recirculation at start-up may be detrimental [62].

Elevation change and weight loss

The experiment measured waste matrix elevation daily, showing a significant decrease in waste height from days 1-5. Reduced waste height during heating and declining phases led to uniform temperature distribution, enhancing heat penetration and microbial activity, thus optimizing biodrying efficiency. Figure 7 shows the relationship between elevation change and leachate accumulation during biodrying. The maximum waste height reduction was observed on days 1-3 in all lysimeters, with Lysimeter 1 showing the highest reduction of 50.83%. Factors contributing to this decrease include residual heat from earlier stages, leachate recirculation, and compaction due to gravitational force and water filling in waste pores.

The weight of the matrix was only measured on the first and last days of the experiment. The highest weight reduction was seen in Lysimeter 2 (72.39%), followed by Lysimeters 3 and 1 (69.94% and 58.56%). However, the output of leachate was rigorously monitored throughout the period.

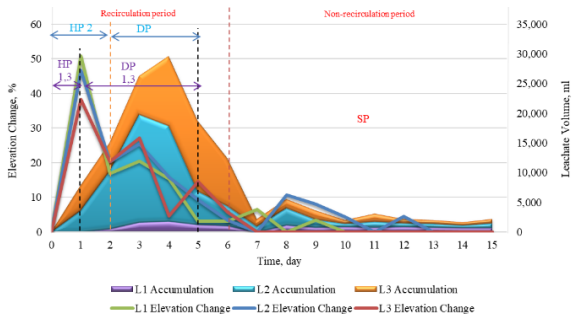

Figure 7 Relationship between elevation change and leachate accumulation during the biodrying process (HP, Heating Phase, DP, Declining Phase, SP, Stable Phase)

Product characteristics

Biodrying involves microorganisms breaking down organic substrate to produce water, gasses, and heat, causing mass loss through biodegradation, moisture removal, and leachate leakage due to waste's higher MC [63]. Furthermore, the gravimetric outflow of water in leachate should be regarded as a parameter influencing wastewater reduction [45].

After the procedure was completed, the final MC and LHV were measured to determine the efficiency of the biodrying process. The initial MC of all lysimeters was around 90.19% by weight. However, following the process, the ultimate MC varied, with decreases of 5.97%, 7.97%, and 2.47% for Lysimeters 1, 2, and 3, respectively, indicating that Lysimeter 2 produced the highest reduction. According to Ngamket et al. (2021), the feedstock should be dried as much as possible with a higher MC reduction to retain the energy content [64]. The LHV of the product for Lysimeters 1, 2, and 3 were 198 kcal/kg, 169.5 kcal/kg, and

134 kcal/kg, respectively. Regarding heating value increases, Lysimeter 1 had the highest increase with 317%, followed by Lysimeters 2 and 3 (257% and 182%). Sutthasil et al. (2022) found that LHV could not be significantly enhanced due to the remaining MC in the waste. The heating value of waste after biodrying for 15 days was lower than its original value in the experiment with water addition during the entire period. As a result, biodrying during water addition was not possible [45]. According to Zhang et al. (2009), organic waste with a high water content and heat from biodegradation is insufficient to evaporate water, making it difficult to lower the water content sufficiently [37].

The biodrying experiments on market waste used three lysimeters with different aeration rates. A comprehensive comparison involving CO_2 concentration, weight loss, leachate volume, and temperature profiles across the lysimeters was conducted. Although biodrying aims to treat market waste using the heat generated from microbial activities under aerobic conditions, excessive moisture addition and returning leachate for six consecutive days hindered the drying mechanism. This leads to sudden heat loss and leachate drainage. Feng et al. (2017) investigated the combination of spray and vertical well (VW) recirculation systems. VW recirculation may not be a viable solution since recycled leachates run directly down to the landfill's leachate collecting system, squandering the recycled leachate. One method for reducing leachate misapplication is to combine a spray VW system with a horizontal leachate flow to allow more MSW to pass through [57].

Lysimeter 1 consistently outperformed in these analyses, indicating its efficiency in the biodrying process. Lysimeter 1 achieved a substantial reduction in MC (5.97%) compared to Lysimeter 2 (7.97%) and Lysimeter 3 (2.47%). The lower aeration rate in Lysimeter 1 appears to have effectively contributed to a more efficient moisture reduction process. The results suggest that the controlled aeration rate in Lysimeter 1 contributed to a more favorable organic content transformation, enhancing the final product's heating value with an LHV increase of 317%. In conclusion, Lysimeter 1, employing the lowest aeration rate, stands out as the most favorable configuration for biodrying market waste based on superior moisture reduction and heating value increase.

Conclusion

This investigation elucidates the efficacy of biodrying in enhancing the LHV and reducing the MC of market waste, focusing on the pivotal role of the aeration rate. Our findings demonstrate that waste abundant in degradable material benefits from biodrying under continuous negative ventilation, where aeration rate optimization is crucial for maximizing biodegradation and thermal efficiency. Initial results showed promising temperature increases due to high organic loads, yet leachate recirculation emerged as a significant impediment to microbial activity, warranting future exclusion from the biodrying process. Significantly, while diminished aeration rates were advantageous for heat preservation, they required careful management to prevent detrimental shifts in moisture and organic material levels. Despite Lysimeter 2 achieving the highest reduction in MC, it fell short of meeting the heating value standards for RDF, highlighting the necessity for further refinement of operational practices. Therefore, future research should refine aeration strategies to comply with industry standards and improve the sustainability of waste management practices. This involves fine-tuning aeration rates and possibly incorporating alternative practices that do not hinder microbial activity. Exploring innovative aeration techniques and their integration with zero-discharge systems could further improve the efficiency of biodrying processes. This study's insights into the interplay between aeration rate and biodrying efficiency pave the way for more effective waste treatment solutions, with implications for environmental sustainability and resource recovery.

Acknowledgement

The authors acknowledge the financial support from The Joint Graduate School of Energy and Environment (JGSEE). This study was supported by the Center of Excellence on

Energy Technology and Environment (CEE), King Mongkut's University of Technology Thonburi (KMUTT), Eastern Energy Plus Co., Ltd., and SCI Eco Services Co., Ltd.

References

[1] Bilgin, M. and Tulun, Ş. 2015. Biodrying for municipal solid waste: volume and weight reduction. Environmental Technology. 36(13): 1691-1697.

[2] Chiemchaisri, C., Chiemchaisri, W., Suksathienwong, P., Boonkongma, P., Towprayoon, S., and Ishigaki, T. 2024. Impact of COVID-19 Pandemic on Greenhouse Gas Emissions from Municipal Solid Waste Disposal of Bangkok Metropolitan. In Proceedings of the Annual Conference of Japan Society of Material Cycles and Waste Management (p. 123). Japan Society of Material Cycles and Waste Management.

[3] Amulah, N. C., Oumarou, M. B. and Muhammad, A. B. 2024. Exergy analysis of waste-to-energy technologies for municipal solid waste management. Environment and Natural Resources. 22(3): 232-243.

[4] Sutthiprapa, S., Wongsaengchan, K., and Wangyao, K. 2023. Effect of Aeration on Bio drying of Municipal Solid Wastes for Utilization as Refuse Derived Fuel (RDF). PTU Journal of Science and Technology. 1(1).

[5] Korai, M. S., Mahar, R. B. and Uqaili, M. A. 2016. Optimization of waste to energy routes through biochemical and thermochemical treatment options of municipal solid waste in Hyderabad, Pakistan. Energy Conversion and Management. 124: 333-343.

[6] Khongkrapan, N., Visvanathan, C., and Cowell, S. J. 2017. Characterization of Municipal Solid Waste in Bangkok. Procedia Environmental Sciences. 38: 118-124.

[7] Esparza, I., Jiménez-Moreno, N., Bimbela, F., Ancín-Azpilicueta, C., and GandíA, L. 2020. Fruit and vegetable waste management: Conventional and emerging approaches. Journal of Environmental Management. 265: 110510.

[8] Bernat, K., Kulikowska, D., Wojnowska-Baryła, I., and Kamińska, A. 2022. Can the biological stage of a mechanical–biological treatment plant that is designed for mixed municipal solid waste be successfully utilized for effective composting of selectively collected biowaste? Waste Management. 149: 291-301.

[9] Thi, N. B. D., Sen, B., Chen, C. C., Kumar, G., and Lin, C. 2014. Food waste to bioenergy via anaerobic processes. Energy Procedia. 61: 307-312.

[10] Popradit, A., Wiangnon, J., Jitrabiab, P., and Pakvilai, N. 2022. Organic fertilizer application using leaf waste according to Maejo engineering method 1. Thai Environmental Engineering Journal. 36(3): 47-54.

[11] Chaiyarit, J. and Intarasaksit, P. 2024. Effect of COVID-19 on Healthcare Waste and Waste-Related the Pandemic: A case study in Nakhon Nayok province, Thailand. Thai Environmental Engineering Journal. 38(1): 21-28.

[12] Bhattarai, K. 2015. Households' willingness to pay for improved solid waste management in Banepa municipality, Nepal. Environment and Natural Resources Journal. 13(2): 14-25.

[13] Suknark, P., Wangyao, K., and Jirajariyavech, I. 2023. From Waste to Resource: An Economic Analysis of Landfill Mining for Refuse-Derived Fuel Production in Five Thai Landfills. Thai Environmental Engineering Journal. 37(2): 1-10.

[14] Wannawilai, P., Poboon, C., and Maneein, J. 2017. Analysis of Solid Waste Management and Strategies for Bangkok Metropolitan. Environment & Natural Resources Journal, 15(2).

[15] Deuja, A., Chuanchit, B., Bunnag, C., Prueksakorn, K., Thongplew, N., Santisukkasaem, U., and Prapaspongsa, T. 2024. Climate Change Mitigation in the Waste Sector: Policies and Measures in Different Countries and the Way Forward for Thailand. Thai Environmental Engineering Journal. 38(1): 37-46.

[16] Thanomnim, B., Papong, S., and Onbhuddha, R. 2022. The methodology to evaluate food waste generation

with existing data in Thailand. Thai Environmental Engineering Journal. 36(1): 1-9.

[17] Ayutthaya, T. K. N., Jakrawatana, N., Nitayavardhana, S., Rakruam, P., and Maneesiri, C. 2021. Evaluation of Alternative Municipal Solid Waste Management Option Towards Circular Economy and Smart City Model. Thai Environmental Engineering Journal. 35(2): 81-91.

[18] Chotiratanasak, J., Vitidsant, T., and Khemkhao, M. 2023. Feasibility Study of Plastic Waste Pyrolysis from Municipal Solid Waste Landfill with Spent FCC Catalyst: 10.32526/ennrj/21/ 202200270. Environment and Natural Resources Journal. 21(3): 256-265.

[19] Mozhiarasi, V. 2022. Overview of pretreatment technologies on vegetable, fruit and flower market wastes disintegration and bioenergy potential: Indian scenario. Chemosphere. 288: 132604.

[20] Tavornpongstid, A., Tripetchkul, S., Towprayoon, S., Chiemchaisri, C., and Wangyao, K. 2022. Biodrying of rejected materials from mechanical separation processes of municipal solid waste for utilization as refuse-derived fuel. Journal of Sustainable Energy & Environment. 13: 59-67.

[21] RenoSam, Rambøll. The most efficient waste management system in Europe: Waste-to-energy in Denmark. published by RenoSam Vesterbrogade 24, 2. sal tv. DK-1620 Copenhagen V. 2016 [Internet]. Available from: https://stateofgreen.com/ files/ download/275.

[22] Itsarathorn, T., Towprayoon, S., Chiemchaisri, C., Patumsawad, S., Phongphipat, A., Bhatsada, A., and Wangyao, K. 2023. The Effect of Aeration Rate and Feedstock Density on Biodrying Performance for Refuse-Derived Fuel Quality Improvement. International Journal of Renewable Energy Development. 12(6): 1091-1103.

[23] Itsarathorn, T., Towprayoon, S., Chiemchaisri, C., Patumsawad, S., Wangyao, K., and Phongphipat, A. 2022. The Situation of RDF Utilization in the Cement Industry in Thailand. 2022 International Conference and Utility Exhibition on Energy, Environment and Climate Change (ICUE). 1-7.

[24] Pudcha, T., Phongphiphat, A., Wangyao, K., and Towprayoon, S. 2023. Forecasting Municipal Solid Waste Generation in Thailand with Grey Modelling. Environment & Natural Resources Journal. 21(1).

[25] Ngamket, K., Wangyao, K., Patumsawad, S., Chaiwiwatworakul, P., and Towprayoon, S. 2021. Comparative Biodrying Performance of Municipal Solid Waste in the Reactor Under Greenhouse and Non-greenhouse Conditions. Quality improvement of mixed MSW drying using a pilot-scale solar greenhouse biodrying system. Journal of Environmental Treatment Techniques. 9(1): 211-217.

[26] Bilitewski, B., Wagner, J., and Reichenbach, J. 2018. Best practice municipal waste management. Information pool on approaches towards a sustainable design of municipal waste management and supporting technologies and equipment. Texte. 40.

[27] Thi, N. B. D., Sen, B., Chen, C. C., Kumar, G. and Lin, C. 2014. Food waste to bioenergy via anaerobic processes. Energy Procedia, 61, 307-312.

[28] Barje, F., Fels, L. E., Hajjouji, H. E., Winterton, P., and Hafidi, M. 2013. Biodegradation of organic compounds during co-composting of olive oil mill waste and municipal solid waste with added rock phosphate. Environmental Technology. 34(21): 2965-2975.

[29] Teerawattana, R., Uyasatian, U., and Nutmagul, W. 2011. Models for higher heating value evaluation of refuse-derived fuel from on-nut composting plant, Bangkok. Environment and Natural Resources Journal. 9(1): 13-23.

[30] Velis, C. A., Longhurst, P. J., Drew, G. H., Smith, R., and Pollard, S. J. T. 2009. Biodrying for mechanical–biological treatment of wastes: A review of process science and engineering. Bioresource Technology. 100(11): 2747-2761.

[31] Sołtysiak, M. and Rakoczy, M. 2019. An overview of the experimental research use of lysimeters. Environmental & Socio-Economic Studies. 7(2): 49-56.

[32] Cai, L., Zheng, S. W., Shen, Y. J., Zheng, G. D., Liu, H. T., and Wu, Z. Y. 2018. Complete genome sequence provides insights into the biodrying-related microbial function of Bacillus

thermoamylovorans isolated from sewage sludge biodrying material. Bioresource technology. 260, 141-149.

[33] Bhatsada, A., Patumsawad, S. and Wangyao, K. 2023. Effect of Negative Aeration Rates on Water Balance in Biodrying of Wet-Refuse-Derived Fuel. Thai Environmental Engineering Journal. 37(1): 55-63.

[34] Shao, L. M., He, X., Yang, N., Fang, J. J., Lü, F., and He, P. J. 2012. Biodrying of municipal solid waste under different ventilation modes: drying efficiency and aqueous pollution. Waste management & research. 30(12): 1272-1280.

[35] Yang, B., Hao, Z., and Jahng, D. 2017. Advances in biodrying technologies for converting organic wastes into solid fuel. Drying Technology. 35(16): 1950-1969.

[36] Francois, V., Feuillade, G., Matejka, G., Lagier, T., and Skhiri, N. 2007. Leachate recirculation effects on waste degradation: Study on columns. Waste Management (Elmsford). 27(9): 1259-1272.

[37] Zhang, D., He, P., and Shao, L. 2009. Effect of pH-neutralized leachate recirculation on a combined hydrolytic–aerobic biopretreatment for municipal solid waste. Bioresource Technology. 100(17): 3848-3854.

[38] Priyambada, I. B. and Wardana, I. W. 2018. Fast decomposition of food waste to produce mature and stable compost. Sustinere (Sukoharjo). 2(3): 156-167.

[39] Hanrinth, W. and Polprasert, C. 2016. Phosphorus Recovery from Co-composting of Faecal Sludge and Fresh Food Market Waste. GMSARN International Journal. 10(2016): 171-174.

[40] Wang, Q., Matsufuji, Y., Dong, L., Huang, Q., Hirano, F., and Tanaka, A. 2006. Research on leachate recirculation from different types of landfills. Waste Management. 26(8): 815-824.

[41] Bilgili, M. S., Demir, A., and Özkaya, B. 2007. Influence of leachate recirculation on aerobic and anaerobic decomposition of solid wastes. Journal of hazardous materials. 143(1-2), 177-183.

[42] Bhatsada, A., Patumsawad, S., Itsarathorn, T., Towprayoon, S., Chiemchaisri, C., Phongphiphat, A., and Wangyao, K. 2023. Improvement of energy recovery potential of wet-refuse-derived fuel through bio-drying process. Journal of Material Cycles and Waste Management. 25(2): 637-649.

[43] Bhatsada, A., Patumsawad, S., Towprayoon, S., Chiemchaisri, C., Phongphiphat, A., and Wangyao, K. 2023. Modification of the Aeration-Supplied Configuration in the Biodrying Process for Refuse-Derived Fuel (RDF) Production. Energies. 16(7).

[44] Bilgili MS, Top S, Sekman E, Varank G., and Demir, A. 2012. Aerobic landfill application in developing countries: a case study. In: International exhibition and conference, 28–31 March 2012, Kharkiv, Ukraine.

[45] Sutthasil, N., Ishigaki, T., Ochiai, S., Yamada, M., and Chiemchaisri, C. 2022. Carbon conversion during biodrying of municipal solid waste generated under tropical Asian conditions. Biomass Conversion and Biorefinery. 13(18): 16791-16805.

[46] Awasthi, M.K., Wang, Q., Wang, M., Chen, H., Ren, X., Zhao, J., and Zhang, Z., 2018. In-vessel co-composting of food waste employing enriched bacterial consortium. Food Technology and Biotechnology. 56(1): 83.

[47] Wijerathna, P. A. K. C., Udayagee, K. P. P., Idroos, F. S., and Manage, P. M. 2024. Formulation of novel microbial consortia for rapid composting of biodegradable municipal solid waste: An approach in the circular economy. Environment and Natural Resources. 22(3): 283-300.

[48] Ma, J., Li, Y. and Li, Y. 2021. Effects of leachate recirculation quantity and aeration on leachate quality and municipal solid waste stabilization in semi-aerobic landfills. Environmental Technology & Innovation. 21: 101353.

[49] Luo, L. and Wong, J. W. 2019. Enhanced food waste degradation in integrated two-phase anaerobic digestion: effect of leachate recirculation ratio. Bioresource technology. 291: 121813.

[50] Calabrò, P. S., Gentili, E., Meoni, C., Orsi, S., and Komilis, D. 2018. Effect of the recirculation of a reverse osmosis concentrate on leachate generation: A case study in an Italian landfill. Waste Management. 76: 643-651.

[51] Payomthip, P., Towprayoon, S., Chiemchaisri, C., Patumsawad, S.,

and Wangyao, K. 2022. Optimization of aeration for accelerating municipal solid waste biodrying. International Journal of Renewable Energy Development. 11(3): 878-888.

[52] Jalil, N. A., Basri, H., Basri, N. E. A., and Abushammala, M. F. 2016. Biodrying of municipal solid waste under different ventilation periods. Environmental Engineering Research. 21(2): 145-151.

[53] Sakulrat, J. 2019. Duration of elevated starting temperature influencing food waste composting. Thai Environmental Engineering Journal. 33(2): 51-56.

[54] Thammabut, P., Tripetchkul, S., Wangyao, K., and Towprayoon, S. 2022. Application of Solar Greenhouse for Nigh-soil Sludge and Yard Waste Co-Composting Process Enhancement. Journal of Sustainable Energy & Environment. 13(2022): 31-37.

[55] Zaman, B., Oktiawan, W., Hadiwidodo, M., Sutrisno, E., and Purwono, P. 2021. Calorific and greenhouse gas emission in municipal solid waste treatment using biodrying. Global Journal of Environmental Science and Management. 7(1). 33-46.

[56] Kumar, A., Reinhart, D., and Townsend, T. 2008. Temperature inside the landfill. Effects of liquid injection. In Global Waste Management Symp., Environment Research and Education Foundation, Raleigh. NC. 1-10.

[57] Feng, S., Cao, B., and Xie, H. 2017. Modeling of leachate recirculation using Spraying–Vertical well systems in bioreactor landfills. International Journal of Geomechanics. 17(7).

[58] Sandoval-Cobo, J. J., Caicedo-Concha, D. M., Marmolejo-Rebellón, L. F., Torres–Lozada, P., and Fellner, J. 2022. Evaluation of leachate recirculation as a stabilisation strategy for landfills in developing countries. Energies (Basel). 15(17): 6494.

[59] Francois, V., Feuillade, G., Matejka, G., Lagier, T., and Skhiri, N. 2007. Leachate recirculation effects on waste degradation: Study on columns. Waste Management (Elmsford). 27(9): 1259-1272.

[60] Top, S., Akkaya, G. K., DemiR, A., Yıldız, Ş., Balahorli, V., and Bilgili, M. S. 2019. Investigation of leachate characteristics in Field-Scale landfill test cells. International Journal of Environmental Research. 13(5): 829-842.

[61] Tran, H., Münnich, K., Fricke, K., and Harborth, P. 2013. Removal of nitrogen from MBT residues by leachate recirculation in combination with intermittent aeration. Waste Management & Research. 32(1): 56-63.

[62] Kusch, S., Oechsner, H., and Jungbluth, T. 2012. Effect of various leachate recirculation strategies on batch anaerobic digestion of solid substrates. International Journal of Environment and Waste Management. 9(1/2): 69.

[63] Park, J. and Lee, D. 2021. Effect of aeration strategy on moisture removal in bio-drying process with auto-controlled aeration system. Drying Technology. 40(10): 2006-2020.

[64] Ngamket, K., Wangyao, K., Patumsawad, S., Chaiwiwatworakul, P., and Towprayoon, S. 2021. Quality improvement of mixed MSW drying using a pilot-scale solar greenhouse biodrying system. Journal of Material Cycles and Waste Management. 23(2): 436-448.

Thai Environmental Engineering Journal Vol. 38 No. 2 (2024) : 35-46
www.eeat.or.th

Impact of Feedstock Density on Biodrying for Enhancing Heat Retention and Moisture Reduction

Eka Wahyanti[1,2], Abhisit Bhatsada[1,2], Sirintornthep Towprayoon[1,2], Noppharit Sutthasil[3], Suthum Patumsawad[4] and Komsilp Wangyao[1,2*]

[1]The Joint Graduate School of Energy and Environment (JGSEE), King Mongkut's University of Technology Thonburi, Bangkok 10140, Thailand
[2]Center of Excellence on Energy Technology and Environment (CEE), Ministry of Higher Education Science, Research and Innovation (MHESI), Bangkok 10400, Thailand
[3]Environmental Health Programme, School of Health Science, Mae Fah Luang University, Chiang Rai 57100, Thailand
[4]Department of Mechanical and Aerospace Engineering, Faculty of Engineering, King Mongkut's University of Technology North Bangkok, Bangkok 10800, Thailand
[*]E-mail : komsilp.wan@kmutt.ac.th

Article History; *Received: 18 July 2024, Accepted: 18 July 2024, Published: 30 August 2024*

Abstract

This study examines the effect of varying feedstock densities on the performance of biodrying processes to enhance waste management efficiency. Three different densities of wet-refuse-derived fuel 3 (wet-RDF3) from Bangkok's On Nut Transfer Station were tested using lysimeter reactors with constant aeration rates (0.6 m^3/kd.day). Results revealed that a moderate density (230 kg/m^3) achieved the highest temperature integration index (7218.01°C) and demonstrated effective moisture reduction and minimal volatile solids consumption. The higher densities improved heat retention and prolonged thermophilic conditions, optimizing the biodrying process. These findings highlight the importance of feedstock density in biodrying, suggesting that optimal density can significantly improve waste drying efficiency and produce better quality refuse-derived fuel. This approach offers a sustainable solution for waste management, particularly in developing countries.

Keywords : Refuse-Derived Fuel; Temperature Integration Index; Waste Management; Thermal Performance; Volatile Solids Consumption

Introduction

The increase in municipal solid waste (MSW) is unavoidable due to population growth, where everyone produces their own. The prediction of waste generation in low-income countries, especially in Asia, accounts for 0.5-0.9 kg/capita/day until 2050 [1]. This condition has a potential environmental problem if the waste generated piles up without further processing. Especially in developing countries, the widespread types for managing waste are open dumping and untreated landfills [2-4]. This is undertaken because the operation is easy and cheap. However, proper sustainable waste management is needed to develop in developing countries.

One reliable waste management method is biodrying technology. In its implementation, biodrying has been applied to produce biodried waste capable of reuse as an alternative fuel [5]. This process aims to produce treated waste with high low heating value (LHV) and low moisture content (MC) and subsequently be applied to the cement industry and power plants. Biodrying is a biological drying process that utilizes microorganisms in the waste to degrade the materials' organic fraction and water content. Biodrying applications have been widely applied in developing countries

because of low operation expenses. In waste management, the types of material commonly used are MSW, kitchen waste, dewatered sludge, and other materials that have organic fractions [6-8].

Several parameters are affecting the biodrying process's performance, such as the initial MC of feedstock, the operational conditions involving aeration rate (AR) supply, and the kind of material used to produce bioheat for evaporation [9-11]. This experiment was set up under different feedstock densities in three trials. Itsarathorn *et al.* (2023) evaluated the relationship between density variations and AR supply in the biodrying of wet-RDF2. According to their findings, 232 kg/m^3 density was the optimal condition at AR0.5, and 250 kg/m^3 was the efficient outcome at AR0.6. Furthermore, Tom *et al.* (2016a) conducted biodrying on mixed MSW with different initial MC and density conditions. This was carried out to evaluate how well biodrying works in waste management to lower the amount and volume of MSW [12].

RDF2, a coarse RDF, involves coarsely shredding or cutting combustible waste. RDF3, a fluff RDF, separates non-combustible components and shreds the remaining waste to a size smaller than 2 inches for 95% of the material. This creates differing air/void ratios, impacting air distribution and temperature retention during biodrying. Despite these differences, no study has ever focused on the effects of varying densities in wet-RDF3. Addressing this gap could optimize biodrying performance by providing crucial insights. This study aims to investigate the effect of different densities and their changing on the biodrying performance based on temperature integration (TI) index and biodrying index (BI) value, which led to the efficient biodried product in LHV and MC during the process.

Methodology

Feedstock Preparation and Analysis

The feedstock used in this experiment was wet-RDF3 from On Nut Waste Transfer Station, Bangkok, Thailand. A wet-RDF3 is a kind of shredded RDF2, with the air classifier, magnetic separator, and fine shredder primarily consisting of plastic [13]. The wet-RDF3 from the stockpile was sampled for 1.5 kg to measure the chemical properties before the biodrying (the same treatment as the product after biodrying). Furthermore, a thermogravimetric analyzer was used to measure MC and volatile solid (VS) content in the feedstock and biodried product following the ASTM D7582 standard. The LHV also was analyzed using a bomb calorimeter according to the ASTM D2015 standard. Three different conditions were set up in this experiment through lysimeter reactor, designated as L1, L2, and L3, respectively.

This experiment was set up with a constant AR supply and various densities. The constant AR of 0.6 m³/kg.day was chosen based on previous findings where different ARs (0.2, 0.4, and 0.6 m³/kg.day) were tested. The 0.6 m³/kg.day rate produced the best results, yielding the highest low heating value (LHV) and lowest moisture content (MC) [14, 15]. For this experiment, the objective was to investigate the effect of variations in initial feedstock density on biodrying performance while maintaining a constant AR. The initial condition during the experiment is shown in Table 1.

Table 1 Initial condition of feedstock

Conditions	L1	L2	L3
Density (kg/m^3)	208.86	230.00	250.00
Weight (kg)	50.1	55.8	60.1
High (m)		1.20	
AR (m^3/kg.day)		0.6	
MC (%)		47	
LHV (kcal/kg)		3,119	

Lysimeter Description

The biodrying experiment used three lysimeters, with each being 1.5 m high, 0.5 m deep, and 0.5 m wide. A perforated metal plate was placed above the ventilation pipe at the bottom side of the reactor to help material distribute air. The ventilation pipe, condensation pipe, and centrifugal pump to provide airflow were installed at the system's base. A U-trap pipe was installed at the legs of the lysimeter to collect leachate. The gas measuring inside the system was recorded through the pipe. More

details on the installation location and design are shown in Figure 1.

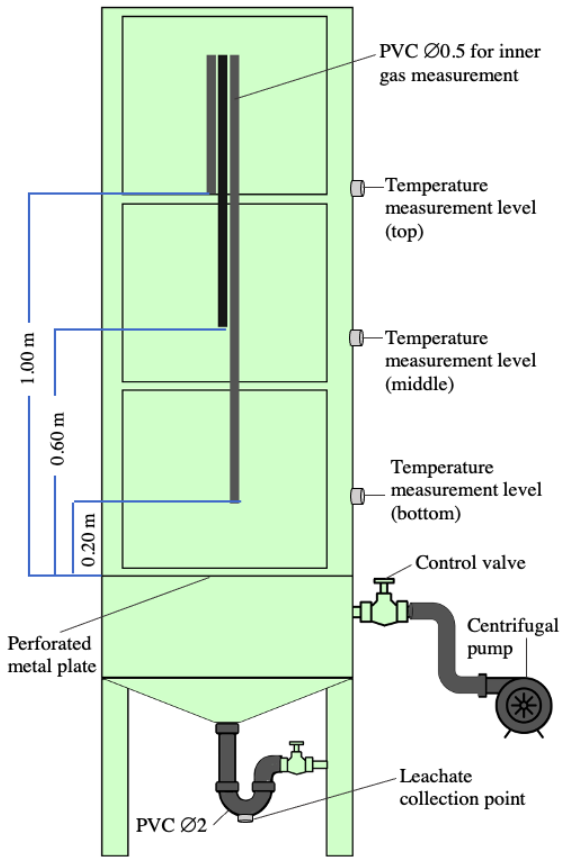

Figure 1 Schematic design of lysimeter

Experimental Monitoring

The temperature was measured using a thermocouple connected to cables at three locations (Figure 1), and another probe was placed in the surrounding environment to record the ambient temperature. The temperature data was recorded hourly using a midi-data logger (Graphtec GL220). Those data were subsequently used to determine the temperature integration (TI) index. The TI index can be calculated using the following equation:

$$\mathbf{TI} = \sum_{t=1}^{n}(t_s - t_{amb})\ x\ \Delta t \qquad (1)$$

Where t_s is sample temperature at time t (ºC), t_{amb} is ambient temperature at time t (ºC), and Δt is the difference between the measured time points.

A hoist and a digital scale were used to measure daily weight reduction. The following equation describes the weight loss:

$$\textbf{weight loss}\ (\%) = \frac{\Delta w}{w_i}\ x\ 100 \qquad (2)$$

Where Δw is the change in weight of the dried product relative to the initial material weight (kg) and w_i is the initial material weight (kg).

Gas measurements were taken using a Biogas 5000 portable gas analyzer (Geotech, UK). Carbon dioxide (CO_2) and oxygen (O_2) levels were measured daily in the morning during the biodrying process. For CO_2 exhaust gas measurement, the value was determine using information from direct gas measured by Biogas 5000, and with the following equation:

$$\Sigma CO_{2\ exhaust} = Av\ x\ A\ x\ CO_{2\ measurement} \qquad (3)$$

Where Av is the air velocity (m/s), A is the cross-sectional area of the pipe (m^2), and CO_2 measurement is the value recorded by the Biogas 5000 instrument (%).

O_2 utilization refers to the amount of O_2 microorganisms required to degrade organic matter. The amount of O_2 utilization is based on the total mass remaining on the day of each measurement, as it relates to the remaining nutrient supply needed by the microbes. The calculation method to determine O_2 utilization (volume in m^3) was adopted by Contreras-Cisneros (2021) in the following equation:

$$\Sigma O_{2\ u} = \left(\frac{O_{2amb} - O_{2ex}}{O_{2amb}}\right) x\ V \qquad (4)$$

Where O_2amb is the O_2 concentration in the surrounding environment (%), O_2ex is the oxygen concentration in the exhaust pipe recorded by the Biogas 5000 portable gas analyzer (%), and V is air volume in the day (m^3). Air volume can be determined using the following equation:

$$V = \frac{AR}{Wt} \qquad (5)$$

Where AR is the exact aeration rate flowed based on air velocity when the monitoring daily (m^3/kg.day), and Wt is the waste mass at the monitoring (kg).

For biodrying index (BI) determination, parameter used was MC reduction and VS consumption. To find VS consumption was adopted method from Li *et al.* (2022) in the following:

$$VS\ consumption\ (\%) = \frac{\Delta VS}{VS_i} x100 \qquad (6)$$

Where ΔVS is subtraction VS between initial and final, and VS_i is initial VS.

Statistical analysis

The correlation test was used to determine the relationship between two parameters, and single-factor ANOVA was used to analyze the variance in temperature with a confidence level of 95% ($p<0.05$). Both statistical tests were conducted using Microsoft® Excel for Mac Version 16.77.1 Software.

Results and Discussion

Temperature Profile

Temperature evolution

Temperature is a parameter that indicates microbial activity in degrading organic matter. The heat produced is a byproduct of microbial metabolism–heat metabolic. The highest temperature achieved by L1 on day 3 of the experiment was 65°C. This maximum temperature was reached more quickly than in other trials. A sudden significant drop in temperature (with a difference of 20°C) occurred on day 4. After that, it entered the stable phase at a moderate temperature and was maintained under thermophilic conditions, this study used 50°C as the starting point for the shift from the mesophilic to the thermophilic phase [4], in the middle layer and mesophilic conditions in the top and bottom layers. The maintaining temperature occurs from day 5 to 12. The temperature evolution trend in L1 is shown in Figure 2(a).

In L2, the highest temperature was obtained in the bottom layer from day 1 to 6. Upon entering the HP, the middle layer showed the highest temperature trend. The maximum temperature reached was 74°C in the middle layer and occurred for two days (days 8 and 9). If the heat in the system is a byproduct of aerobic degradation, then in L2, microbial growth occurs maximally from day 7 to 12. The temperature evolution trend in L2 is shown in Figure 2(b).

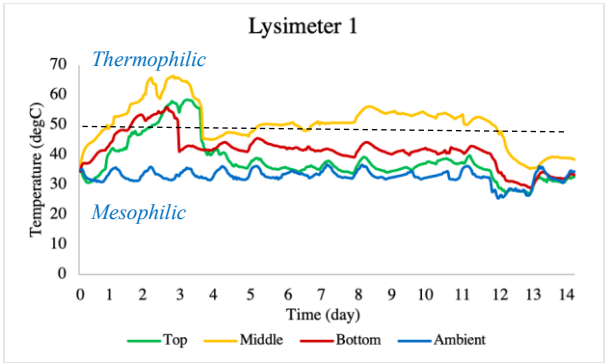

(a)

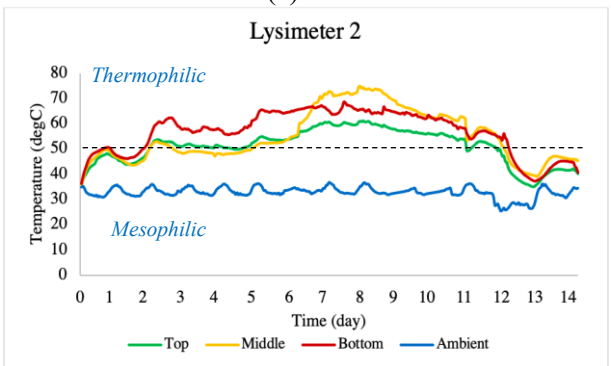

(b)

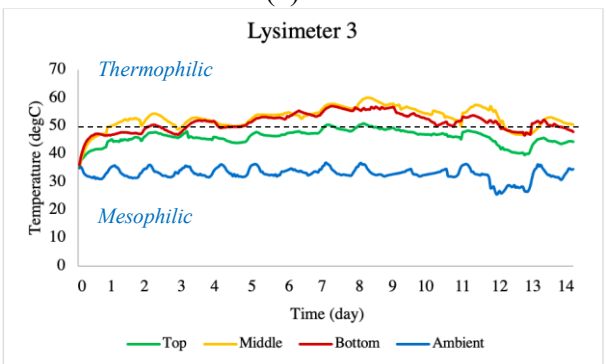

(c)

Figure 2 Temperature evolution trend in each layer of (a) L1, (b) L2, and (c) L3

Meanwhile, in L3, the temperature in the middle and bottom layers was extremely high. The remaining maintained temperature was also under thermophilic conditions from day 3 to 11. The temperature range during this time was 49.5-47.9°C, with a slight decrease in temperature (to 53°C) entering day 12. The temperature evolution trend in L3 is presented in Figure 2(c). This trial had almost no declining

phase, suggesting that aerobic degradation still occurred and was not completed by day 14.

Similar findings were reported by Tom *et al.* (2016b), who conducted biodrying experiments of mixed solid waste with different densities (density Case A > Case B) under the same airflow supply. They reported that the temperature profile in Case A reached a higher maximum temperature (65°C < T < 70°C) compared to the maximum temperature in Case B (55°C < T < 60°C). Based on physical assessments, this occurred because a high density can hinder the system in the reactor from returning to the surrounding temperature [16]. Based on the availability of organic matter in the waste, the highest temperature can be achieved if degradation continues. This was reported by Hao and Jahng (2019), who analyzed the levels of organic substances in bulking agents during the biodrying of dewatered sludge. Degradation occurs when volatile solids are consumed, with the degradation ability ranked as lipid > hemicellulose > protein. The highest temperature obtained in the experiment with bulking agents contained more lipids and hemicellulose, reached 70°C, and was maintained at around 65°C until the final experimental day. This result indicated a higher degradation process because lipids and hemicellulose are more easily degraded than proteins [17].

Temperature integration index

The largest cumulative TI value was obtained from the L2, which was 7,218.01°C. This temperature achievement was significantly higher compared to the other two trials. The next most considerable TI value was in the L3 experiment, which reached 5,803.67°C. The lowest one obtained in L1 is 3,524.43°C. The higher TI value obtained from the higher density trial due to the system maintaining thermophilic conditions for longer than L1 during the process. The L1, which has the lowest density, made it easier to escape the temperature from the system, so the temperature recorded in the system was relatively low. The cumulative TI trend in the whole process is presented in Figure 3(a), and the TI index by phase is shown in Figure 3(b).

From the three separate phases of TI, all trials show the maximum TI value obtained during HP. This was caused by the longer retention time and heat produced within metabolic reaction considering material's type. Trial L2 with moderate density achieved greatest value. A similar finding was found in Itsaratorn *et al.* (2023), which revealed that moderate density during biodrying of wet-RDF2 for five days obtained the highest TI value at 2,108.10°C. Their TI value is smaller than this experiment's because of the different retention times during biodrying. Furthermore, Payomthip *et al.* (2022) reported that the highest TI reached 365°C during the biodrying of shredded MSW over seven days. Their higher TI obtained was consistent with the temperature evolution.

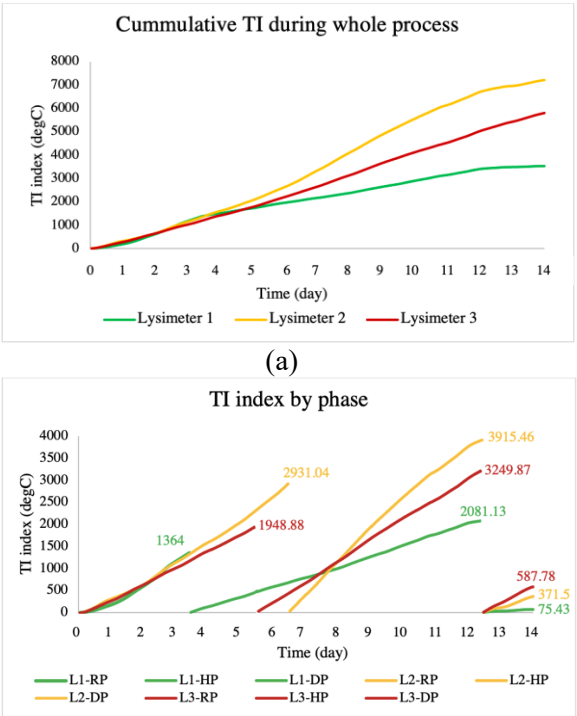

Figure 3 Cumulative TI index of (a) whole process, and (b) by phase

The effective condition to show biodrying performance based on the TI index was in moderate to high obtained value. Suppose the concept of biodrying is utilized as much as heat generated from the degradation of organic materials. In that case, a high TI value indicates maintaining control during the process. However, each trial was set up in this experiment with different density and mass-loaded conditions. So, one of the rationales that the higher-density trials have a greater TI value

is that the denser waste and the capability to provide more organic to degraded. Yuan *et al.* (2019) conducted that biodrying with additional bulking agents causes the highest TI value due to material density. The increasing density effect decreases free air space and leads to low heat loss in the system [8].

CO_2 Production

The trial with higher densities showed significant value of CO_2 levels in the inner gas measurement. The CO_2 levels increased on day 2 in the L1 trial, corresponding to the maximum temperature achieved during that period. The CO_2 concentration then decreased on day 3 and continued to decline until the end of the experiment. The process in L1 was finished when the experiment stopped. Meanwhile, the L2 and L3 produced more CO_2 than the L1. This condition might occur because the availability of organic fraction was higher along with increased density. Reports show that denser waste can provide more organic and lead to more VS consumption [8]. The CO_2 production trend in each experiment is presented in Figure 4.

A similar finding was reported by Itsarathorn *et al.* (2023), who conducted biodrying experiments on RDF2 with different densities (232, 250, 270 m^3/kg) under the same AR supplied (0.6 m^3/kg/day). His experiments found that the largest CO_2 was produced by experiments with a density of 270 m^3/kg. Furthermore, Sutthasil *et al.* (2022) revealed that the availability of more organic fractions is a factor that influences the speed of CO_2 production in aerobic degradation because organic acts as a substrate that microorganisms digest. This was very likely in this study when an increase in feedstock density caused the amount of waste loaded into the lysimeter reactor to increase, and a large amount of waste increased the availability of organic material [18].

O_2 Utilization

The representation shows how much O_2 is utilized during aerobic degradation by the microorganism. The calculation of O_2 utilization is necessary since O_2 is a crucial component in the success of aerobic degradation. This compares the volume of O_2 used and CO_2 produced [19]. In some literature, O_2 utilization is

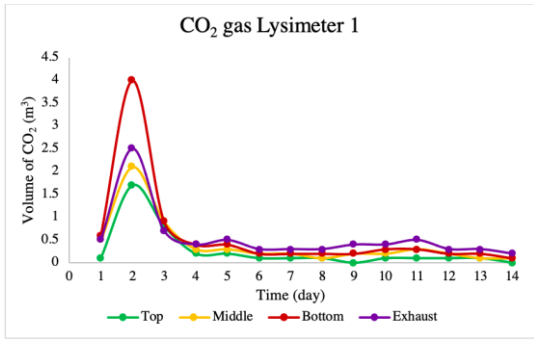

(a)

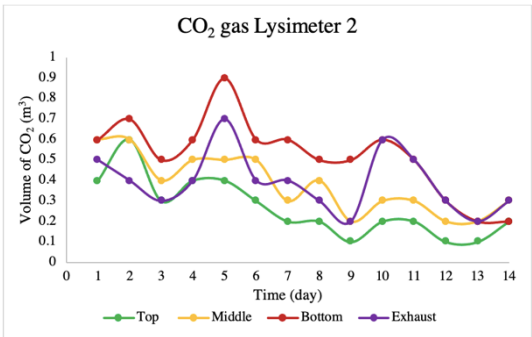

(b)

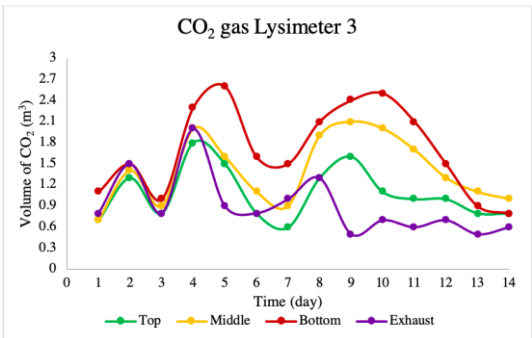

(c)

Figure 4 CO_2 production in each layer of (a) L1, (b) L2, and (c) L3

closely related to the amount of CO_2 produced during biodrying. However, in this experiment, there was a very weak correlation in one of the three phases based on temperature evolution. The correlation between O_2 utilization and CO_2 production is shown in Table 2, and the trend of O_2 utilization is shown in Figure 5.

As an optimum condition for aerobic degradation, which occurs under thermophilic, the O_2 should be uptake high due to thermal assistance when the system enters HP, which can stimulate microbial growth more than natural thermal effects. Increased biogenic heat can reduce external heat energy consumption.

Table 2 Correlation of O_2 utilization and CO_2

Trial	RP		HP		DP	
	r	Stdv.	*r*	Stdv.	*r*	Stdv.
L1	0.99	±4.70	0.34	±1.53	0.23	±0.80
L2	0.55	±2.92	0.81	±2.06	0.97	±1.69
L3	0.93	±7.72	0.74	±3.23	0.36	±2.92

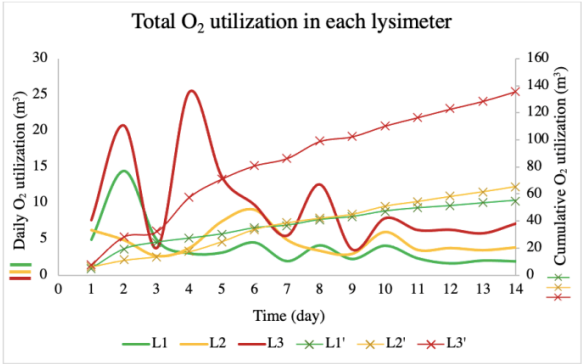

Figure 5 Total O_2 utilization during biodrying

For L1, the trend was consistent with CO_2 production and maximum temperature reached to describe the degradation condition. Özbay *et al.* (2021) revealed the significance of O_2 in aiding aerobic microbes during biodrying, which enhances the effectiveness of the drying process. This highlights the crucial role O_2 plays in establishing suitable conditions for microbial action and the decomposition of organic matter [7]. Furthermore, Payomthip *et al.* (2022) monitored O_2 levels during the biodrying process and highlighted the significance of this parameter in understanding the dynamics of biodrying. However, for L2 and L3, the O_2 trend did not always match the CO_2 production. It may occur because of the density effect. Huiliñir *et al.* (2020) measured the behavior of dynamic respiration index (DRI) on the dewatered secondary sludge biodrying, which is represent the O_2 consumption for enhance microbial activity. Higher DIR values were favorable conditions for microbial growth, which was similar to this experiment and related to organic mass in the system [20].

Weight Loss and Density Changes

Weight loss is described as the MC successfully evaporating and the organic fraction being broken down into gases–the water removal phenomenon. In the L1 trial, the maximum weight loss was achieved on day 3. This trend followed the maximum temperature produced in the system and CO_2 production in the inner gas. The L2 trial reached a maximum on days 5 to 7, during which the HP and the highest CO2 production were entered. While in the L3 trial, the maximum weight loss occurred on day 4, and the greater CO_2 production occurred. Daily weight loss in each trial is shown in Figure 6.

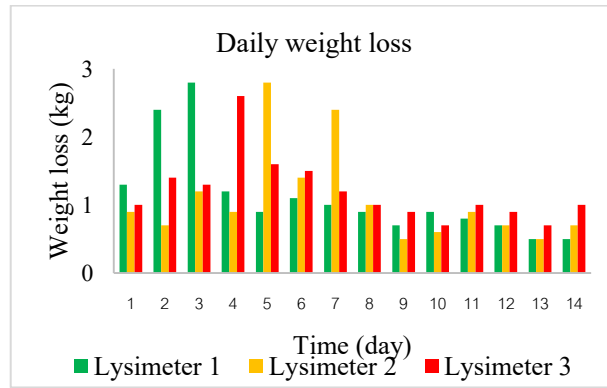

Figure 6 Trend of daily weight loss

Besides evaporation, which reduces the weight and volume of waste, in many cases of biodrying, especially for waste rich in organics, the leachate production also influences the weight loss. This occurs because water vapor condenses after it reaches its maximum temperature and turns into leachate. This study implements the negative ventilation system (suction airflow) to force more leachate. However, this study's cumulative leachate production was less than 1 L for each trial. The total volume of leachate produced in L1, L2, and L3 were 640, 169, and 450 mL, respectively. Bhatsada *et al.* (2023) revealed that water removal mainly occurs due to bioactivity, and the water phase changes as water vapor evaporation during biodrying. In their experiment, the low leachate generation caused leachate to be a nominal proportion of the water balance in the system with less removal [21]. Bosilj *et al.* (2023) experimented on the sample with a higher initial MC, which led to a more significant overall mass loss. Most samples had a mass loss that occurred on

day 2 of the experiments. The rate then stabilized to a lower level (around 0.3-0.4 kg/day). However, this experiment showed that maximum loss occurred on day 4. This happened due to variations in organic content compared to [11] study.

Density changes were obtained through daily weight loss and waste height reduction measurements. Density affects the free-air space (FAS) in the waste pile in the reactor. This FAS affects the distribution of heat resulting from the degradation of organic matter, which subsequently affects the water vapor evaporation rate to leave the system. Higher density limits FAS availability and leads to higher temperatures being trapped in the waste pile [8]. Due to enhanced FAS, typical bulking agents support organics degradation and water migration [22]. Their results showed that suitable feedstock, with appropriate bulk density, affects bio-heat generation, extracellular polymeric substances (EPS) release, and potentially contributes to the maturity of the biodried product.

For this experiment, the density changes between the initial and final occurred not too much in all trials. The final percentage changes in L1, L2, and L3 were 6.64, 3.22, and 3.94%, respectively. The initial density in L1, L2, and L3 was 195, 226, and 240 kg/m^3. This relatively small change in density can be attributed to the nature of RDF3, which primarily consists of plastic. As the moisture content in RDF3 decreases, the plastic components tend to dry out and may expand slightly. This behavior is different from wet plastics, which can become compact when they retain moisture. The reduction in moisture allows RDF3 to retain some of its bulk, preventing significant compaction and leading to only minor changes in density throughout the biodrying process. The trend of daily density change is shown in Figure 7.

Based on the trend in Fig. 7, each trial has a change in density increase. L1 and L2 trials showed an increase in the early stages of the biodrying process. Meanwhile, the L3 trial showed an increase after day 5. L2 and L3 had the same density on days 4 to 5, where both trials entered a phase of maintaining high temperatures during that time. Unlike trial L1, the significant decrease in density occurred until the last day of the process. This can be stated as consistent with the trend of temperature changes, in which L1 reached its maximum temperature only for three days of the experiment.

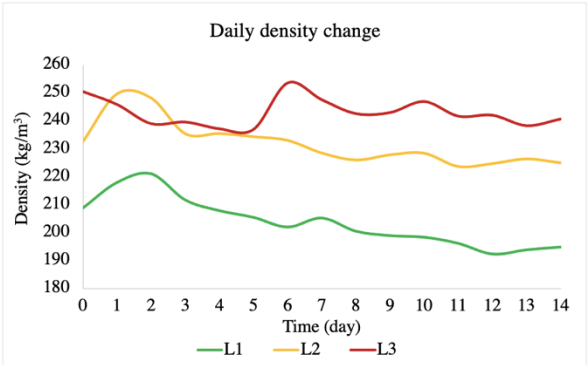

Figure 7 Daily density change

Despite the density changes, the trial with a higher initial density still resulted in a higher final density in the experiment. This can be explained by the fact that FAS critically affects the high-temperature resistance experienced by L2 and L3. The degradation process in L3 might have been still undergone until the last day of biodrying stopped. The temperature and CO_2 production were also still relatively high in L3.

Moisture Content and Low Heating Value

The moisture reduction is related to the effectiveness of evaporation of water molecules during the biodrying process. Suppose numerous water molecules are successfully released from the system. In that case, the moisture reduction will also be considerable, positively impacting the final LHV value obtained. In this second experiment, the highest moisture reduction was achieved in L1, with a final MC value reaching 15%. Daily moisture reduction has been investigated in this study, with the manual calculation adopted from Ham (2020). The detailed pathways equation is shown in Table 3, and the trend of daily moisture reduction in each trial is shown in Figure 8. Xu *et al.* (2023) highlighted that optimal nutrient utilization (C/N ratio) promotes microbial growth, leading to faster decomposition of organic matter and the release of water. This study emphasizes the impact of density on heat retention, which can significantly influence the

moisture reduction rate. However, optimizing the biodrying process affects microbial degradation, producing high-quality biodried products with fine LHV [23].

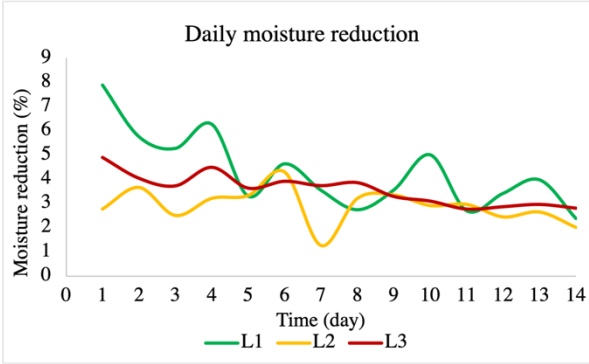

Figure 8 Daily MC reduction in each trial

The declining graph in L1 was very significant until the last day of the biodrying process. As cumulative, the MC percentages for L1, L2, and L3 were 68, 43, and 55%, respectively. This final MC value affected the LHV obtained, where L1 had the largest LHV. If we return to the initial meaning of biodrying, which is a biological drying process that utilizes metabolic heat from aerobic degradation [4]. So, the sufficient AR supply is a factor that enhances the degradation. However, if excessive aeration is intended to accelerate the process, the drying that occurs may not be biodrying. This was what might have happened in the L1 trial. Looking back at the cumulative TI and temperature evolution, a significant temperature decrease occurred rapidly on day 3. In addition, CO_2 production also sharply decreased during that period. The drying process from the excess AR supply subsequently helps significantly decrease MC and the large final LHV. The LHV values for each experiment are presented in Table 4.

Some studies mentioned the relationship between MC and LHV. Sagala *et al*. (2018) reported that the final LHV of RDF can reach 3,000 kcal/kg or more with an MC below 20%, which indicates that the drying process can significantly enhance the LHV value of RDF by reducing its MC. Furthermore, Dharmasyah (2023) reported that processed fluff RDF presented an LHV of 4,708 kcal/kg with a low MC of 2.1%, which confirms the potentially high LHV values that can be achieved in RDF when the MC is effectively reduced.

Biodrying Index

This parameter is related to water losses and volatile solid (VS) removal. The amount of BI is closely related to the material and the operational condition. A higher BI value indicates that the experiment is the most effective for removing water because the system can escape as much water vapor as possible with measly organic consumption. This condition is good when the system preserves more carbon, which would affect the final LHV obtained. Normally, materials with high organic content undergo significant VS consumption during degradation [24, 25]. Li *et al.* (2022) reported that VS consumption of kitchen waste during biodrying was 26.26%, with an MC reduction of 34.47%. Furthermore, Wang *et al.* (2024) reported that VS consumption of biodrying sludge was 8.79%, Similar to this experiment with unrich organic matter, the VS consumption is not over 10%. The VS information before and after biodrying is shown in Table 5.

Table 3 Equations for daily moisture reduction [26]

Contents	Symbols	Unit	Equations	Remarks
Water vapor pressure	pv	Pa	$pv = RH\ x\ pvs$	RH = direct humidity measured
Saturated water vapor pressure	pvs	Pa	$pvs = 6.1078\ x\ 10\text{^}\frac{7.5\ x\ T}{T + 237.3}$	T = temperature (°C)
Specific humidity	SH	%	$SH = \frac{0.622\ x\ pv}{Ptotal - pv} x100$	P total = standard atmosphere, 101,325 Pa
Estimated dry feed mass	m_d	kg	$m_d = 1 - \left(\frac{RH}{100}\right) x\ m_f$	m_f = daily mass measured
Daily moisture reduction	ΔMC	%	$\Delta MC = SH\ x\ m_d$	

The greatest BI value for this study was obtained from the L1. Meanwhile, the largest VS consumption was obtained from L2. The availability of organic matters in the feedstock influenced big or small amounts of VS consumption. As mentioned in the CO_2 production section, higher-density trials have denser waste, which provides more organic availability. It was very reasonable that the less VS consumed, the greater the BI value produced [27-29]. This finding was reinforced by Payomthip *et al.* (2022), who reported that the highest BI value was reached with the maximum moisture removal (65.6%) and lowest VS consumption (2.87%). That condition obtained the greatest LHV (4,938 kcal/kg). Furthermore, Cao *et al.* (2024) reported the highest BI value from a trial that has the highest LHV (5,843 kJ/kg) and maximum moisture removal (61.71%) simultaneously. Quan *et al.* (2023) reported that a biodrying sludge pile exhibited a significantly higher BI due to more efficient water removal and less VS consumption. Similarly, the L2 condition provided high-temperature evolution in this experiment, resulting in maximum VS loss.

Table 4 LHV and MC changing after biodrying

Trial	LHV (kcal/kg)		Change (%)	MC (%)		Change (%)
	Before	After		Before	After	
L1		6,020	(+) 93		15	(-) 68
L2	3,119	4,931	(+) 58	47	27	(-) 43
L3		5,628	(+) 80		21	(-) 55

Table 5 Information on VS before and after biodrying

Trials	Volatile solid (%)		ΔVS	VS consumption (%)	MC reduction (%)	BI value
	Initial	Final				
L1		43.42	6.14	12.0	68	5.67
L2	49.4	40.96	8.60	17.4	43	2.47
L3		41.81	7.78	15.7	55	3.50

Conclusion

This study demonstrated that varying feedstock densities significantly influence the efficiency of the biodrying process. Among the tested densities, a moderate density (230 kg/m³) achieved the highest temperature integration index (7218.01°C). However, exhibited superior moisture reduction and minimal volatile solids consumption was reached in the lowest density trial (208.86 kg/m³). These findings highlight the critical role of feedstock density in optimizing the biodrying process, suggesting that careful density adjustment can enhance heat retention and extend thermophilic conditions. Consequently, this leads to more efficient drying and higher-quality refuse-derived fuel production. The results of this study provide valuable insights for developing sustainable waste management strategies, particularly in developing countries where efficient and cost-effective solutions are crucial. Future research should explore the long-term impacts of different feedstock compositions and densities on biodrying performance and evaluate the economic feasibility of large-scale applications. By continuing to refine these methods, the potential for significant environmental and economic benefits in waste management can be realized.

Acknowledgement

The authors acknowledge the financial support from The Joint Graduate School of Energy and Environment (JGSEE). This study was supported by Center of Excellence on Energy Technology and Environment (CEE), King Mongkut's University of Technology Thonburi (KMUTT), Eastern Energy Plus Co. Ltd. and SCI Eco Services Co. Ltd.

References

[1] Khan, A. H., Lopez-Maldonado, E. A., Khan, N.A., *et al.* 2022. Current solid waste management strategies and energy

recovery in developing countries - State of art review. Chemosphere, 29(3): 133088.

[2] Shovon, S. M., Akash, F. A., Rahman, W., *et al.* 2024. Strategies of managing solid waste and energy recovery for a developing country – A review. Heliyon, 10(2): e24736

[3] Ferronato, N. and Torretta, V. 2019. Waste Mismanagement in Developing Countries: A Review of Global Issues. Inter J Environ Res Public Healt, 16(6): 1060.

[4] İnce, E., İnce, M., and Önkal E. G. 2017. Comparison of thermophilic and mesophilic anaerobic treatments for potato processing wastewater using a contact reactor. Glob. Nest J, 19: 318-326.

[5] Zaman, B., Hardyanti, N., Purwono, P., Suryantara, A. R., Putri, N.S. and Failusuf, T.A.M. 2023. Application of biodrying with hot air aeration system to process solid waste into rdf. IOP Conference Series: Earth and Environmental Science, 1268(1): 12034.

[6] Guerra-Gorostegi, N., González, D., Puyuelo, B., *et al.* 2021. Biomass fuel production from cellulosic sludge through biodrying: Aeration strategies, quality of end-products, gaseous emissions and techno-economic assessment. Waste Management, 126: 487-496.

[7] Özbay, İ., Özbay, B. and Akdemir, U. 2022. Biodrying for fuel recovery from sewage sludge: An integrated evaluation by ultimate and proximate analyses. Environmental Progress and Sustainable Energy, 41(1).

[8] Yuan, J., Li, Y., Wang, G., *et al.* 2019. Biodrying performance and combustion characteristics related to bulking agent amendments during kitchen waste biodrying. Bioresourch Technology, 284: 56-64.

[9] Contreras-Cisneros, R.M., Orozco-Álvarez, C, Piña-Guzmán, A.B., *et al.* 2021. The Relationship of Moisture and Temperature to the Concentration of O_2 and CO_2 during Biodrying in Semi-Static Piles. Processes, 9(3).

[10] Pecorini, I., Bacchi, D. and Iannelli, R. 2020. Biodrying of the Light Fraction from Anaerobic Digestion Pretreatment in Order to Increase the Total Recovery Rate. Processes, 8(3).

[11] Bosilj, D., Petrovic, I., Hrnic, N. and Kaniski, N. 2024. Biodrying of municipal solid waste–correlation between moisture content, organic content, and end of biodrying process. Environmental Science and Pollution Research, 1-14.

[12] Tom, A. P., Haridas, A. and Pawels, R. 2016a. Biodrying Process Efficiency: Significance of Reactor Matrix Height. Procedia Technology, 25: 130-137.

[13] Itsarathorn, T., Towprayoon, S., Chiemchaisri, C., *et al.* 2023. The Effect of Aeration Rate and Feedstock Density on Biodrying Performance for Refuse-Derived Fuel Quality Improvement. International Journal of Renewable Energy Development, 12(6): 1091-1103.

[14] Dharmasyah, D.F., Anasstasia, T.T., Utami, A., Widiarti, I.W. and Alfiani, O.D. 2023. Inorganic Waste Management and Energy Potential: Implications for Agricultural Sustainability. IOP Conference Series: Earth and Environmental Science, 1242(1).

[15] Sagala, G., Kristanto, G.A., Kusuma, M.A. and Rizki, S. 2018. Assessment of Municipal Solid Waste as Refuse Derived Fuel in the Cement Industry. International Journal on Advanced Science Engineering and Information Technology, 8(4).

[16] Tom, A. P., Haridas, A. and Pawels, R. 2016b. Biodrying process: A sustainable technology for treatment of municipal solid waste with high moisture content. Waste Management, 49: 64-72.

[17] Hao, Z. and Jahng, D. 2019. Variations of organic matters and extracellular enzyme activities during biodrying of dewatered sludge with different bulking agents. Biochemical Engineering Journal, 147: 126-135.

[18] Sutthasil, N., Ishigaki, T., Ochiai, S., Yamada, M. and Chiemchaisri, C. 2022. Carbon conversion during biodrying of municipal solid waste generated under

tropical Asian conditions. Biomass Conversion and Biorefinery, 13: 16791-16805.

[19] Ma, J., Zhang, L., Mu, L., Zhu, K. and Li, A. 2019. Energetic enhancement of thermal assistance in the cooling stage of biodrying by stimulating microbial degradation. Waste Management, 89: 165-176.

[20] Huiliñir, C., Leiva, E., Stegmaier, F., Castillo, A., Cottet, L. and Montalvo, S. 2020. Biodrying of dewatered secondary sludge: behavior of dynamic respiration index (DRI) and energy release under different operating conditions. Journal of Chemical Technology & Biotechnology, 95(1): 94-101.

[21] Bhatsada, A., Patumsawad, S. and Wangyao, K. 2023. Effect of Negative Aeration Rates on Water Balance in Biodrying of Wet-Refuse-Derived Fuel. Thai Environmental Engineering Journal, 37(1): 55-63.

[22] Hu, Z., Hao, Z., Lei, H., *et al.* 2023. Effect of Bulking Agents on Dewatered Sludge Biodrying Followed by Thermal Drying. Processes, 11(5): 1392.

[23] Xu, M., Sun, H., Yang, M., *et al.* 2023. Effect of biodrying of lignocellulosic biomass on humification and microbial diversity. Bioresource Technology, 384: 129336.

[24] Li, J., Ju, T., Lin, L., *et al.* 2022. Biodrying with the hot-air aeration system for kitchen food waste. Journal of Environmental Management, 319: 115656.

[25] Wang, K., Chen, Y., Cao, M. K., Zheng, G.D. and Cai, L. 2024. Influence of microbial community succession on biodegradation of municipal sludge during biodrying coupled with photocatalysis. Chemosphere, 349: 140901.

[26] Ham, G.Y. 2020. Study on Bio-drying MBT by modelling of moisture removal and evaluation as MSW management system for energy recovery. (Doctoral Dissertation, Hokkaido University).

[27] Payomthip, P., Towprayoon, S., Chiemchaisri, C., Patumsawad, S., and Wangyao, K. (2022). Optimization of Aeration for Accelerating Municipal Solid Waste Biodrying. International Journal of Renewable Energy Development, 11(3): 878-888.

[28] Cao, X., Gao, J., Wang, Z., *et al.* 2024. Rapeseed cake (RSC) as a novel bulking agent for accelerated biodrying of dewatered sludge. Journal of Environmental Chemical Engineering, 12(3): 112526.

[29] Quan, H., Zhu, T., Ma, F., *et al.* 2023. Enhanced bio-drying effect in low-temperature: Characteristics of sludge hyperthermophilic aerobic bio-drying by inoculating with thermophilic bacteria and full-scale operation. Drying Technology, 41(12): 1977-1990.

Thai Environmental Engineering Journal Vol. 38 No. 2 (2024) : 47-55
www.eeat.or.th

The Effect of Bromide Ions on the Formation of Brominated Haloacetic Acids (Br-HAAs) in Tropical Rivers, Thailand

Nattharika Phongmanee[1], Yuto Tada[2], Shinya Echigo[3] and Suwanna Kitpati Boontanon[4*]

[1,4]Graduate Program in Environmental and Water Resources Engineering, Department of Civil and Environmental Engineering, Faculty of Engineering, Mahidol University, Nakhon Pathom 73170, Thailand, and Graduate School of Global Environmental Studies, Kyoto University, Japan
[2,3]Graduate School of Global Environmental Studies, Kyoto University, Japan
[*]E-mail : suwanna.boo@mahidol.ac.th

Article History; *Received: 16 August 2024, Accepted: 16 August 2024, Published: 30 August 2024*

Abstract

With the presence of bromide ions in chlorination during water purification, hypobromous acid (HOBr) is formed, leading to the formation and distribution of brominated disinfection by-products (Br-DBPs) in tap water. Brominated haloacetic acids (HAAs) in tap water are known to be significantly harmful and toxic to human health. Bromide ions are naturally present in groundwater and surface water, primarily as affected by seawater intrusion. Conventional treatment methods face difficulty in completely eliminating bromide ions. This study investigated the concentration of bromide ions and the haloacetic acid formation potentials (HAAFPs) in three tropical river sources in Thailand: the Tha-Chin River, the Chao Phraya River, and the Mae Klong River. The bromide ion concentrations were 44.79, 41.34, and 18.22 µg/L, respectively. In these three rivers, chlorinated and brominated HAAs (trichloroacetic acid (TCAA), dichloroacetic acid (DCAA), bromodichloroacetic acid, and bromochloroacetic acid) were detected after chlorination. The sum of only DCAAFPs and TCAAFPs were significantly higher than the US EPA regulations of 60 µg/L for total HAA5 (the sum of monochloroacetic acid, monobromoacetic acid, DCAA, dibromoacetic acid, and TCAA). The DCAAFPs in the Chao Phraya River were relatively high, surpassing the WHO guidelines of 50 µg/L. This study also found that the Tha-Chin River had high levels of bromide ions and brominated HAAFPs, resulting from seawater intrusion from the estuary Gulf. These findings highlighted the formation of brominated HAAFPs, which were particularly significant in water sources with higher levels of bromide ions in the water.

Keywords : Bromide ion; disinfection by-products; dissolved organic matter; haloacetic acids; tropical river

Introduction

Chlorination, a commonly used method to eliminate pathogens in the water supply, leads to the formation of disinfection by-products (DBPs), which include carcinogenic trihalomethanes (THMs) and haloacetic acids (HAAs). HAAs are one of the DBPs that have been detected frequently in many regions [1-3]. Nine HAA species commonly occur: three chlorinated HAAs (i.e., monochloroacetic acid (MCAA), dichloroacetic acid (DCAA), trichloroacetic acid (TCAA)), three brominated HAAs (i.e., monobromoacetic acid (MBAA), dibromoacetic acid (DBAA), tribromoacetic acid (TBAA)), and three chlorinated and brominated HAAs (i.e., bromochloroacetic acid (BCAA), bromodichloroacetic acid (BDCAA), and dibromochloroacetic acid (DBCAA)).

Many studies have shown bromine incorporation into DBPs (including THMs and HAAs) when bromide ion (Br^-) are present in source waters [4, 5]. The presence of Br^- changes the reaction pathways of chlorine and dissolved organic matter (DOM) [6, 7]. Br^- is oxidized by chlorine to produce hypobromous acid (HOBr). HOBr reacts more rapidly than hypochlorous acid (HOCl) with DOM, leading to the more formation of brominated DBPs [8, 9]. Brominated DBPs are generally known to be more mutagenic and toxic compared with chlorinated ones [10, 11]. Many studies show that Br^- concentrations in water can vary widely. In the US, the average concentration of Br^- in water supplies is around 62 μg/L, though in certain coastal regions, levels may exceed 500 μg/L [12]. Sohn et al. (2006) found that Br^- concentrations in surface and groundwater ranged from 7 to 312 μg/L, leading to variations of brominated THMs and HAAs [13]. In China, the Yangtze, Huangpu, Tai, and Qiantang Rivers have Br^- concentrations ranging from 100 to 720 μg/L, leading to the formation of brominated HAAs, such as BCAA and BDCAA [14].

In tropical areas like Thailand, higher temperatures, intensive rainfall, and various other conducive factors increase the concentration of DOM in water sources. Br^- naturally occur in groundwater and surface water due to seawater intrusion and discharges from agricultural areas and industries [15]. Conventional water treatment processes (i.e., coagulation, sedimentation, and rapid sand filtration) struggle to remove Br^-. Consequently, concentrations of carcinogenic brominated DBPs in tap water can increase. This study aimed to comprehensively investigate the relationship of the concentration of bromide ions and HAA formation potentials (FPs) in the three water sources used for water supply in Thailand (the Chao Phraya River, the Mae Klong River, and the Tha-Chin River). This study also focused on the relationship between Br^- concentrations and HAAFPs and various factors, including pH, temperature, and conductivity.

Methodology

Study Area

The sampling points of surface water from three rivers, including the Chao Phraya River (14°2'26.9"N, 100°33'21.0"E), the Mae Klong River (13°44'22.5"N 99°50'34.0"E), and the Tha-Chin River 13°55'45.1"N 100°12'01.9"E) (as shown in Figure 1) were investigated. Water samples from raw water sources were collected from a depth of 1.0 meter below the water surface and promptly stored in 10-liter bottles. The sampling was conducted on different dates, with the Mae Klong and Tha-Chin Rivers being sampled on 21 September 2023, and the Chao Phraya River on 1 October 2023. Each river was sampled only once at a single designated point. The collected water samples were prepared for dissolved organic carbon (DOC) analysis by filtering them through 0.7 μm cellulose acetate membrane filters (GF/F, Whatman) using a vacuum pump (N820, Labsort) within 24 h of collection [16].

Analytical Methods

1. Measurement of water quality parameters

The pH and temperature were determined using a pH meter (pHTestr30, EUTECH), and conductivity was measured using a conductivity meter (ECTestr11, Eutech). DOC was analyzed using a TOC analyzer (TOC-V, Shimadzu).

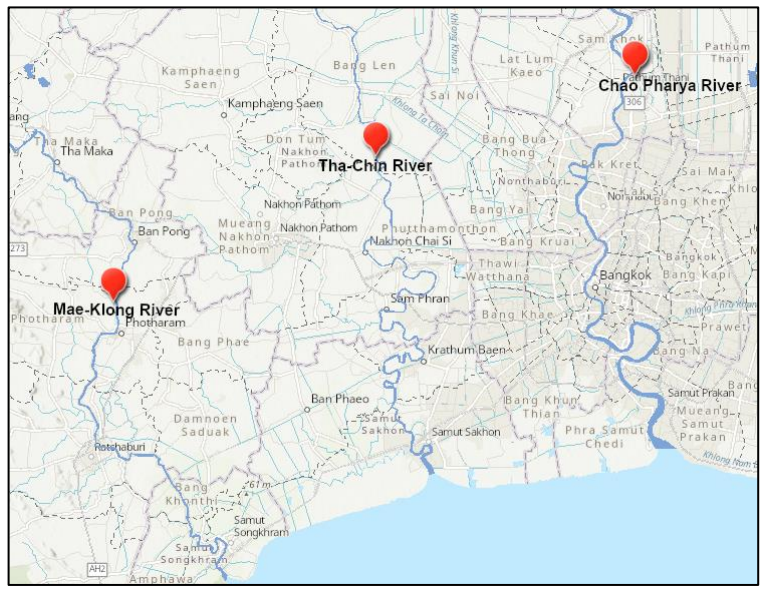

Figure 1 Sampling sites in tropical rivers in Thailand

2. Determination of bromide ion concentrations

Br^- concentrations were determined by LC-MS/MS (6500 QTARP, Sciex, Massachusetts, USA) equipped with an Acclaim Trinity P1 column (3 µm, 2.1×100 mm, Thermo Fisher Scientific). The mobile phases consisted of 200 mM ammonium acetate added with 0.5% acetic acid and acetonitrile. The gradient conditions of organic solvent are as follows: 96% (0-2.5 min), 86% (15.5 min), 5% (16-24.5 min), and 96% (25-34.5 min). The flow rate was maintained at 0.3 mL/min, and the injection volume was set at 10 µL. Quantification of Br^- concentration was performed using negative electrospray ionization (ESI) mode, with multiple reaction monitoring (Q1= *m/z* 79, Q3=*m/z* 79). Calibration curves were prepared using standard solutions containing bromide ions at concentrations of 1, 3, 10, 30, and 100 µg/L, with each calibration point run in triplicate to ensure accuracy and precision. Quality control samples were periodically analyzed to monitor the stability and consistency of the instrument throughout the analytical sequence.

3. HAAFP in chlorination

The chlorination condition for HAAFPs was as follows: 10 mL of sample volume, initial chlorine dose (by sodium hypochlorite) at 30 or 50 mg Cl_2/L, the reaction time 24 h, pH 7 (maintained by 5 mM phosphate buffer), temperature 30 °C in a dark place. After 24 h of the reaction, residual free chlorine was measured using the DPD colorimetric method and quenched with ammonium chloride (50 mg N/L). HAA concentrations were determined by LC-MS/MS (6500 QTARP, Sciex) equipped with a reverse phase column (zorbax SB-Aq, 5 µm, 4.6×150 mm, Agilent technologies, CA, USA). The mobile phases consisted of methanol and 0.3% formic acid solution. The methanol gradient conditions are as follows: 1% (0-0.5 min), 50% (20 min), 99% (21-31 min), and 1% (32-35 min). Calibration curves were prepared using five levels of working standard solutions containing the nine HAA compounds at identical concentrations of 1, 3, 10, 50, 70, and 100 µg/L.

Results and Discussion

Water quality characteristics of rivers in tropical area in Thailand

The water quality of three tropical rivers in Thailand are shown in **Table 1**. The results showed that all rivers had a pH of 7.1-8.0, a temperature of 28.8-32.7 °C, and conductivity (EC) of 160–250 µS/cm. The Tha-Chin River had the highest conductivity value, followed by the Chao Phraya River. The lowest level was found in the Mae-Klong River. Br^- concentrations varied from 18.22 to 44.79 µg/L. The highest values of Br^- are in the Tha-Chin River, followed by the Chao Phraya

Table 1 River water quality characteristics (Br^-, and DOC are expressed as average ± standard deviation in triplicate.)

Source water	pH	Temp. (°C)	EC. (µS/cm)	Br^- (µg/L)	DOC (mg/L)
Chao Phraya River	7.1	31.5	210	41.34 ± 1.17	4.85 ± 0.44
Tha-Chin River	7.3	28.8	250	44.79 ± 5.72	3.41 ± 0.02
Mae-Klong River	8.0	32.7	160	18.22 ± 1.75	2.07 ± 0.06

River, and the lowest in the Mae-Klong River. Most freshwater systems typically exhibit Br^- concentrations ranging from 10 to 500 µg/L [15, 17], whereas seawater typically maintains a concentration of 65 mg/L [18]. In other studies, Br^- in the range of 20-63 µg/L was reported for the Bangphakong River [19], 26.2 µg/L in the China Wu River, and 54.01 µg/L in the Qiantang River [20]. The highest value of conductivity was in the Tha-Chin River, followed by the Chao Phraya River and the Mae-Klong River. The conductivity had a positive relationship with Br^- concentrations. As a result, seawater intrusion from the Gulf of Thailand estuary or human activities might contribute to the high conductivity of the Tha-chin River and Chao Phraya River.

The DOC concentrations are at 4.85 mg/L for the Chao Phraya River, 3.41 mg/L for the Tha-Chin River and 2.07 mg/L for the Mae-Klong River. The Chao Phraya River had the highest value among all the three rivers. The high DOCs in the waters indicated the presence of a wide range of organic substances, resulting from complex interactions between natural processes and human activities, including the decay of vegetation, the impacts of eutrophication, the occurrence of algal blooms, and the release of wastewater. Nevertheless, the Mae-Klong River had the lowest DOC because of limited urban development along the river's path. Other research investigated water sources in Thailand and reported that the concentrations of DOC in river waters were 2 to 12 mg/L [21, 22], showing that the DOCs in the rivers examined in our study were within the range observed in previous research conducted in Thailand.

Haloacetic acid formation potential

Figure 2A shows the HAAFPs of the samples collected during the rainy season. Focusing on chlorinated HAA species (i.e., MCAA, DCAA, and TCAA), high DCAAFPs and TCAAFPs in the three source waters were found, while MCAAFPs were not quantified (less than LOQ at < 3µg/L). TCAAFPs in source waters collected from the Chao Phraya, Tha-Chin rivers, and Mae Klong were 165 µg/L, 103 µg/L, and 52 µg/L, respectively. In addition, DCAAFPs were 69 µg/L, 47 µg/L, and 25 µg/L, respectively. The orders of FPs were the same for DOC. The DCAAFPs in the Chao Phraya River largely exceeded the WHO guideline values in tap water (i.e., 50 µg/L) [23], suggesting that appropriate treatment is necessary for drinking of tap water. TCAAFPs in the Chao Phraya River were close to the WHO guideline (i.e., 200 µg/L) and in all three rivers considerably larger than regulations developed by several countries such as Japan (i.e., 30 µg/L), which means that TCAA is also needed to control for drinking of safe tap water. Considering the total FP concentration, all three rivers had high HAA5 levels significantly exceeding the US EPA and EU regulations (i.e., 60 µg/L) [24], also strongly indicating the risk of DBPs in the tap water.

Moving to brominated HAA species (i.e., MBAA, BCAA, DBAA, BDCAA, DBCAA, and TBAA), only BCAAFP and BDCAAFP were quantified in all three rivers in this study, while the others were less than LOQ (1 µg/L). BCAAFP of the river waters of the Chao Phraya, Tha-Chin, and Mae Klong rivers were 4.12 µg/L, 4.73 µg/L, and 1.72µg/L respectively. BDCAAFP were 15.33 µg/L,

13.01 µg/L, and 6.20 µg/L, respectively. The magnitude relationship among them is the same as for chlorinated HAAs. Although the FPs were much lower than those of DCAAFPs and TCAAFPs (approximately one-tenth), it is not negligible considering their higher toxicity than the chlorinated forms. Although no standard or guideline values have been established for individual brominated HAAs, the substances are subject to monitoring in public water systems in many countries like U.S and Japan. The results of this study are the first successful determination of the brominated HAAFPs in raw waters in Thailand and will be valuable data for future water supply operations.

In a previous study conducted in China, TCAAFP was 168 µg/L and DCAAFP 236 µg/L in the Qiantang River [20]. Similarly, in Büyükçekmece Lake in Turkey, the levels of HAA5 were 87.0 µg/L, TCAAFP 23.9 µg/L, and DCAAFP 51.2 µg/L, respectively [25]. Comparatively, our study revealed that the levels of TCAAFPs in river waters in Thai were higher than DCAAFPs, meaning that the composition of the DOM may be different. Subsequently, the treatability may be different from the other areas, and a comprehensive treatment approach may need to be considered for ensuring the safety and proper water quality in the water supply system in Thailand.

Figure 2B shows the concentrations of HAAFPs per DOC in the three samples. The Chao Phraya, Mae Klong and Tha-Chin rivers had TCAAFPs of 31.2, 24.4, and 26.5 µg/mg C, and DCAAFP concentrations of 13.1, 11.1 and 12.0 µg/mg C, respectively. No significant differences were found between rivers. Not much difference was also found for brominated HAAFP. Since trihaloacetic acid FPs were greater than dihaloacetic acid FPs, major precursors of HAAs were likely to have aromatic moieties.

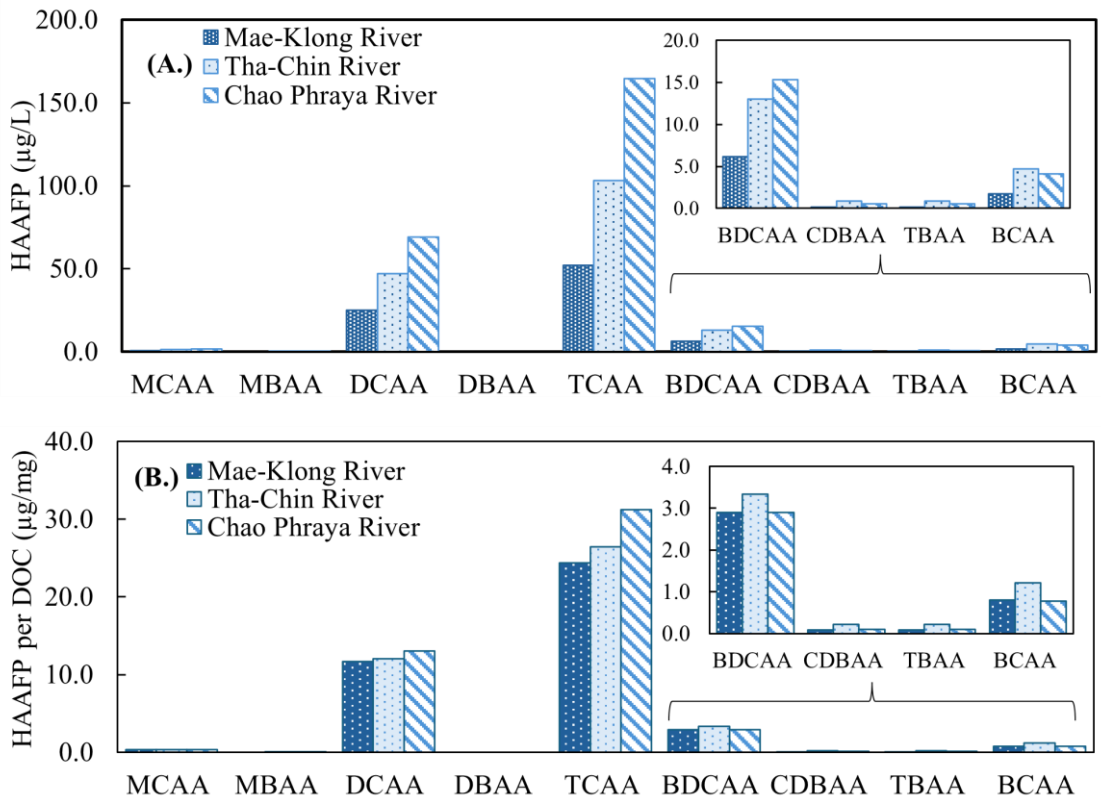

Figure 2 (A) HAAFPs and (B) HAAFPs per DOC of the river waters

Figure 3A illustrates the correlation between the sum of HAAFP per DOC and DOC levels in the Chao Phraya River, Mae- Klong River and Tha-chin River. Figure 3B depicts the correlation between the values of brominated HAAFP/DOC and the concentration of bromide ions. The Tha-Chin River displays a notable presence of brominated HAAFP, characterized by elevated levels of bromide ions. Consequently, after chlorination, the Br^- levels exhibited an increasing proportion of brominated HAA compared to chlorinated HAAFP. These results suggest that the concentration of DOC and Br^- have an impact on the increase in the HAAFP. The presence of Br^- specifically causes a shift in the distribution of HAAs towards more brominated species, leading to an increase of brominated HAAs [25].

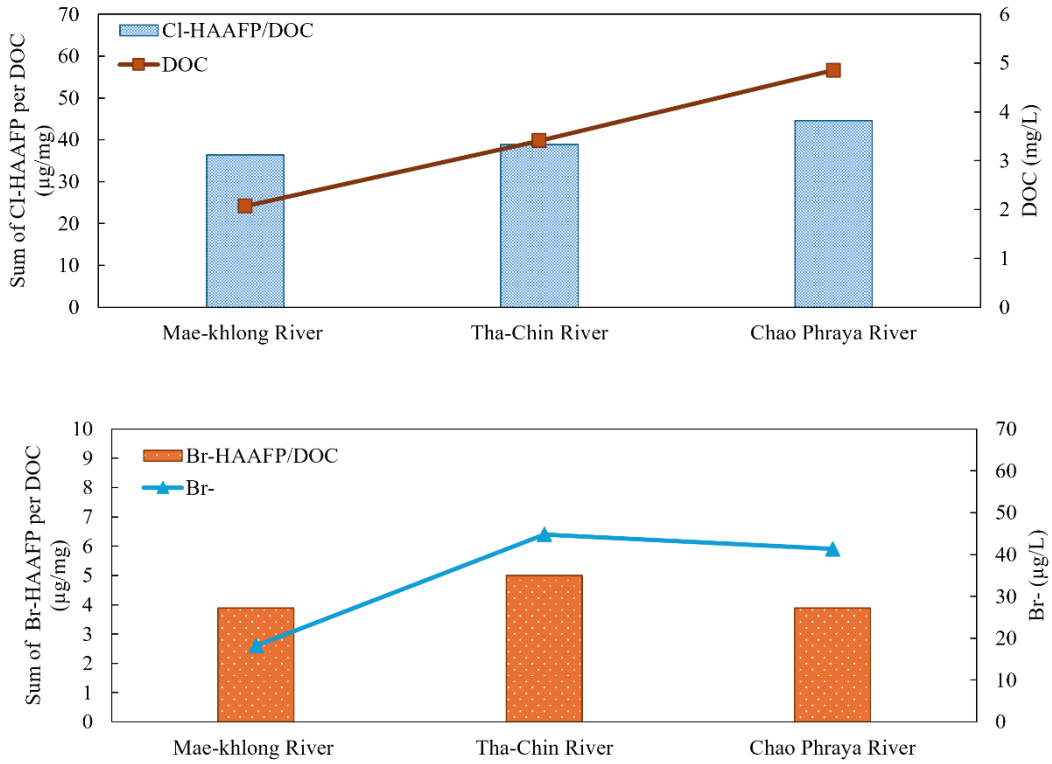

Figure 3 Relationships between (A) the sum of HAAFPs per DOC and DOC, (B) the sum of only brominated HAAs and Br^- concentrations

HAAFP percentage occurring in three tropical rivers in Thailand

Figure 4 displays the distribution percentage of HAAFPs in the three rivers: the Chao Phraya, Tha-Chin, and Mae Klong rivers. The patterns of HAAFPs were similar across all rivers, with TCAAFP and DCAAFP predominantly comprising over 90% of all HAAFPs. The identified HAAFP types included TCAAFP, DCAAFP, BDCAAFP, and BCAAFP. TCAAFP was the most prevalent, accounting for approximately 60%–64% across the three rivers, with the highest proportion found in the Chao Phraya River. DCAAFP comprises 27%–29% of the total, with the highest proportion observed in the Mae-Klong River. BDCAAFP accounts for 6%–7.6% and is most commonly found in the Tha-Chin River, while BCAAFP constitutes 1.6%–2.7%. Additionally, other HAAFP types are present in minute amounts, including MCAA (0.6%–0.8%), CDBAAFP (0.21%–0.50%), TBAAFP (0.21%–0.50%), MBAAFP (0.06%–0.14%), and DBAA (< detection limit).

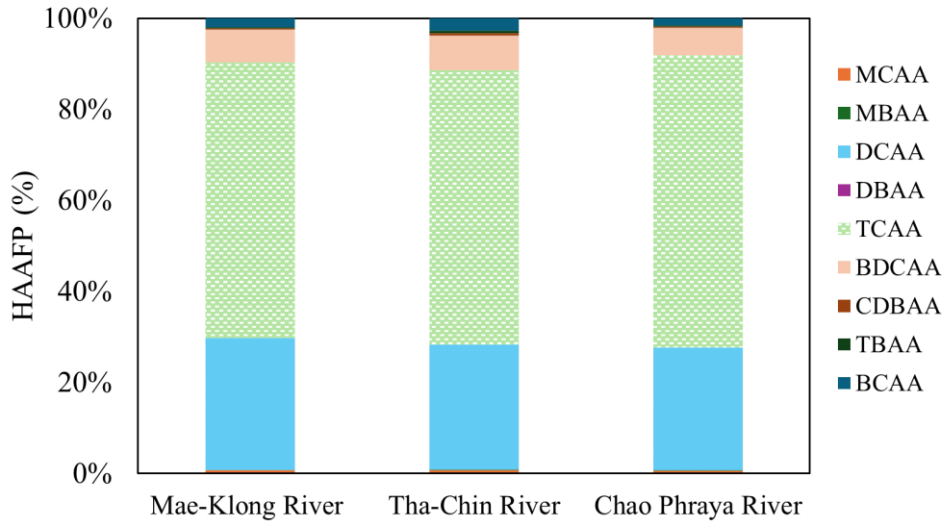

Figure 4 The percentage of HAAFP in tropical rivers in Thailand

Conclusion

A significant finding is the presence of Br^- in tropical rivers in Thailand, with concentrations detected in the Tha-Chin (44.79 µg/L), Chao Phraya (41.34 µg/L) and Mae-Klong rivers (18.22 µg/L). The bromide ion concentrations of these rivers were influenced by seawater intrusion from the Gulf of Thailand.

The occurrence of TCAAFP, DCAAFP, BDCAAFP and BCAAFP were identified in these rivers, with HAA5 (the sum of chlorinated HAAs, MBAA and DBAA were not detected.) levels significantly exceeding the US EPA and EU regulations (60 µg/L). DCAAFPs in the Chao Phraya River exceeded WHO guideline values (50 µg/L), indicating treatment is necessary for drinking tap water. TCAAFPs in the Chao Phraya River were close to WHO guidelines (200 µg/L) but in all three rivers greatly exceeded the regulations in Japan's regulations (30 µg/L), which means that TCAA is also needed to monitor for safe tap water. The HAAFP distribution in the Chao Phraya, Tha-Chin, and Mae Klong rivers shows TCAAFP (60%–64%) and DCAAFP (27%–29%) as the most prevalent, with minor contributions from BDCAAFP, BCAAFP. The presence of Br^- in river samples, notably in the Tha-Chin River, correlated with increased levels of brominated HAAFP (BDCAAFP, BCAAFP), indicating a positive correlation between Br^- levels and HAAFP formation.

Consequently, using chlorine in the water treatment process in the presence of Br^- can lead to the formation of brominated HAAFP, posing potential health risks. Therefore, the significant formation of brominated HAAFP is considerable in water sources with increased bromide levels. To build upon these findings, further research should extend the duration of data collection and incorporate information on rainfall amounts at each sampling site. Precipitation significantly impacts seawater intrusion and Br^- concentrations. A thorough understanding of these dynamics is essential for a comprehensive analysis of their influence on water quality. This approach will elucidate the relationship between environmental conditions and the formation of DBPs, ultimately leading to more efficient water treatment strategies.

Acknowledgement

The authors are grateful to the On-Site Laboratory Initiative of the Graduate School of Global Environmental Studies at Kyoto University for additional funding. Additionally, this study was financially supported by JSPS KAKENHI (Grant Numbers JP23K04088).

References

[1] Krasner, S.W., Westerhoff, P., Chen, Z., Amy, G., and Croué, J.P. 2006. Occurrence of a new generation of disinfection byproducts. Environmental Science & Technology, 40(23): 7175-7185.

[2] Richardson, S.D., Plewa, M.J., Wagner, E.D., Schoeny, R., and DeMarini, D.M. 2007. Occurrence, genotoxicity, and carcinogenicity of regulated and emerging disinfection by-products in drinking water: A review and roadmap for research. Mutation Research, 636 (1-2): 178-242.

[3] Park, K.-Y., Kim, J., Lee, Y., and Shin, H. 2019. Natural organic matter removal from algal-rich water and disinfection by-products formation potential reduction by powdered activated carbon adsorption. Journal of Environmental Management, 235: 310-318.

[4] Liang, L. and Singer, P.C. 2003. Factors influencing the formation and relative distribution of haloacetic acids and trihalomethanes in drinking water. Environmental Science & Technology, 37(13): 2920-2928.

[5] Ersan, M.S., Wols, B., Harmsen, D., and Medema, G. 2019. The interplay between natural organic matter and bromide on bromine substitution. Science of the Total Environment, 646: 1172-1181.

[6] Kumar, K. and Margerum, D.W. 1987. Kinetics and mechanism of general-acid-assisted oxidation of bromide by hypochlorite and hypochlorous acid. Inorganic Chemistry, 26(16): 2706-2711.

[7] Liu, Y., Yu, L., Huang, J., and Wang, Y. 2022. Formation of regulated and unregulated disinfection byproducts during chlorination and chloramination: Roles of dissolved organic matter type, bromide, and iodide. Journal of Environmental Sciences, 117: 151-160.

[8] Cowman, G.A. and Singer, P.C. 1995. Effect of bromide ion on haloacetic acid speciation resulting from chlorination and chloramination of aquatic humic substances. Environmental Science & Technology, 30(1): 16-24.

[9] Alsulaili, A.D. 2009. Impact of bromide, NOM, and pre-chlorination on haloamine formation, speciation, and decay during chloramination. Water Research, 43(5): 1432-1440.

[10] Heller-Grossman, L., Heller, M., and D. S. M. Barak. 1993. Formation and distribution of haloacetic acids, THM, and TOX in chlorination of bromide-rich lake water. Water Research, 27(8): 1323-1331.

[11] Westerhoff, P., Chao, P., and Mash, H. 2004. Reactivity of natural organic matter with aqueous chlorine and bromine. Water Research, 38(6): 1502-1513.

[12] Siddiqui, M.S., Amy, G.L., and Rice, R.G. 1995. Bromate ion formation: a critical review. Journal - American Water Works Association, 87(10): 58-70.

[13] Sohn, J., Amy, G., and Yoon, Y. 2006. Bromide ion incorporation into brominated disinfection by-products. Water, Air, and Soil Pollution, 174(1-4): 265-277.

[14] Liu, S., Zhang, Y., Wang, Y., and Chen, Y. 2011. Seasonal variation effects on the formation of trihalomethane during chlorination of water from Yangtze River and associated cancer risk assessment. Journal of Environmental Sciences (China), 23(9): 1503-1511.

[15] Kampioti, A.A. and Stephanou, E.G. 2002. The impact of bromide on the formation of neutral and acidic disinfection by-products (DBPs) in Mediterranean chlorinated drinking water. Water Research, 36(10): 2596-2606.

[16] Tada, Y., Nakagawa, T., Matsumoto, S., and Sakurai, K. 2023. High formation of trichloroacetic acid from high molecular weight and ultra-hydrophilic components in freshwater raphidophytes upon chlorination. Science of the Total Environment, 879: 163000.

[17] Cowman, G.A. and Singer, P.C. 1995. Effect of bromide ion on haloacetic acid speciation resulting from chlorination and chloramination of aquatic humic substances. Environmental Science & Technology, 30(1): 16-24.

[18] Kharkar, D., Turekian, K.K., and Bertine, K.J. 1968. Stream supply of dissolved silver, molybdenum, antimony, selenium, chromium, cobalt, rubidium, and cesium to the oceans. Geochimica et Cosmochimica Acta, 32(3): 285-298.

[19] Marhaba, T.F., Murthy, S.K., and Parulekar, S.J. 2006. Trihalomethanes formation potential of shrimp farm effluents. Journal of Hazardous Materials, 136(2): 151-163.

[20] Zheng, L., Xu, Z., Huang, Y., and Zhang, H. 2020. Precursors for brominated haloacetic acids during chlorination and a new useful indicator for bromine substitution factor. Science of the Total Environment, 698: 134250.

[21] Volk, C., Hübner, U., and Koch, C. 2002. Monitoring dissolved organic carbon in surface and drinking waters. Journal of Environmental Monitoring, 4(1): 43-47.

[22] Wang, Y., Small, M.J., and VanBriesen, J.M. 2017. Assessing the risk associated with increasing bromide in drinking water sources in the Monongahela River, Pennsylvania. Journal of Environmental Engineering, 143(3): 04016089.

[23] World Health Organization. 2011. WHO Guidelines for Drinking-Water Quality, 4th edition. Geneva: World Health Organization.

[24] U.S. Environmental Protection Agency. 2010. Stage 2 Disinfectants and Disinfection By-Products Rule: A Quick Reference Guide for Schedule 1 Systems. EPA 815-K-09-003.

[25] Uyak, V. and Toroz, I. 2007. Investigation of bromide ion effects on disinfection by-products formation and speciation in an Istanbul water supply. Journal of Hazardous Materials, 149(2): 445-451.

Thai Environmental Engineering Journal Vol. 38 No. 2 (2024) : 57-64
www.eeat.or.th

Effect of In-situ Aeration on Leachate Qualities under Uncompacted Municipal Solid Waste Disposal Conditions

Chattrapha Suethep[1], Noppharit Sutthasil[1,2], Chart Chiemchaisri[1*], Wilai Chiemchaisri[1], Kazuto Endo[3] and Masato Yamada[3]

[1]Department of Environmental Engineering, Faculty of Engineering, Kasetsart University, Bangkok 10900, Thailand
[2]School of Health Science, Mae Fah Luang University, Chiang Rai 57100, Thailand
[3]National Institute for Environmental Studies, Ibaraki 305-8506, Japan
[*]E-mail : fengccc@ku.ac.th

Article History; *Received: 15 August 2024, Accepted: 21 August 2024, Published: 30 August 2024*

Abstract

This research was carried out to investigate the effect of in-situ aeration on leachate qualities in simulated lysimeters containing uncompacted municipal solid wastes representing typical municipal solid waste disposal conditions in Thailand. The study was performed by applying different aeration conditions to the lysimeters and leachate volume and its chemical characteristics were monitored over 6 months. The air supply conditions varied from natural ventilation to active aeration at rates of 0.18 and 0.36 l/min. The generated leachate was compared to the control lysimeter representing typical anaerobic disposal conditions. The lysimeters operated at a high airflow rate of 0.36 l/min and natural ventilation had their leachate qualities in terms of organic (BOD, COD) and nitrogen (TKN) well stabilized by more than 90% within 30 days. Under low aerated conditions (0.18 l/min), organic stabilization in leachate required more than 100 days whereas TKN removals were also highly fluctuated. Based on the results from this study, waste disposal operation under natural aeration through a ventilation pipe installed into the uncompacted waste layer would be sufficient to reduce organic and nitrogen pollutants in leachate to the same level as the highly aerobic landfill condition.

Keywords : Landfill aeration; Leachate generation; Leachate quality; Waste stabilization

Introduction

Direct land disposal of fresh municipal solid wastes (MSW) is practiced in most developing countries. Conventional landfills are mostly designed so that the disposed wastes are kept isolated from the outside environment causing a dry anaerobic environment, which is unfavorable for microbial decomposition. Therefore, waste stabilization processes take a long time, and products from land disposal of MSW such as gas and leachate are continuously generated, demanding long-term monitoring and pollution control [1]. To mitigate these problems, new operating techniques were developed in an attempt to accelerate the waste stabilization process and reduce pollutant discharge such as the use of the bioreactor concept through leachate recirculation and storage [2, 3] or the development of the aerobic condition in the waste matrix [4].

The aeration concept has been introduced for waste stabilization and reduction of environmental impacts. The introduction of air could accelerate the microbial degradation process and reduce pollutant emissions both in terms of gaseous and leachate forms. Aerobic conditions in waste disposal areas can be promoted either through passive or active aeration methods. In Japan, naturally aerated landfills so-called "semi-aerobic landfills" have been developed by Fukuoka University where leachate and gas are continuously removed from the waste mass using leachate collection and gas venting systems allowing ambient air flows into the waste body [5]. Meanwhile, the active aeration method using a mechanical air-pressurized system is popularly implemented in

European countries [6]. In-situ aeration through pipes applied in a shallow landfill provided a widespread distribution of air into the waste body [7]. The air intrusion into the waste body leads to the subsequent improvement of waste stabilization and leachate qualities due to the enhancement of aerobic microbial activities within the waste cell [8]. Under aerobic conditions, organic matter present in wastes is subjected to biodegradation by aerobic microorganisms to carbon dioxide and water. Enhancement of organic carbon mineralization under aerobic treatment compared to that of anaerobic treatment has been confirmed [9]. Development of aerobic conditions in landfills resulted in rapid reduction of organic pollutants and reduction of methane emission [10]. In this regard, it was reported that aerobic treatment led to lower emissions due to the increased sorption capacity of aerated wastes than a lower overall pollutant potential [9]. Leachate qualities were found to be significantly improved under semi-aerobic and aerobic conditions in the landfills when compared to conventional anaerobic landfills [11, 12]. Ma et al. [13] reported the effects of aeration on the improvement of leachate qualities reaching 97% of Chemical Oxygen Demand (COD) and 88% of ammonium nitrogen (NH_4^+) removals. Liu et al. [14] also reported the beneficial effects of providing micro-aeration and leachate recirculation on the acceleration of landfill stabilization through promoting hydrolytic activities.

Despite the obvious advantages of providing semi-aerobic and aerobic conditions in MSW disposal sites, the effect of aeration either provided through active or passive aeration operation on the waste matrix is still unclear. Some previous attempts have been performed using intermittent aeration operation [12, 15] pre-aeration [16], or aeration during leachate recirculation [17]. In a previous review of landfill aeration research [18], optimum aeration rates were found to vary widely ranging from 0.00006-4.51 l/min/kg dry mass depending on aeration mode (continuous or intermittent), waste characteristics (fresh or old) and disposal condition (low or high waste densities) and operating conditions such as temperature and leachate recirculation practice. Meanwhile, clear operation guidelines to achieve appropriate aerobic conditions in MSW disposal sites under different waste disposal and climatic conditions have not been developed especially those disposed as uncompacted waste under high moisture conditions which is the predominated condition of MSW in Thailand. In this study, the effect of in-situ aeration on leachate characteristics was experimentally investigated to determine appropriate conditions for reducing leachate pollution from MSW disposal sites in Thailand.

Materials and Methods

Experimental set-up

Laboratory-scale lysimeters were made of acrylic with 0.3 m diameter and 1.5 m height (Figure 1). They were filled with MSW obtained from a local authority in Thailand to an initial height of 1.0 m and covered with a sand layer of 0.3 m. Major waste components were 63.5% food waste, 4.9% paper, 14.4% plastic, and 10.2% glass (Table 1), representing typical MSW composition received at solid waste disposal sites in Thailand. Four lysimeters were operated under different conditions. The first lysimeter was operated under anaerobic conditions as the control experiment. Another two lysimeters were operated at different aeration rates of 0.18 and 0.36 l/min supplied by an air blower. The other lysimeter was operated under passive aeration (natural ventilation) through a vertical pipe (1 in. diameter). The amount of MSW placed in each lysimeter was 25.7 kg wet weight (or 7.7 kg dry mass) except for that of natural aeration in which 23.9 kg of wet wastes (or 7.2 kg dry mass) were added due to lower active lysimeter volume from vertical aeration pipe placement. The initial waste densities in all lysimeters were set equally at 385 kg/m^3. The aeration rates in aerated lysimeters were set equivalent to 0.023 and 0.046 l/min/kg dry mass of solid waste which were reported as optimum conditions in previous landfill aeration studies [19-20]. In those researches, aeration rates of 0.027-0.043 l/min/kg dry mass were reported as appropriate conditions for fresh waste disposed under low compaction densities (350-384 kg/m^3).

Table 1 presents the physical composition and chemical characteristics of solid wastes used in this study. The chemical analyses of solid wastes were performed according to the procedures provided by the Soil and Plant Analysis Council [21]. During the lysimeter operation, waste temperature and settlement were also monitored weekly.

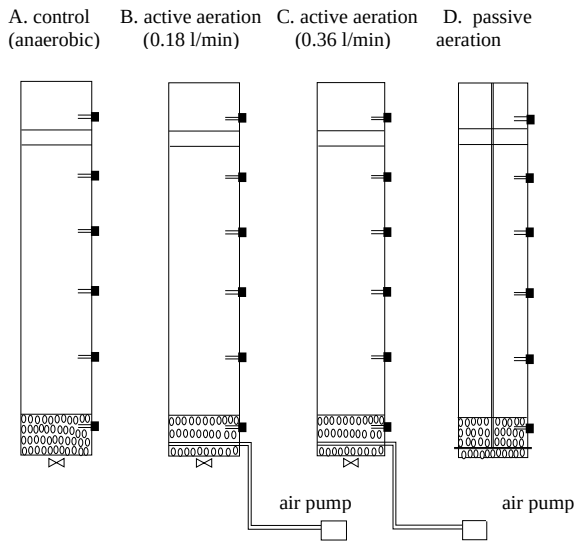

Figure 1 Experimental lysimeters with different aeration set-up

Table 1 Composition and chemical characteristics of MSW

Composition	Percentage (wet wt.)
Food wastes	63.55
Paper/Newsprint/cardboard	4.86
Plastics	14.44
Rubber	0.32
Textile	2.07
Wood	0.84
Glass	10.21
Metals	1.60
Others	2.11
Chemical characteristics	**Percentage**
Moisture	69.92 (wet wt.)
Volatile solids (VS)	93.45 (dry wt.)
Carbon (as TOC)	56.20 (dry wt.)
Nitrogen (as TKN)	3.34 (dry wt.)

Lysimeter operation, sampling, and analyses

The lysimeters were operated and monitored for 6 months. The temperature inside the lysimeters was measured at four different levels along the waste height, i.e. 0.2, 0.4 m, 0.6, and 0.8 m. from the bottom of lysimeters using thermometers. During the experimental period, waste layer height, leachate volume, and chemical characteristics were monitored regularly. The determining parameters included pH, biochemical oxygen demand (BOD), chemical oxygen demand (COD), total Kjeldahl nitrogen (TKN), nitrite (NO_2^-), and nitrate (NO_3^-). All water quality analyses were performed according to Standard Methods for the Examination of Water and Wastewater [22].

Results and Discussion

Waste characteristics in lysimeter

Figure 2 shows waste subsidence in the lysimeters during 6 months of operation. The control lysimeter had about 10% settlement, significantly lower than the other aerobic lysimeters (25-35%). Comparatively, the

lysimeters with active aeration had higher waste subsidence than passively aerated lysimeters, especially after about 100 days of operation. The higher settlement rate observed in the aerobic lysimeters could relate to faster biodegradation of organic wastes under aerobic conditions. Figure 3 shows the average temperature of solid waste in the lysimeters. While the temperatures were found to fluctuate with time, it was noticed that higher average temperatures were temporally detected in aerated lysimeters compared to the control lysimeters, especially during the first 100 days of operation. This temperature rise indicated the heat released from the aerobic decomposition of organic wastes. It was also noted that higher temperature was detected at the bottom part of the lysimeters where aeration was introduced. This observation suggests that aerobic conditions prevailed in the aerated lysimeters. The temperatures in the lysimeter supplied with a higher aeration rate (0.36 l/min) were found relatively stable than the others, especially during the early stage of operation. Meanwhile, the lower aerated lysimeter (0.18 l/min) had its temperature highly fluctuated possibly due to the occurrence of facultative or semi-aerobic conditions with temporal temperature rise observed twice during the experimental period, i.e. after the first week and towards 100 days of operation. These results also suggested that a more uniform distribution of supplied air took place in the lysimeter operated at a higher aeration rate of 0.36 l/min. These temperature-rise incidents were followed by high waste subsidence observed in the lysimeter so they are expected to be associated with the waste degradation. Under natural ventilation conditions, the highest temperature was observed during the start-up period and it declined to the same level as the other lysimeters and mostly became stable afterward whereas the waste subsidence suggested its conditions were between the control (anaerobic) and active aeration conditions.

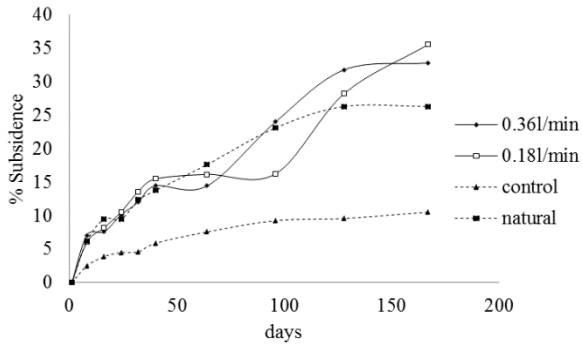

Figure 2 Waste subsidence in the lysimeters

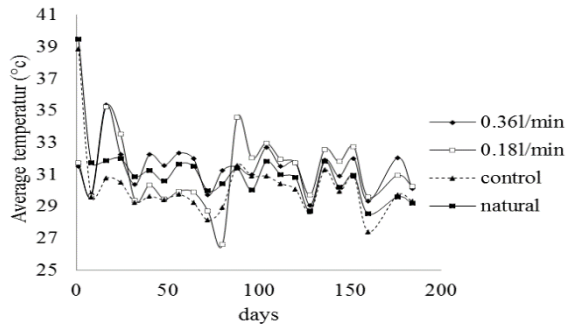

Figure 3 Variation of temperatures of waste in the lysimeters

Leachate quantity and qualities

During the lysimeter operation, the amount of leachate formed and drained from the lysimeters was recorded. The total cumulative volume of leachate from the control lysimeter was found to be approximately 2 liters whereas the highest detected volume was 8 liters from the naturally ventilated lysimeter as shown in Figure 4. The two aerated lysimeters have about the same volume of leachate at about 6.5 liters but it was found that the lysimeter with a higher aeration rate produced leachate faster than the other during the early stage of operation. The amount of leachate produced primarily comes from the original moisture content in waste as well as that produced from organic waste degradation. The reduction of organic matter in solid waste during its degradation also reduced water holding capacity of landfilled waste whereas a greater ventilation rate resulted in lower water content of landfilled waste due to the water evaporation effect [23]. Comparing aerated and naturally ventilated lysimeters, a higher volume of leachate was observed in naturally ventilated lysimeter as most of the moisture loss occurred only through leachate formation in the lysimeter whereas those aerated lysimeters had their moisture loss occurred through leachate formation as well as evaporation of water.

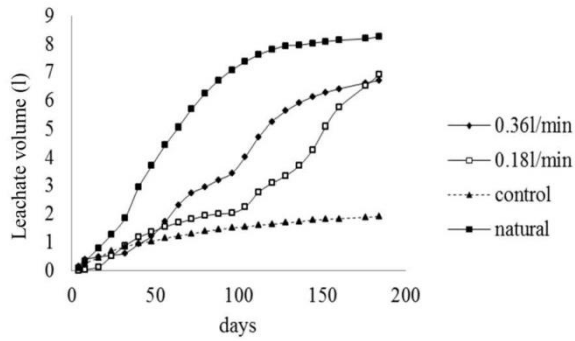

Figure 4 Cumulative leachate volume produced during lysimeter operation

Figures 5a) to 5e) show the chemical characteristics of leachate from the lysimeters in terms of pH, BOD, COD, TKN, and oxidized nitrogen. Leachate from the control lysimeter was found to be acidic and contained higher organic and nitrogen concentrations. Meanwhile, other aerobic lysimeters produce more stabilized leachate, being alkaline while containing low BOD, COD, and TKN concentrations after 30 days of operation and became stable mostly during the whole experimental period. The oxidized nitrogen was also detected in leachate from those aerobic lysimeters but at much lower concentrations when compared to TKN. These results indicate that aerobic condition in the lysimeters has significantly improved leachate qualities and simultaneous nitrification and denitrification reactions possibly took place in the lysimeters according to the following reactions assuming organic matter available for denitrification reaction was in the form of acetic acid.

- Nitrification reaction:

$NH_3 + 2O_2 \rightarrow H^+ + NO_3^- + H_2O$

- Denitrification reaction:

$5CH_3COOH + 8NO_3^- \rightarrow 4N_2 + 10CO_2 + 6H_2O + 8OH^-$

Among the aerated lysimeters, the lysimeter with the highest aeration rate (0.36 l/min) had the lowest organic pollutant leaching out during its operation. Meanwhile, the lysimeter with natural ventilation conditions also yielded good and stable leachate qualities which suggested that the air supply was sufficiently provided for its leachate stabilization. Under lower aeration conditions (0.18 l/min), the qualities of leachate fluctuated and it took longer time up to more than 100 days to be stabilized. However, this stabilization period (100 days) is similar to that reported for leachate stabilization in the semi-aerobic recirculation process [24] but comparatively shorter than that of large-scale simulated semi-aerobic landfills reported at 48 weeks [25]. These results also suggested that air supply into un-compacted waste under natural ventilation conditions was similar to that of a higher aeration rate of 0.36 l/min whereas there was no uniform distribution of air at a lower aeration rate of 0.18 l/min for leachate stabilization.

The pollutants load from produced leachate was determined from the leachate amount and pollutant concentrations at the end of the lysimeter operation. Comparing among the lysimeters, it was found that the lysimeter operated at a higher aeration rate (0.36 l/min) yielded the lowest pollutant load as it had their organic and nitrogen pollutants well stabilized whereas its leachate amount was similar to that observed in lower aerated condition and lower than of natural ventilation lysimeter. However, pollutant load from natural ventilation conditions was also not very much higher due to a similar degree of leachate stabilization achieved though a larger volume of leachate of about 20% was observed. Meanwhile, the control lysimeter had the highest pollutant load due to high pollutant concentrations contained in leachate even though it produced a lesser amount of leachate.

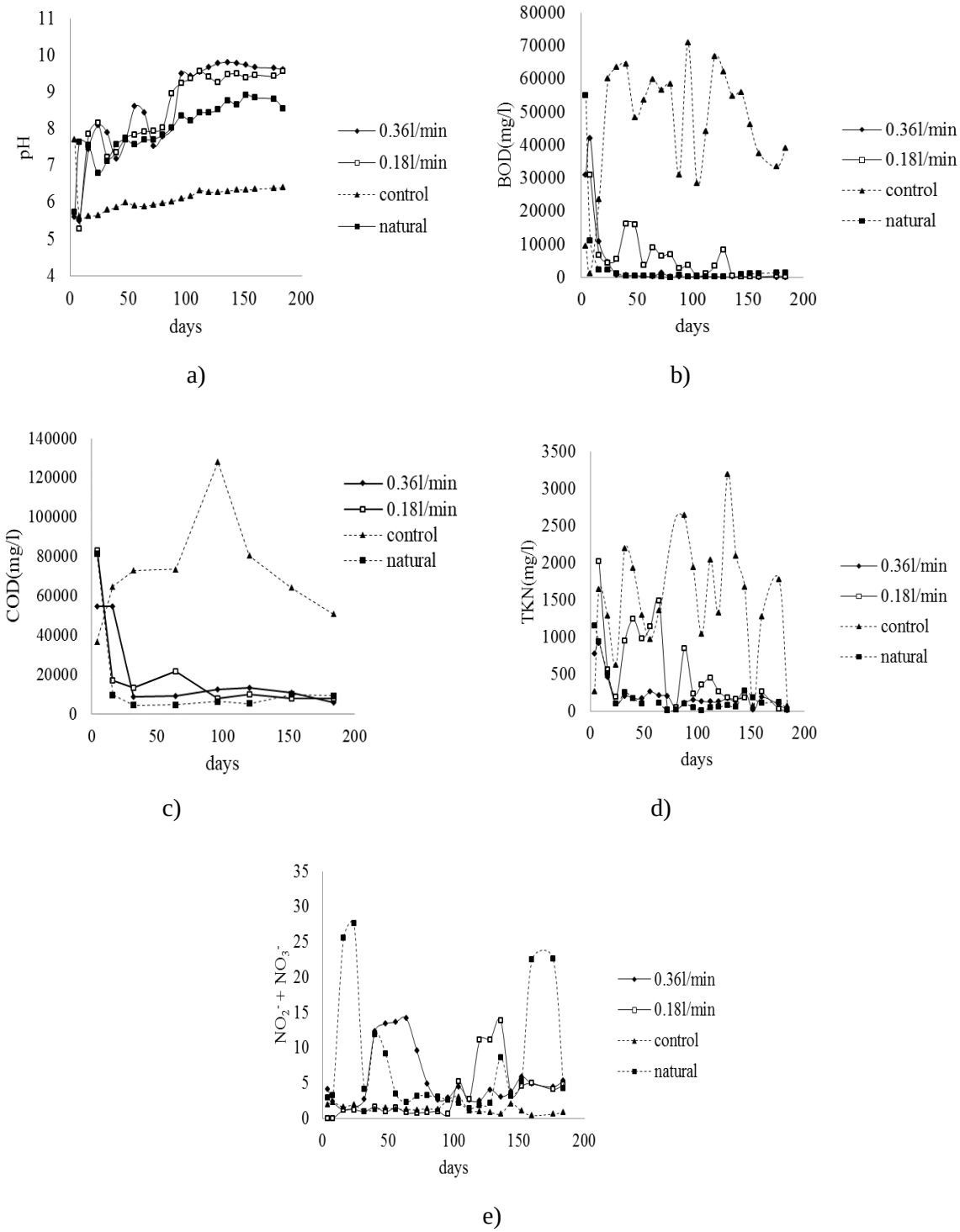

Figure 5 Variations of leachate characteristics a) pH, b) BOD, c) COD, d) TKN, e) NO_X of the lysimeters

Conclusions

The effect of aeration on improved leachate qualities from uncompacted solid waste disposal was confirmed in lysimeter experiments. The lysimeters operated at a higher air flow rate (0.36 l/min) and natural ventilation had their leachate qualities in terms of BOD and COD well stabilized by more than 90% within 30 days whereas those in low airflow condition (0.18 l/min) required more than 100 days. Meanwhile, organic substances in leachate were not stabilized during the whole experimental period under anaerobic conditions. TKN removals of more than 90% were also achieved in the lysimeters with 0.36 l/min air flow rate and natural ventilation after 30 days whereas their removals fluctuated under low air flow rate and anaerobic conditions. The majority of nitrified nitrogen was denitrified in the lysimeters resulting in low oxidized nitrogen in the leachate. The supply of sufficient air through active aeration at a higher rate (0.36 l/min) or natural ventilation significantly improved and accelerated organic waste degradation and leachate stabilization from the traditional anaerobic conditions. This in-situ aeration utilizing ventilation pipes installed into the uncompacted waste layer could help reduce leachate pollution from solid waste disposal sites in Thailand, similar to that of aerated landfills.

Acknowledgments

This research was carried out as an activity under the Collaborative Research Laboratory (CRL) between Kasetsart University, and National Institute for Environmental Studies (NIES), Japan.

References

[1] Warith, M.A. and Takata, G.J. 2004. Effect of aeration on fresh and aged municipal solid waste in a simulated landfill bioreactor. Water Quality Research Journal of Canada. 39(3): 223-229.

[2] Chiemchaisri, C., Chiemchaisri, W., Sittichoktam, S. and Tantichatakarun, T. 2009. Application of partially submerged bioreactor landfill for leachate management in the tropics. International Journal of Environment and Waste Management. 3(1/2): 78-90.

[3] Weerasekara, R., Chiemchaisri, C. and Chiemchaisri, W. 2010. Influence of solid waste disposal conditions on organic pollutants discharged from tropical landfill. Asian Journal of Water, Environment and Pollution. 7(1): 107-112.

[4] Erses, A.S., Onay, T.T. and Yenigun, O. 2008. Comparison of aerobic and anaerobic degradation of municipal solid waste in bioreactor landfills. Bioresource Technology. 99: 5418-5426.

[5] Theng, L.C., Matsufuji, Y. and Hassan, M.N. 2005. Implementation of the semi-aerobic landfill system (Fukuoka method) in developing countries: A Malaysia cost analysis. Waste Management. 25: 702-711.

[6] Ritzkowski, M. and Stegmann, R. 2012. Landfill aeration worldwide: Concepts, indications and findings. Waste Management. 32: 1411-1419.

[7] Brandstätter, C., Prantl, R. and Fellner, J. 2020. Performance assessment of landfill in-situ aeration - a case study. Waste Management. 101: 231-240.

[8] Gómez, M.A., Baldini, M., Marcos, M., Martínez, A., Fernández, S. and Reyes, S. 2012. Aerobic microbial activity and solid waste biodegradation in a landfill located in a semi-arid region of Argentina. Annals of Microbiology. 62: 745-752.

[9] Fricko, N., Brandstätter, C. and Fellner, J. 2021. Enduring reduction of carbon and nitrogen emissions from landfills due to aeration? Waste Management. 135: 457-466.

[10] Sutthasil, N., Chiemchaisri, C., Chiemchaisri, W., Wangyao, K., Towprayoon, S., Endo, K. and Yamada M. 2014. Comparison of solid waste stabilization and methane emission from anaerobic and semi-aerobic landfills operated in tropical condition. Environmental Engineering Research. 19(3): 261-268.

[11] Aziz, A.Q., Aziz, H.A., Yusoff, M.S. and Barshir, M.J.K. 2010. Leachate characterization in semi-aerobic and anaerobic sanitary landfills: a comparative study. Waste Management. 91: 2608-2614.

[12] Nag, M., Shimaoka, T. and Komiya, T. 2016. Impact of intermittent aerations on

leachate quality and greenhouse gas reduction in the aerobic-anaerobic landfill method. Waste Management. 55: 71-82.

[13] Ma, J., Li, Y. and Li, Y. 2021. Effects of leachate recirculation quantity and aeration on leachate quality and municipal solid waste stabilization in semi-aerobic landfills. Environmental Technology and Innovation. 21: 101353.

[14] Lui, K., Lv, L., Li, W., Wang, X., Han, M., Ren, Z., Gao, W., Wang, P., Liu, X., Sun, L. and Zhang, G. 2023. Micro-aeration and leachate recirculation for the acceleration of landfill stabilization: enhanced hydrolytic acidification by facultative bacteria. Bioresource Technology. 387: 129615.

[15] Ko, J.H., Ma, Z., Jin, X. and Xu, Q. 2016. Effects of aeration frequency on leachate quality and waste in simulated hybrid bioreactor landfills. Journal of the Air and Waste Management Association. 66(12): 1245-1256.

[16] Li, W., Sun, Y., Wang, H. and Wang, Y. 2018. Improving leachate quality and optimizing CH_4 and N_2O emissions from a pre-aerated semi-aerobic bioreactor landfill using different pre-aeration strategies. Chemosphere. 209: 839-847.

[17] Traitaned, P. and Sakulrat, J. 2016. Effect of aerated leachate recirculation on decomposition condition in municipal solid waste (MSW) landfill. Thai Environmental Engineering Journal. 30(2): 49-56.

[18] Ma, J., Liu, L., Xue, Q., Yang, Y., Zhang, Y. and Fei, X. 2021. A systematic assessment of aeration rate effect on aerobic degradation of municipal solid waste based on leachate chemical oxygen demand removal. Chemosphere. 263: 128218.

[19] Rendra, S. 2007. Comparative Study of Biodegradation of Municipal Solid Waste in Simulated Aerobic and Anaerobic Bioreactors Landfills. University of Ottawa, Canada.

[20] Morello, L., Raga, R., Lavagnolo, M.C., Pivato, A., Ali, M., Yue, D. and Cossu, R. 2017. The S.An.A.® concept: semi-aerobic, anaerobic, aerated bioreactor landfill. Waste Management. 67: 193-202.

[21] Soil and Plant Analysis Council. 1999. Soil Analysis Handbook of Reference Method. CRC Press. Washington DC.

[22] APHA. 2012. Standard Methods for the Examination of Water and Wastewater, 22nd Edition, American Public Health Association, Washington DC.

[23] Jin, P., Bian, S., Yu, W., Guo, S., Lai, C., Wu, L., Zhao, H., Xiao, K., Liang, S., Yuan, S., Huang, L., Wang, S., Duan, H., Gan, F., Chen, W. and Yang, J. 2023. Insights into leachate reduction in landfill with different ventilation rates: balance of water, waste physicochemical properties, and microbial community. Waste Management. 156: 118-129.

[24] Sun, Y., Sun, X. and Zhao, Y. 2011. Comparison of semi-aerobic and anaerobic degradation of refuse with recirculation after leachate treatment by aged refuse bioreactor. Waste Management. 31: 1202-1209.

[25] Huang, Q., Yang, Y., Pang, X. and Wang, Q. 2008. Evolution on qualities of leachate and landfill gas in the semi-aerobic landfill. Journal of Environmental Sciences. 20: 499-504.

Thai Environmental Engineering Journal Vol. 38 No. 2 (2024) : 65-77
www.eeat.or.th

Assessment of Airborne Microbial Contamination in Cosmetics Manufacturing Facilities: Skincare Cream Production in Thailand

Suda Sinsuwanrak[1*], Piyarat Premanoch[1], Wongsakorn Phongsopitanun[2], Suchart Leungprasert[3], Seree Tuprakay[1] and Nannapasorn Inyim[1]

[1]Faculty of Engineering, Ramkhamhaeng University, Bangkok 10240, Thailand
[2]Faculty of Pharmaceutical Sciences, Chulalongkorn University, Bangkok 10330, Thailand
[3]Faculty of Engineering, Kasetsart University, Bangkok 10900, Thailand
[*]E-mail : sudaning@yahoo.com

Article History; *Received: 19 August 2024, Accepted: 22 August 2024, Published: 30 August 2024*

Abstract

Skincare is a variety of practices to maintain skin integrity, enhance appearance, and alleviating skin conditions. Thailand's skincare market has seen substantial growth, becoming the dominant sub-sector in cosmetics. Microbial contamination in the skincare can occur when the manufacturing process are not well controlled. The objective of this research is to establish criteria for managing appropriate levels of microbial quantities in the air of Good Manufacturing Practice (GMP) cosmetics production facilities. Airborne microbial samples are collected using both active air sampler and settle plate techniques at varying time intervals, followed by a comparative analysis. The skincare creams as representatives showed that the total airborne microbial counts using the air sampling method, ranged from 85 to 252 cfu/m^3. For the settle plate method for 4 and 1 hours ranged from 8 to 90 cfu/4h and 1 to 59 cfu/h. The action limits from control charts at 341 cfu/m^3, 107 cfu/4h, and 59 cfu/h for the respective methods. Based on the results of this research, it can be concluded that the monitoring criteria for cosmetics manufacturing facilities, with a specified limit for airborne microbial counts not exceeding 100 cfu/4h (sterile medicinal products at Grade D) or 50 cfu/h (moderate IMA level).

Keywords : airborne microbial contamination; cosmetics; good manufacturing practice (GMP); indoor air quality; microbial environmental monitoring; monitoring criteria

Introduction

Cosmetic products, as non-sterile health products, require production in clean environments to prevent contamination risks that can compromise product quality, consumer safety, and industry reputation. Although not subjected to the same aseptic standards as vaccine production, high-risk cosmetic products are susceptible to contamination, which can have repercussions on both health and product quality.

Skincare encompasses a range of practices designed to preserve skin integrity, enhance its appearance, and address various skin conditions such as lotions, facial creams, eye creams, sunscreens, skin serums, hair and scalp treatments, and non-colored lip balms. The skincare market in Thailand has witnessed substantial growth in recent years, establishing itself as the predominant sub-sector within the cosmetic industry.

To prevent microbial cross contamination during production, it is imperative to maintain the cleanliness of five key sources: water, raw materials, equipment, personnel, and the environment [1]. FDA data from 2004-2011 reveal that 31% of cosmetic product recalls were attributed to microbial contamination, predominantly the Pseudomonads group, with *Burkholderia cepacia* (formerly *Pseudomonas cepacia*) accounting for 34% of cases. This marked an increase from the 22% prevalence observed during 1998-2006 [2]. Furthermore, between 2002 and 2016, there were 313 cosmetic recalls, with the majority linked to bacterial contamination. These recalls included 14 level 1 recalls (indicating severe health risks), 266 level 2 recalls (associated with temporary health effects), and 33 level 3 recalls (with no significant health concerns) [3].

Due to these global concerns, regulations such as Good Manufacturing Practice (GMP) have gained significance in ensuring the safety and quality of health products. These guidelines focus on controlling personnel hygiene, production facilities, equipment, environmental conditions, manufacturing processes, quality control, and storage.

Microbiological standards for cosmetics establish limits, with a maximum total microbial count (including yeast and mold) of 1000 cfu/g or ml. Prohibited microorganisms in 1 g or 1 ml include *Pseudomonas aeruginosa*, *Escherichia coli*, *Staphylococcus aureus*, and *Candida albicans* [4]. Cosmetics are categorized under various classifications, such as skincare, foundation, powder, hair color, and fragrance products [5]. The risk associated with these products depends on factors such as pH, alcohol content, hydrogen peroxide, filling temperature, and water activity, as detailed in ISO 29621 [6] guidelines for low-risk products. High-risk products, such as skincare creams, can remain susceptible to contamination during production, even within controlled environments, highlighting the necessity for microbiological environmental monitoring.

Criteria of cleanroom for pharmaceutical production

Microbiological Environmental Monitoring (EM) is a means of demonstrating acceptable microbiological quality in a controlled environment and detecting changes in time. It involves collecting data on microbial counts recovered from air, surfaces, and people in pharmaceutical production area. EM describes the microbiological testing for evaluating the cleanliness of manufacturing environments of both sterile and nonsterile products [7]. In the context of sterile pharmaceutical control, EM encompasses four tests: active air samples or volumetric sampling, settle plates, contact plates, and fingerprint sampling during cleanroom monitoring. The limits for microbial EM listed in Table 1 apply exclusively to sterile pharmaceuticals, such as vaccines. These standards serve the purpose of prequalification, distinguishing grades A, B, C, and D, where "A" denotes operations in at-risk areas, "B" for sterile areas, "C" for control areas, and "D" for support areas [8-9].

Table 1 Microbiological cleanliness levels in operation

Grade	Air Sample (cfu/m^3)	Dia. 90 mm. Settle Plate (cfu/4h)	Dia. 55 mm. Contact Plate (cfu/plate)	Glove print (cfu/glove)
A	< 1	< 1	< 1	< 1
B	10	5	5	5
C	100	50	25	-
D	200	100	50	-

Cleanroom environments are established based on ISO 14644-1 and ISO 14698-1 standards to ensure cleanliness and control [10], with the Pharmaceutical and Healthcare Sciences Society [11] consolidating several cleanroom standards. The microbiological limits in cleanrooms are typically classed as follows: Class 100000, comparable to ISO 8 and EU Grade D, with values of 200 CFU/m^3 or settle plates (90 mm) at 100 CFU/4 hours; Class 10000, similar to ISO 7 and EU Grade C, with values of 100 CFU/m^3 or settle plates (90 mm) at 50 CFU/4 hours; and Class 100, which aligns with ISO 6,5 and EU Grade A and B.

Another criterion, as proposed by Pasquarella et al. [12], is the index of microbial air contamination (IMA), which is based on microbial fallout counts on Petri dishes exposed to the air according to the 1/1/1 scheme (for 1 hour, 1 meter from the floor, at least 1 meter away from walls or any obstacles). IMA is classified into five categories: 1) very good: 0-5; 2) good: 6–25; 3) fair: 26–50; 4) poor: 51–75; and 5) very poor: > 76.

However, there is currently a lack of specific microbial contamination control criteria for cosmetics or non-sterile health product manufacturing facilities. This absence of standardized control criteria has left manufacturers without reliable benchmarks. Utilizing criteria from pharmaceuticals may not be suitable for cosmetics due to variations in product characteristics. Implementing stringent control measures such as fumigation to eliminate contaminants within production areas can be costly and disruptive. In contrast, the food industry provides guidelines for microbiological laboratory working areas, setting a limit of no more than 15 cfu/15 minutes (FDA–BAM, 2001).

Salaman [13] advises manufacturers to create their own suitable control criteria by assessing the risks associated with microbial cross-contamination in the environment. Subsequently, control criteria for microbes can be developed through the generation of statistical control charts. Furthermore, Pitzurra et al. [14] recommend generating scientific data to select dependable and appropriate methods tailored to the facility's needs. Validation and verification of these methods should precede implementation. Additionally, it is advisable to establish Standard Operating Procedures (SOPs) concerning environmental microbial sampling, data interpretation, and ensuring precise and consistent understanding among personnel.

This research-intensive approach can pose challenges for microbiologists in industrial settings, as it entails routine work and significant responsibilities. These challenges can be quite demanding for microbiologists in the industry, typically employed in laboratories as quality control or quality assurance officers. Their workload is generally characterized by routine tasks and more.

The objective of this study is to establish criteria for managing appropriate levels of airborne microbial contamination in Good Manufacturing Practice (GMP) cosmetics production facilities to ensure product quality and safety, with a focus on skincare cream production.

Materials and Methods

Selection of Sampling Sites

To comprehensively analyze microbial contamination within the cosmetic cream manufacturing sector, five manufacturing facilities in Thailand were chosen. During the selection process, careful attention was given to identifying high-risk zones characterized by direct interaction between the air and products or raw materials. These zones included areas such as weighing rooms, mixing rooms, semi-product storage rooms, filling rooms, and packaging rooms.

We selected five skincare cream manufacturing facilities certified under the ASEAN Cosmetic GMP guidelines [15], representing the cosmetics industry. The choice to emphasize skincare cream manufacturing is rooted in the significant expansion of the skincare market in Thailand, where skincare has emerged as the dominant sub-sector among all cosmetic categories. The susceptibility of skincare products to microbial contamination arises from insufficient control measures during both the manufacturing process and storage.

Sampling Techniques and Equipment

A multifaceted approach to airborne microbial sampling was employed, utilizing various techniques and equipment: Volumetric Air Sampling - One cubic meter (1 m^3) of air within the manufacturing chambers was

collected using the Sampl'Air Lite device by BIOMERIEUX [8, 16]. Settle Plate Method (4-Hour Exposure) - Standard Petri dishes with a 90 mm diameter were used [8]. Settle Plate Method (1-Hour Exposure, per the Index of Microbial Air Contamination, IMA) - following the 1/1/1 scheme, involving placement 1 meter from the floor and at least 1 meter away from walls or any relevant physical obstacles. Petri dishes with a 90 mm diameter were employed [12].

Environmental parameters that could influence the study outcomes, including personnel count, temperature & humidity [thermo-hygro-meter], and wind speed [anemometer], were measured and recorded.

Culture and Analysis

TSA (Tryptic Soy Agar, [HIMEDIA]) and DG-18 ([HIMEDIA]) were used for bacterial and fungal analysis, respectively [17]. MacConkey Agar ([HIMEDIA]) was employed for the cultivation of Gram-negative bacteria [18]. Bacterial sample agar plates underwent incubation at 35°C for 48 hours, while fungal culture plates were incubated at 25°C for 5-7 days.

Microbial Identification

Following incubation, each sample underwent meticulous examination to determine the presence or absence of colony forming units (CFU). Bacterial identification involved Gram's staining and morphological characterization, while fungal species were identified based on colony and hyphal morphology, with the assistance of staining using lactophenol blue.

The 16S rRNA gene analysis was used for identifying bacterial isolates. 'The amplification and sequencing of the 16S rRNA gene were performed by Macrogen (Seoul, South Korea) using universal primers [19]. BLAST was performed using the EzBiocloud 16S database [20].

Risk assessment

To conduct a risk assessment for microbial contamination, we will assess the "likelihood" and "impact" of contamination. Likelihood is associated with the contamination rate from the airborne environment, expressed as a percentage of the contamination rate (% CR). Meanwhile, the impact pertains to the results of total microbial and Gram-negative bacterial counts that the cosmetic product is from each production room, as presented in Table 2

Table 2 The five levels of impact from the the microbial count and types

Score Level	Microbial count and types (CFU)	Impact Level
1	Total count <10 & No Gram -	Negligible
2	Total count 10-100 & No Gram -	Minor
3	Total count 100-500 & No Gram -	Moderate
4	Total count 500-1000 and/or found Gram -	Major
5	Total count >1000 and/or found Gram -	Critical

To evaluate this, we will create a risk matrix based on the likelihood-impact relationship, using the % CR values to generate likelihood tables for contamination at five levels, as presented in Table 3. The likelihood levels are determined by referencing the IMA table, and the maximum value in each IMA table range is used to calculate the contamination rate (%CR) according to Sandle's Numerical Approaches to Risk Assessment [7] as follow;

$$\%\,CR = \text{Settle plate count} \times \frac{\text{Area of product}}{\text{Area of Petri-dish}} \times \frac{\text{Time product exposure}}{\text{Time settle plate}} \times 100$$

%CR calculation is based on the surface area of the product, determined by the cross-sectional area of the cream container (4 cm) and the surface area of the agar plate (9 cm). The product's exposure to air lasts 1 minute, while the agar plate is exposed for 1 hour, following the IMA method.

Table 3 The five likelihood levels of microbial contamination

Likelihood Level	IMA value	% Contamination rate (%CR)	Score Level
Very good	0 - 5	< 2 %	1
Good	6 - 25	>2 - 8 %	2
Fair	26 - 50	>8 - 16 %	3
Poor	51 - 75	>16 - 25 %	4
Very poor	> 75	> 25 %	5

We can multiply each likelihood and impact level to establish the risk matrix shown

in Table 4. The microbial contamination risk can be estimated from the risk matrix. This matrix contains five colored boxes. The red boxes are very high-risk, the orange boxes are high-risk, the yellow boxes are moderate-risk, the light blue boxes are low risk, and the green boxes are very low-risk.

Table 4 The risk matrix by multiplying likelihood and impact

Matrix	Impact level					
Likelihood Levels	Risk Rating	Negligible	Minor	Moderate	Major	Critical
	Frequent	5	10	15	**20**	**25**
	Probable	4	8	12	**16**	**20**
	Occasional	3	6	9	12	15
	Remote	2	4	6	8	10
	Improbable	1	2	3	4	5

The control chart calculation

The Shewhart Control Chart Method [21] involves establishing statistical control criteria by sampling microbial data. Typically, 20-30 consecutive samples are collected to construct a variable control chart. The mean and standard deviation (SD) are calculated to set the warning limit at mean ± 2SD and the action limit at mean ± 3SD, providing a robust framework for monitoring and controlling contamination risks.

Results and Discussion

Airborne Microbial Assessment in Cosmetics Manufacturing Factories

1. **Factory 1: skincare creams and powder**

Microbial counts in the air at critical points within Factory 1 were sampled in 9 rooms. It was found that the total microbial count in the air, using the air sampling method, ranged from 87 to 252 cfu/m^3 (colony-forming units per cubic meter). Count placed on agar plates for 4 hours ranged from 9 to 49 cfu/4h, and those placed on agar plates for 1 hour ranged from 1 to 18 cfu/h, as shown in Table 5. The fungal count in the air, using the same air sampling method, ranged from 87 to 203 cfu/m^3 and agar plates for 4 hours, ranged from 10 to 45 cfu/4h. The gram-negative bacterial count in the air, using agar plates for 4 hours, ranged from 0 to 5, as shown in Table 7.

It was observed that the total microbial count in the air in all rooms was relatively low when compared to the microbial control standards for cosmetics. However fungal counts obtained from air sampling were also high (87 to 203 cfu/m^3) which is above the ISO 7218 [22] recommendation that suggests using agar plates with a diameter of 90 mm for fungal counts with a range between 10-150 cfu (for bacteria, the range should be between 10-300 cfu). Therefore, in the subsequent research within the factory, the fungal testing was discontinued using the air sampling method.

2. **Factory 2: skincare creams**

Microbial counts in the air at critical points within Factory 2 were sampled in 5 rooms. It was found that the total microbial count in the air, using the air sampling method, ranged from 105 to 240 cfu/m^3. Count placed on agar plates for 4 hours ranged from 25 to 90 cfu/4h, and those placed on agar plates for 1 hour ranged from 14 to 41 cfu/h, as shown in Table 5. The fungal count in the air on agar plates for 4 hours, ranged from 18 to 74 cfu/4h. The gram-negative bacterial count in the air, using agar plates for 4 hours, ranged from 0 to 1, as shown in Table 7.

3. **Factory 3: skincare, mascara, hair dye**

Microbial counts in the air at critical points within Factory 3 were sampled in 14 rooms. It was found that the total microbial count in the air from skincare and makeup products, using the air sampling method, ranged from 108 to 270 cfu/m^3. Count placed on agar plates for 4 hours ranged from 26 to 164 cfu/4h, and those placed on agar plates for 1 hour ranged from 4 to 58 cfu/h.

The airborne microbial assessment of hair dye products, conducted using the air sampling method, revealed a range of 262 to 400 cfu/m^3. The counts placed on agar plates for 4 hours varied from 134 to 701 cfu/4h, while those placed on agar plates for 1 hour showed a range of 52 to 100 cfu/h, as detailed in Table 3.

Observations were carried out in the Hair Care Mixing A room, designated for hair dye mixing. The total microbial count in this room reached as high as 701 cfu/4h and 100 cfu/h. This elevation in microbial counts can be attributed to the use of water spray within the room to regulate temperature, resulting in a substantial increase in airborne contamination levels. However, the air

sampling method yielded a lower count of 400 cfu/m^3. This variance may be associated with the air sampling technique, which entails drawing air through approximately 300 holes.

The fungal count in the air on agar plates for 4 hours, ranged from 5 to 110 cfu/4h. The gram-negative bacterial count in the air, using agar plates for 4 hours, ranged from 0 to 91, as shown in Table 7.

4. Factory 4: skincare creams

The results of microbial analysis in the air within Factory 4 which only skincare creams products were examined in 6 rooms. It was found that the total microbial count in the air, using the air sampling method ranged from 85 to 240 cfu/m^3, agar plates for 4 hours and 1 hour ranged from 8 to 34 cfu/4h. and 1 to 26 cfu/h, respectively as shown in Table 5. The fungal count in the air, using agar plates incubated for 4 hours, ranged from 3 to 17 cfu. The gram-negative bacterial count in the air, using agar plates incubated for 4 hours, ranged from 0 to 3.

5. Factory 5: skincare creams and powder

The results of microbial analysis in the air within Factory 5, were examined in 7 rooms. It was found that the total microbial count in the air, using the air sampling method and agar plates incubated for 4 hours and 1 hour, ranged from 124 to 242 cfu/m^3, 37 to 73 cfu/4h, and 16 to 59 cfu/h, respectively. as shown in Table 5. The fungal count in the air, using agar plates incubated for 4 hours, ranged from 28 to 74 cfu, and no gram-negative bacteria were detected in the air.

From all the data, Factory 4 had the lowest microbial count, with production room walls and ceilings made of ISOWALL and PU (Polyurethane) flooring, both of which are easy to clean. The next lowest microbial count was found in Factory 1, where, despite using smooth concrete or partition walls, the facility was well-managed and maintained in terms of cleanliness.

The comparison of results from airborne microbial examinations across 41 rooms in five Cosmetics Manufacturing Factories showed that using the air sampler with the European Union Good Manufacturing Practice (EU GMP) method [8], and a settle plate for 4 hours with the EU GMP method, and a settle plate for 1 hour with the IMA method, yielded mean values of 194 cfu/m^3, 84 cfu/4h, and 28 cfu/h, respectively. The corresponding standard deviations (SD) were 84 cfu/m^3, 116 cfu/4h, and 24 cfu/h. Elevated SD values, surpassing the mean, raise concerns about data reliability. Individual factory analysis revealed that Factory 3 had significantly higher levels of total microbes, gram-negative bacteria, and fungi compared to others. To identify outliers, a Huge Error method was applied, uncovering values exceeding 4 for all hair care production rooms and some skincare production rooms.

Consequently, an additional risk assessment was conducted to validate the reliability of the test results, focusing on product types: skincare, makeup, and hair care products. Each production area for different cosmetic product groups was distinctly separated according to their respective categories. The outcomes of this risk assessment led to the following conclusions:

Risk assessment for cosmetics plant

The results of the risk assessment for the cosmetics manufacturing plant indicate that, during the risk identification survey of the production area in Factory 3, it was found that this factory produces skincare, makeup, and hair care products. Samples of airborne microbes were collected in 14 risk rooms, which are rooms directly in contact with raw materials and products, as illustrated in the factory layout in Figure 1

According to Table 6, the raw material weighing and mixing rooms in Factory 3 pose the highest risk probability, reaching level 5. Similarly, three packing rooms also exhibit the highest risk probability, yet the microbial quantities for each product in these rooms are minimal (less than 10 cfu/g), with no gram-negative bacteria, resulting in negligible impact levels. The risk matrix by multiplying likelihood and impact, places the overall risk levels between 1 and 3, deemed acceptable (see Table 4).

The comprehensive analysis of airborne microbial contamination risk in Factory 3 indicates the production of various cosmetic groups, spanning skincare, makeup, and hair care. Notably, the hair care group has comparatively lower cleanliness standards, resulting in a medium risk level.

Table 5 Comparison method of air sampling, settle plates 4 hours and 1 hour from 5 cosmetics factories

Factory	Room	Air Sampler (cfu/m^3)	90 mm. Settle Plate (cfu/4h)	90 mm. Settle Plate (cfu/h)
1	Raw Material Weighing	222	20	N/D
	Cream Mixing	87	13	2
	Skin Cream Filling	252	49	18
	Dust Powder Mixing	121	9	4
	Dust Powder Filling	115	18	5
	Cake Powder Mixing	116	14	1
	Powder Grinding	124	40	15
	Powder Sieving	105	32	15
	Cake Powder Pressing	91	30	10
2	Raw Material Weighing	162	84	32
	Cream Mixing Room	240	60	41
	Semi-product Storage	105	25	14
	Skin Cream Filling F1	156	54	14
	Skin Cream Filling F2	195	90	36
3	Raw Mat. Weighing YK	135	81	24
	Raw Mat. Weighing NB	197	103	36
	Skin Care Mixing D	270	42	16
	Cream Filling A	250	151	49
	Skin Care Filling K	208	104	37
	Skin Care Filling L	135	164	58
	Make up Filling M	161	38	25
	Make up Filling N	108	26	4
	Raw Mat. Weighing Fl.1	368	229	66
	Hair Care Mixing A	400	701	100
	Hair Care Mixing B	350	205	52
	Hair Care Mixing H	265	134	61
	Hair Care Filling C	262	222	71
	Hair Care Filling D	391	199	69
4	Raw Mat. Weighing 1	240	32	16
	Raw Mat. Weighing 2	219	18	9
	Cream Mixing	85	8	1
	Bulk & Labelling	194	34	2
	Cream Filling	127	9	6
	Assembly	95	34	26
5	Raw Mat. Weighing	235	54	21
	Drying	124	52	24
	Cream Mixing	212	73	59
	Semi-product Storage	241	37	22
	Cream Filling	208	60	28
	Packaging & Labelling	242	56	25
	Storage	137	44	16
	Average / Mean	194	84	28
	Standard Deviation	84	116	24

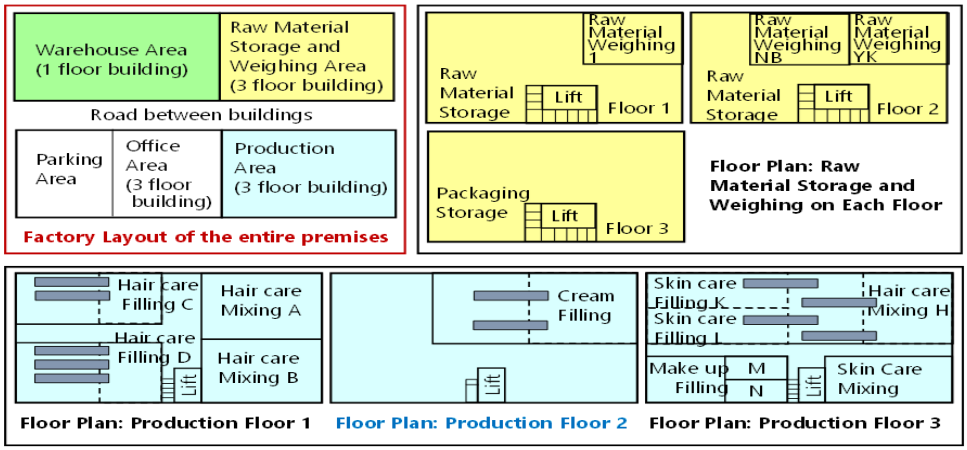

Figure 1 Layout of Factory 3 – Cosmetic Production plant skincare, mascara, hair dye

Table 6 Contamination rate values (% CR) for all 14 risk rooms in Factory 3 to determine the likelihood level

Room in Factory 3	Settle Plate (cfu/h)	Area of product	Time product exposure	% CR	Likelihood level
Raw Mat.Weigh YK	24	79	2	99	5
Raw Mat.Weigh NB	36	79	2	148	5
Skin Care Mixing	16	50	3	63	5
Cream Filling	49	7	1	9	3
Skin Care Filling K	37	0.5	1	19	4
Skin Care Filling L	58	20	1	30	5
Make up Filling M	25	7	1	5	2
Make up Filling N	4	1	1	0.1	1
Raw Mat. Weigh 1	66	79	2	272	5
Hair Care Mixing A	100	7	3	395	5
Hair Care Mixing B	52	50	3	205	5
Hair Care Mixing H	61	39	1	62	5
Hair Care Filling C	71	39	1	72	5
Hair Care Filling D	69	7	1	13	3

Table 7 The environment on microbial quantities in the air

Factory	Temperature (C)	Relative Humidity (%)	Wind speed (km/h)	Total Microbial Count (cfu/4 h)	Fungi (cfu/4 h)	Gram Neg. (cfu/4 h)
1	23.3 – 33.5	36.1 – 63.5	0 – 1.7	9 - 69	10 - 45	0 - 5
2	25.6 – 30.6	59.7 – 71.9	0 – 2.0	25 - 90	18 - 74	0 - 1
3	18.4 – 31.2	46.5 – 66.8	0 – 1.9	8 - 701	5 - 110	0 - 91
4	21.1 – 28.8	45.1 – 56.0	0 – 0.8	8 - 34	3 - 17	0 - 3
5	19.7 – 25.5	40.5 – 58.9	0 – 0.1	37 - 73	28 - 74	0

The influence of the environment on microbial quantities in the air

The results of microbial testing in the air of each room were examined in relation to the environmental conditions to assess the influence of the environment on microbial quantities in the air, as detailed in Table 7. It was found that environmental factors such as temperature, humidity, and wind speed in each room of all five factories did not show a significant correlation with the quantity of microbes in the air. Generally, the temperature in each room, measured in each factory, ranged from 20-33°C, which is a normal temperature range for microbial growth. Meanwhile, the relative humidity in the air generally ranged between 40-60%, with some rooms having humidity exceeding 60%, posing a higher risk of mold formation. Rooms with humidity below 40% were drier, and moisture from agar plates could be released into the air, potentially affecting the microbial assessment results [23].

Regarding wind speed within the rooms, the measured values were generally low. Continuous sampling throughout the year revealed that temperature and relative humidity influenced higher concentrations of airborne fungi during the rainy season, aligning with the findings of studies conducted in chocolate factories [24] and in post-harvest fruit environments [25]. These studies demonstrated that temperature and humidity played a role in increased airborne fungal concentrations during the rainy season.

The classification of microbiology in the air of cosmetic manufacturing

The classification of microbial types in the air of cosmetic manufacturing factories 1 to 5 revealed variations among the factories. The percentages for Gram-positive cocci were 78, 62, 63, 75, and 3%; Gram-positive rods were 7, 16, 16, 15, and 3%; Gram-negative bacteria were 13, 2, 4, 9, and 0%. As for molds, the percentages were 2, 20, 1, 1, and 93%. Additionally, Gram-positive filamentous bacteria were found to be 1%. A detailed comparison of microbial classification for each cosmetic factory in Figure 2.

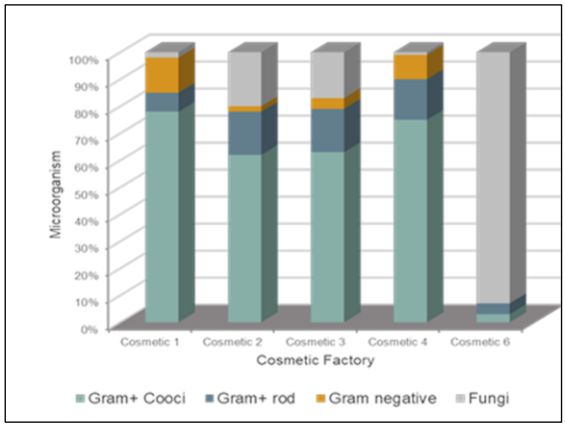

Figure 2 Comparison of type of Microorganism

In general, the predominant bacteria found in most factories were Gram-positive cocci, ranging from 62% to 78%. These bacteria are commonly present on human skin. Factory 5, however, showed a dominance of fungi as the primary microorganisms, reflecting the influence of external air where molds are prevalent (299 cfu/4h or 87%). Despite efforts to control microbial levels, Factory 5 continued to have proportions similar to those found outside.

These research findings align with the study conducted by Sandle [26], which investigated bacteria in cleanrooms with over 9000 samples over 9 years. The study found that Gram-positive cocci, originating from human skin, accounted for 81%, 63%, and 41% in Grade A-B, C, and D rooms, respectively. Gram-positive rods, sourced from soil, followed, and Gram-negative bacteria, derived from water and raw materials, were also identified. Fungi (only molds) constituted 1-8%, with higher prevalence in humid conditions [27].

The identification of bacteria and fungi in the air of cosmetic manufacturing

The results of sequencing the 16S rRNA gene show that the bacteria can be classified at the species level, as indicated in Table 8. Additionally, the fungi were classified at the genus level based on morphology of the conidia using a light microscope. All detected bacteria are non-prohibited types in cosmetics.

Table 8 Identification of microbial contaminants in cosmetics manufacturing factories

Microbial types	Genus / Species
Gram-positive cocci	*Brachybacterium muris*, *Kocuria rhizophila*, *Macrococcus brunensis*, *Micrococcus luteus*, *Mammaliicoccus sciuri*, *Staphylococcus argenteus*, *Staphylococcus caprae*, *Staphylococcus haemolyticus*, *Staphylococcus ureilyticus*, *Staphylococcus hominis* subsp. *Hominis*
Gram-positive rod	*Bacillus cereus*, *Bacillus paramycoides*, *Bacillus paranthracis*, *Bacillus siamensis*, *Bacillus pumilus*, *Bacillus siamensis*, *Brevibacterium casei*, *Cytobacillus firmus*, *Exiguobacterium acetylicum*, *Mesobacillus thioparans*, *Priestia aryabhattai*
Gram-positive filamentous bacteria	*Streptomyces parvulus*
Gram-negative bacteria	*Acinetobacter baumannii*, *Pantoea stewartii* subsp. *indologenes*, *Pseudomonas stutzeri*, *Pseudomonas oleovorans* subsp. *oleovorans*, *Stutzerimonas stutzeri*
Fungi	*Penicillium* sp., *Aspergillus* sp.

Guidelines for controlling microbes in the air of cosmetics manufacturing

In situations where there are no explicit regulations or standards defining microbial control parameters for the air within cosmetics manufacturing factories, statistical calculations become necessary. For example, the Shewhart Control Chart Method [21] can be employed.

Based on microbial air assessment data from four skincare cosmetics manufacturing factories (a total of 27 samples), mean values were calculated as 18 cfu/h, 39 cfu/4h, and 165 cfu/m^3, with corresponding standard deviations of 14, 23, and 59, respectively. Utilizing these values, warning limits for each method were determined as 45 cfu/h, 84 cfu/4 h, 282 cfu/m^3. Action limits were set at 59 cfu/h, 107 cfu/4h, 341 cfu/m^3, as illustrated in Figure 3. This approach aligns with Salaman [13] suggesting manufacturers can establish suitable control criteria by evaluating the risk of environmental cross-contamination and comparing continuous microbial assessment results with risk assessment reports. Subsequently, control criteria can be defined through statistical control chart creation, considering warning and action levels for existing bioburden in water for pharmaceutical production [28].

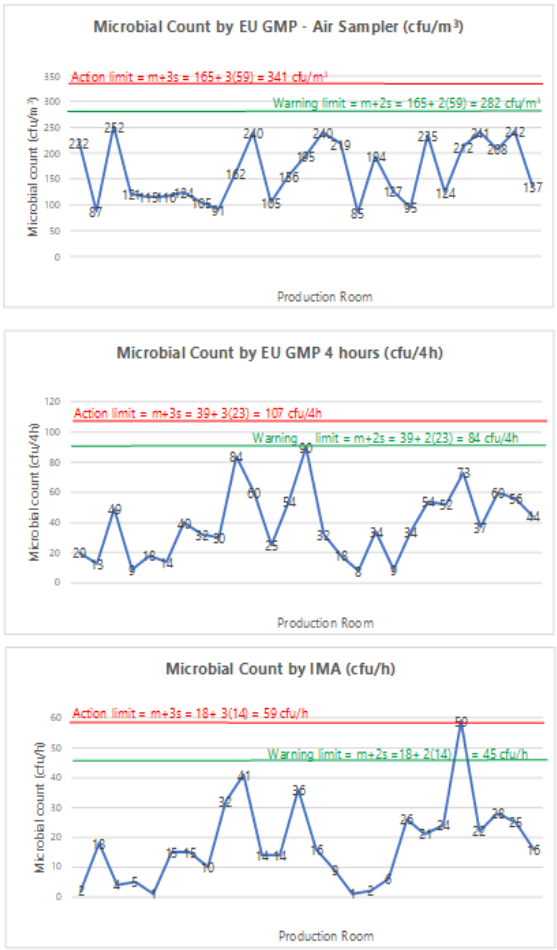

Figure 3 Shewhart Control Chart of air sampling, settle plates 4 hours and 1 hour from skincare cream rooms.

Adopting guidelines from EU GMP [8], the airborne microbial assessments conducted in each skincare factory revealed total microbial counts ranging from 8 to 90 cfu/4h. These values consistently remained below 100 cfu/4h. According to the EU GMP method, the recommended limits for microbiological monitoring in clean areas during operation involve the use of the settle plate technique for 4 hours at Grade D level (areas where

pharmaceutical products are not directly exposed to air). The established warning limit is 84 cfu/4h., and the action limit is 107 cfu/4h., which closely aligns with the 100 cfu/4h criteria. Therefore, it is advisable to establish criteria that do not exceed 100 cfu per 4 hours, in accordance with pharmaceutical regulations.

Derived from the Index of Microbial Air Contamination (IMA) [12], the one-hour settle plate method revealed counts ranging from 1 to 59 cfu/h. Applying the IMA criteria, these counts do not exceed 50 cfu per hour, indicating a fair class. The established warning limit is 45 cfu/h, and the action limit is 59 cfu/h, closely aligned with the 50 cfu/h criteria. Therefore, it is recommended to establish criteria that do not exceed 50 cfu/h, in accordance with the IMA.

However, the active air sampler method in these skincare facilities cannot comply with the guidelines from EU GMP [8] which recommends limits at Grade D level of 200 cfu/m^3. This is evident as the airborne microbial assessments conducted in each skincare factory revealed total microbial counts ranging from 85 to 252 cfu/m^3. The established warning limit is 282 cfu/m^3, and the action limit is 341 cfu/m^3, exceeding the value specified by the EU GMP method for Grade D level. Despite the fact that air sampling devices offer the advantage of providing more detailed information on microbial quantities compared to the basic method of placing agar plates, active air sampling is not commonly employed in most cosmetics factories due to its high cost (150,000 - 300,000 Baht). Therefore, the study recommends a suitable method for microbial sample collection in cosmetics factories, suggesting the use of the settle plate method for both 4 hours and 1 hour.

The statistical analysis and risk assessment underscore the importance of selecting cosmetic product groups for airborne microbial control. This stems from the notably high total microbial count observed in the production area for hair care products. However, the risk assessment maintains an acceptable level due to the low risk of microbial contamination in certain products, such as hair dye, containing substantial amounts of ammonia and hydrogen peroxide. Consequently, the recommendation is to prioritize cosmetic product groups that necessitate microbial control in the air, with a specific focus on collecting samples from high-risk products, in accordance with ISO 29621 [6] standards, particularly within the domain of skincare cosmetics.

Conclusions

The assessment of airborne microbes in cosmetics manufacturing factories 1, 2, 4, and 5 revealed variations in microbial counts, highlighting differences in contamination levels across these facilities. Despite these levels, the overall risk of contamination is manageable according to the risk matrix. Factory 3, producing low-risk hair dye products with high hydrogen peroxide levels, does not require stringent microbial control measures.

Routine operations can rely solely on testing for total microbial counts, as neither fungal nor Gram-negative bacterial counts were observed. Predominant bacteria, identified as Gram-positive cocci ranging from 62% to 78%, were consistent with those commonly found on human skin. If source verification is necessary, selective media for Gram-positive bacteria can be employed, as indicated in the study.

Given the quasi-field experimental nature of this study within active production facilities adhering to GMP for cosmetics, the influence of environmental factors (temperature, humidity, and wind speed) on microbial air quality control, as per GMP guidelines, might not be prominently discernible.

The establishment of control charts in alignment with statistical principles resulted in action limits set at 59 cfu/h, 107 cfu/4h, and 341 cfu/m^3 for the respective methods. Adherence to monitoring criteria in cosmetics manufacturing facilities should follow specified limits for airborne microbial counts, ensuring they do not surpass 100 cfu/4h (Grade D for sterile medicinal products) or 50 cfu/h (fair IMA level). Active air sampling is infrequently utilized in the majority of cosmetics factories.

Acknowledgments

The authors would like to thank Asst. Prof. Dr. Ek Sangvichien, Faculty of Science, Ramkhamhaeng University, for supporting the volumetric air sampler in this study.

References

[1] The United States Pharmacopeial Convention. 2018. The United States Pharmacopeia and the National Formulary (USP 41-NF36). Rockville, MD.

[2] Sutton, S. and Jimenez, L. 2012. A Review of Reported Recalls Involving Microbiological Control 2004-2011 with Emphasis on FDA Considerations of "Objectionable Organisms". American Pharmaceutical Review. http://www.americanpharmaceuticalreview.com/Featured-Articles/38382-A-Review-of-Reported-Recalls-Involving-Microbiological-Control-2004-2011-with-Emphasis-on-FDA-Considerations-of-Objectionable-Organisms/

[3] Franki, R. 2018. Bacterial contamination behind most cosmetics recalls. Dermatology News. https://www.mdedge.com/dermatology/article/191072/health-policy/bacterial-contamination-behind-most-cosmetics-recalls

[4] ISO 17516. 2014. Cosmetics - Microbiology - Microbiological limits. The International Organization for Standardization, Geneva.

[5] Regulation (EC). 2009. No 1223/2009 of the European Parliament and of the Council of 30 November 2009 on cosmetic products.

[6] ISO 29621. 2017. Cosmetics - Microbiology - Guidelines for the risk assessment and identification of microbiologically low-risk products. The International Organization for Standardization, Geneva.

[7] Sandle, T. 2019. Biocontamination Control for Pharmaceuticals and Healthcare. Academic Press, London.

[8] European Commission. 2008. Good Manufacturing Practice (EU GMP) guidelines. European Commission.

[9] World Health Organization. 2011. WHO Technical Report Series, No. 961, Annex 6. WHO Good Manufacturing Practices for sterile pharmaceutical products. http://www.who.int/medicines/areas/quality_safety/quality_assurance/GMPSterilePharmaceutical ProductsTRS961 Annex6.pdf

[10] World Health Organization. 2012. Environmental Monitoring of Clean Rooms in Vaccine Manufacturing Facilities, E.M.a.H.P. (EMP), Editor. World Health Organization, Geneva.

[11] Parenteral Drug Association (PDA). 2001. Fundamentals of an Environmental Monitoring Program. Technical Report No. 13 Revised - Supplement TR13. 55(5).

[12] Pasquarella, C., Pitzurra, O. and Savino, A. 2000. The index of microbial air contamination. Journal of Hospital Infection. 46(4): 241-256.

[13] Salaman-Byron, A.L. 2018. Limitations of Microbial Environment Monitoring Methods in Cleanrooms. American Pharmaceutical Review. https://www.americanpharmaceuticalreview.com/Featured-Articles/349192-Limitations-of-Microbial-Environmental-Monitoring-Methods-in-Cleanrooms/

[14] Pitzurra, M., Savino, A., and Pasquarella, C. 1997. LINEE GUIDA Il monitoraggio microbiologico negli ambienti di lavoro Campionamento e analisi Il Monitoraggio ambientale microbiologico (MAM). Annali di Igiene, 9: 439-454. https://www.inail.it/cs/internet/docs/alg-il-monitoraggio-microbiologico-negli-ambienti-lavoropdf.pdf

[15] ASEAN Cosmetic Committee. 2003. ASEAN Guidelines for Cosmetic Good Manufacturing Practices. http://www.fda.moph.go.th/sites/Cosmetic/SitePages/ViewGMP.aspx?IDitem=4

[16] ISO 16000-18. 2011. Indoor air Part 18: Detection and enumeration of moulds - Sampling by impaction. The International Organization for Standardization, Geneva.

[17] ISO 11133. 2014. Microbiology of food, animal seed and water - Preparation, production, storage and performance testing of culture media. The International Organization for Standardization, Geneva.

[18] American Public Health Association (APHA). 1999. Standard Methods for the Examination of Water and Wastewater. American Water Works Association, Water Environment Federation, Washington DC. #9215

[19] Lane, D. J. 1991. 16S/23S rRNA sequencing. In: E. Stackebrandt & M. Goodfellow (Eds.), Nucleic Acid Techniques in Bacterial Systematics. John Wiley and Sons, New York. 115-175.

[20] Yoon, S.H., Ha, S.M., Kwon, S. and add *et. al*. 2017. Introducing EzBioCloud: a taxonomically united database of 16S rRNA gene sequences and whole-genome assemblies. International Journal of Systematic and Evolutionary Microbiology. 67(5): 1613-1617.

[21] ISO 8258. 1991. Shewhart control charts. The International Organization for Standardization, Geneva.

[22] ISO 7218. 2007. Microbiology of food and animal feeding stuffs – General requirements and guidance for microbiological examinations. The International Organization for Standardization, Geneva.

[23] Sandle, T. 2020. Microbiological environmental monitoring - a review of current standards. [Webinar]. https://www.youtube.com/watch?app=desktop&v=nTpWcwjfmfE

[24] Anaya, M., Gámez-Espinosa, E., Falco, A.S., Benítez, E., and Carballo, G. 2019. Characterization of indoor air mycobiota of two locals in a food industry, Cuba. Air Quality, Atmosphere & Health. 12: 797-805.

[25] Scholtz, I., Siyoum, N. and Korsten, L. 2017. Penicillium air mycoflora in postharvest fruit handling environments associated with the pear export chain. Postharvest Biology and Technology. 128: 153-160.

[26] Sandle, T. 2011. A Review of Cleanroom Microflora: Types, Trends, and Patterns. PDA Journal of Pharmaceutical Science and Technology. 65(4): 392-403. https://journal.pda.org/content/65/4/392

[27] Dao, H., Lakhani, P., Police, A., and add *et. al*. 2017. Microbial Stability of Pharmaceutical and Cosmetic Products. AAPS PharmSciTech. 19(1): 60-77. https://doi.org/10.1208/s12249-017-0875-1

[28] Clontz, L. 2008. Microbial limit and bioburden tests: validation approaches and global requirements (2nd ed.). https://pharmprobeg.ru/download/Suzdal_2021-05/Lucia_Clontz_Microbial_Limit_and_Bioburden_TestsBookFi.org1_.pdf

Thai Environmental Engineering Journal Vol. 38 No. 2 (2024) : 79-90
www.eeat.or.th

Adsorption Mechanisms of Haloacetonitriles on Adsorbent Derived from Canvas Fabric

Kanlayanee Yimyam[1,2,3], Aunnop Wongrueng[3] and Pharkphum Rakruam[3*]

[1]Graduate School, Chiang Mai University, Chiang Mai 50200, Thailand
[2]Doctor of Engineering Program in Environmental Engineering, Faculty of Engineering, Chiang Mai University, Chiang Mai 50200, Thailand
[3]Department of Environmental Engineering, Faculty of Engineering, Chiang Mai University, Chiang Mai 50200, Thailand
[*]E-mail : pharkphum@eng.cmu.ac.th

Article History; *Received: 23 August 2024, Accepted: 26 August 2024, Published: 30 August 2024*

Abstract

The adsorption mechanisms of HANs on canvas fabric-derived adsorbent and modified adsorbent with ferric chloride and ferric nitrate solution were investigated. With the ferric nitrate modification (CF-Fe$(NO_3)_3$), the pore structure of the adsorbent was mesopore, while other adsorbents were micropore. With the mesopore structure of CF-Fe$(NO_3)_3$, the adsorption occurred both on the outer pore layer and inside the pore surface, which resulted in the highest adsorption efficiency obtained by the CF-Fe$(NO_3)_3$ adsorbent. Furthermore, the adsorption mechanisms of five HAN species were investigated. Physical adsorption is the main mechanism of HANs on CF-Fe$(NO_3)_3$ adsorbent based on the low adsorption energy determined from the D-R isotherm. The fastest HAN species to reach equilibrium and the highest removal by the CF-Fe$(NO_3)_3$ adsorbent was TCAN, which has the lowest solubility and more hydrophobicity. Besides the low solubility of HANs species, the halogen atom of each HANs species also affected the removal efficiency. HANs species with more halogen atoms showed higher removal efficiency than other HANs species with low halogen atoms.

Keywords : adsorption kinetics; adsorption isotherm; chemical activation; haloacetonitriles; low-cost adsorbent

Introduction

Critical to the process of treating drinking water is disinfection. Its objective is to assist in the destruction of waterborne pathogens. The chlorine chemicals used to disinfect water sources not only stop the growth of various pathogens, but they can also react with organic and inorganic compounds to create disinfection by-products (DBPs) [1]. Currently, research shows that aromatic DBPs [2] and nitrogen-containing DBPs (N-DBPs) [3] are more harmful than controlled DBPs. Haloacetonitriles (HANs) are a category of N-DBPs that are detected in disinfected drinking water [4]. Dichloroacetonitrile (DCAN) was the most commonly found HANs compound among the 9 HANs species, followed by bromochloroacetonitrile (BCAN) and dibromoacetonitrile (DBAN) [5, 6]. Its carcinogenic and mutagenic characteristics render it a significant threat to human health [7, 8].

There are various available techniques applied for the removal of HANs, including boiling [9, 10], photocatalytic degradation [11], degradation with the UV/peroxymonosulfate process [12], catalytic hydrolysis [13], and adsorption [14]. The adsorption technique is one of the most prominent methods for removing

HANs from contaminated water. Previous research has examined the absorption of haloacetonitriles using polymerizable surfactant-modified mesoporous silica. The incorporation of a polymerizable surfactant was discovered to enhance the efficacy of HANs adsorption. Furthermore, as the degree of halogen substitution in the HANs molecule increased, so did its hydrophobicity. This had an effect on the organic partition's ability to adsorb things [15]. Later in 2019, Prarat et al. investigated the mechanisms and effects of porous structures on the adsorption of haloacetonitriles on silica-based materials. The researchers discovered that the crystalline and porous structures of the materials, specifically the size and volume of the pores as well as the surface functional group of the adsorbent, had a significant impact on the adsorption of HANs.

Besides the sorbents that have been previously mentioned, activated carbon is an additional intriguing sorbent. Activated carbons are efficient adsorbents widely utilized in various applications, including medical purposes, gas storage, pollutant and odor elimination, gas purification and separation, and catalysis [16]. Numerous varieties of DBPs were adsorbed on activated carbon. Qian et al. [17] investigated the adsorption of haloforms by five various granular activated carbons (GACs). The Freundlich model performed well in describing adsorption isotherms, while the pseudo-second-order model performed well in describing adsorption kinetics. The rate-limiting process was identified as film diffusion, while haloforms were adsorbed through chemical adsorption. In general, there was no relationship between the quantity of haloform adsorption and the surface area of GAC. According to research by Nakamura et al. [18], the amount of absorbed trihalomethane is related to the level of hydrophobicity of the activated carbon fiber surface. The degree of adsorption for trihalomethane containing bromine was greater than that containing chlorine. The polarity of trihalomethane molecules can explain the variations in the amounts adsorbed among trihalomethanes.

Currently, the production of activated carbon uses low-cost materials like durian shells [19], bamboo, coconut shells [20], and fabric [21]. Fabric is an interesting substance that can be used as an adsorbent because its primary component is carbon [22]. Furthermore, there has been a significant increase in the amount of textile waste [23]. Consequently, this issue poses a challenge, necessitating the exploration of recycling or utilization methods to address these concerns.

For an understanding of the adsorption mechanism, this study focused on investigating the relationship between the porous structures of the adsorbent derived from canvas fabric and the adsorption efficiency of DBAN at low concentrations. The data from the experiments were matched with adsorption isotherm models, and the kinetic parameters were figured out to find the most likely adsorption mechanism(s). In addition, the effect of the five species of HANs including BCAN, DBAN, DCAN, monobromoacetonitrile (MBAN), and trichloroacetonitrile (TCAN) on the adsorption mechanism was also investigated.

Methodology

Adsorbent Synthesis

This study synthesized the canvas fabric-derived adsorbent. The methodology for synthesizing canvas fabric derived adsorbent was reported in a previous study [24]. Two ferric chemical solutions were used to activate the adsorbent including ferric chloride ($FeCl_3$) and ferric nitrate ($Fe(NO_3)_3$). The methodology for adsorbent activation was also reported in a previous study [24]. This study used three different adsorbents: canvas fabric-derived adsorbent (CF), activated canvas fabric-derived adsorbent with ferric chloride (CF-$FeCl_3$), and activated canvas fabric-derived adsorbent with ferric nitrate (CF-$Fe(NO_3)_3$). The BET surface areas of CF, CF-$FeCl_3$, and CF-$Fe(NO_3)_3$ are 262.51, 577.25, and 370.83 m^2/g, respectively.

Adsorption Kinetics Experiments

The adsorption kinetics experiments were divided into two experiments. The first experiment examined DBAN adsorption kinetics using CF, CF-$FeCl_3$, and CF-$Fe(NO_3)_3$ adsorbents. In this experiment, DBAN was used to represent HANs. DBAN was prepared as a stock solution by mixing in a 10 mM phosphate buffer at pH 7. The adsorption kinetics were

conducted by using each adsorbent at 0.1 g with an initial DBAN concentration of 50 µg/L. The volume of each sample was fixed at 100 mL. The experiment was performed under shaking at 200 rpm at room temperature by varying the contact time from 0 to 300 minutes. The pH was controlled at 7. The water samples were filtrated through a 0.22 µm nylon unit filter and measured for the remaining DBAN concentration. The residual DBAN concentration in the liquid solution was determined by using a gas chromatograph combined with an electron capture detector (GC/ECD) (Hewlett Packard, HP6890 GC, USA). The procedure adhered to EPA Method 551.1, as specified by the US Environmental Protection Agency [6].

The second experiment was conducted with CF-Fe$(NO_3)_3$ adsorbent. Five HANs species were prepared as stock solutions by mixing in a 10 mM phosphate buffer with a controlled pH of 7. The amount of 0.1 g of CF-Fe$(NO_3)_3$ adsorbent was used in this experiment with the same conditions as the adsorption kinetics of DBAN. The residual HANs species in the liquid was detected by using a gas chromatograph combined with an electron capture detector (GC/ECD) (Hewlett Packard, HP6890 GC, USA). The procedure adhered to EPA Method 551.1, as specified by the US Environmental Protection Agency [6].

The adsorption rate was investigated by fitting the model, which included a linear driving force model, a pseudo-second-order kinetic model, and an intraparticle diffusion model.

The equation for the pseudo-second-order model was illustrated in Eq. (1) [25], where q_t is the adsorption capacity at time (mg/g) and q_e is the adsorption capacity at equilibrium (mg/g), k_2 is the pseudo-second-order rate constant (g/mg.min), and t is the adsorption time (min), respectively.

$$q_t = \frac{k_2 q_e^2 t}{1+k_2 q_e t} \quad (1)$$

To measure the adsorption rate, the initial adsorption rate, h (µg/g.hr) at t = 0, and the half-life time, $t_{1/2}$ (hr), can be determined according to Eq. (2) and (3), respectively.

$$h = k_2 q_e^2 \quad (2)$$

$$t_{1/2} = \frac{1}{k_2 q_e} \quad (3)$$

The equation for the linear driving force model is illustrated in Eq. (4), where K_p (L/g) is the linear solid/liquid adsorption distribution coefficient, and k_{LDF} is the linear driving force coefficient at time (t) (µg/g). The q_s is the adsorption capacity at the particle surface (µg/g), and X is the adsorbent dose (g/L).

$$q_t = q_e(1\text{-}e^{-(1+K_p X)K_{LDF} t}) \quad (4)$$

The intraparticle diffusion model proposed by Weber and Morris [26] was utilized to determine the adsorption process in cases where the adsorption process was limited by mass transfer or diffusion. The equation for the intraparticle diffusion model can be defined as shown in Eq. (5), where k_p is the intraparticle diffusion rate constant (µg/g/min0.5) and C (µg/g) is the Y-intercept constant that relates to the thickness of the boundary layer. In addition, the intraparticle diffusion coefficient D_p (m^2/s) in the adsorbent particle with a homogeneous structure is simply calculated from Eq. (6) [27].

$$q_t = k_p t^{0.5} + C \quad (5)$$

$$D_p = \frac{R^2 k_{LDF}}{15} \quad (6)$$

The adsorption kinetic models were applied to the experimental data and the relative root mean square error (RRSME) was calculated by nonlinear regression using Microsoft Excel 2011 software.

Adsorption Isotherm Experiments

The adsorption isotherm experiments were divided into two experiments, the same as the adsorption kinetics experiments. The first experiment was conducted with an initial concentration of DBAN ranging from 25 to 150 µg/L under the same conditions as the kinetics experiment, except the contact time that was fixed at 60 minutes. The second experiment was conducted with five species of HANs with concentrations in the range of 25 to 150 µg/L. The adsorption isotherm was investigated by fitting to the models, namely the linear,

Freundlich, Redlich-Peterson (R-P), and Dubinin-Radushkevich (D-R) isotherm models.

The linear model is the simplest isotherm model that can be used to describe the relationship between adsorption capacity and equilibrium concentration, especially at low concentrations. The linear isotherm is described by Eq. (7), where C_e is the equilibrium concentration of DBAN and K_P is the linear partition coefficient obtained from the slope of the relationship between q_e (µg/g) and C_e (µg/L).

$$q_e = K_P C_e \quad (7)$$

The Freundlich isotherm model is an empirical equation used to describe the heterogeneous system as shown in Eq. (8), where K_F (µg/g) and n are Freundlich constants.

$$q_e = K_F C_e^{1/n} \quad (8)$$

The Redlich-Peterson (R-P) isotherm model is a combination of the Langmuir and Freundlich isotherm, which can describe adsorption mechanisms in a mixed system and does not follow the ideal monolayer adsorption. The equation is shown as Eq. (9), where K_R (L/g) is the Redlich-Peterson constant, B (L/µg) is the Redlich-Peterson constant value, and β_R is an exponent that ranges from 0 to 1.

$$q_e = \frac{K_R C_e}{1+BC_e^{\beta_R}} \quad (9)$$

The Dubinin-Radushkevich (D-R) isotherm is one of the empirical models utilized to describe the adsorption mechanisms that are associated with Gaussian energy distribution on the heterogeneous surface. The D-R isotherms equation is shown as Eq. (10) to (12), where ε is the Polanyi potential, β is the Dubinin-Radushkevich constant value (mol^2/J^2), R is the universal gas constant (8.314×10^{-3} KJ mol^{-1} K^{-1}), T is the absolute temperature (°K), q_{DR} is the theoretical isotherm saturation capacity (µg/g), and E is the mean free adsorption energy (J/mol).

$$q_e = q_{DR} exp^{-(\beta\varepsilon^2)} \quad (10)$$

$$\varepsilon = RT\, ln\left(1+\frac{1}{C_e}\right) \quad (11)$$

$$E = \frac{1}{\sqrt{2\beta}} \quad (12)$$

The adsorption isotherm models were applied to the experimental data and the relative root mean square error (RRSME) was calculated by nonlinear regression using Microsoft Excel 2011 software.

Results and Discussions

Adsorption Kinetic

Adsorption kinetic of DBAN removal using CF, CF-$FeCl_3$, and CF-$Fe(NO_3)_3$ adsorbent.

The kinetic curves of DBAN adsorption by three adsorbents are shown in Fig. 1. These curves show the relative adsorption capacity changes over time. According to the results, the adsorption rate of all adsorbents showed a high degree of velocity at an initial stage and then significant deceleration before reaching equilibrium. Based on the kinetic curves shown in Figure 1, DBAN adsorption with all adsorbents reached equilibrium within 60 minutes. However, the adsorbed concentration of DBAN on each adsorbent was varied. CF-$Fe(NO_3)_3$ adsorbent shows the highest adsorbed concentration, followed by CF-$FeCl_3$ and CF, respectively.

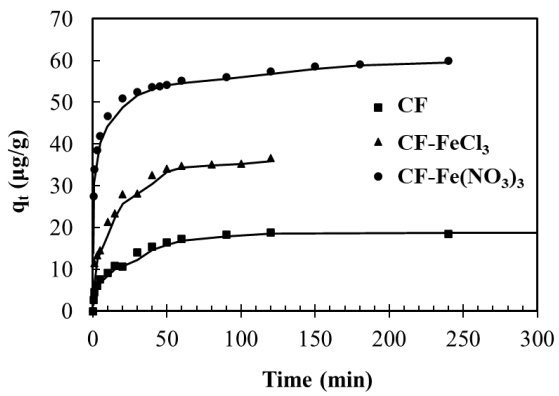

Figure 1 Adsorption kinetic of DBAN on CF, CF-$FeCl_3$, and CF-$Fe(NO_3)_3$

Various mathematical expression models were utilized to characterize the adsorption processes. From the obtained results, it was found that the concentration of adsorbate in the solution is the driving force, and the area represents the number of active sites on the

adsorbent surface. So, the pseudo-second-order model is a better way to describe the mechanism of DBAN sticking to the porous adsorbents when the concentration of the solute is low. Wu et al. [28] revealed that the pseudo-second-order model was suitable to explain the adsorption of low molecular weight compounds on small adsorbent particles. In this case, the adsorption rate is based on the adsorption capacity, not the concentration of the adsorbate. Table 1 shows the adsorption kinetic parameters of CF, CF-$FeCl_3$, and CF-$Fe(NO_3)_3$, which were calculated from the linear driving force and pseudo-second-order models. The D_p value is used to describe the mechanism of adsorption on the outer pore layer of the adsorbent. The high value of D_p indicated that the adsorption occurs in the outer pore layer. The obtained D_p values of DBAN adsorbed onto CF-$Fe(NO_3)_3$, which performed extremely high adsorption capacities, were lower than those of CF and CF-$FeCl_3$. It can be indicated that the adsorption by CF-$Fe(NO_3)_3$ was not only absorbed on the outer pore layer alone but also adsorbed inside the pore surface. While the adsorption by CF and CF-$FeCl_3$ occurs quickly and mainly occupies on the outer pore layer of the adsorbent due to its small porosity. These results corresponded with the porosity of CF, CF-$FeCl_3$, and CF-$Fe(NO_3)_3$ which reported that the porosity of CF and CF-$FeCl_3$ was micropore (<2 nm) while CF-$Fe(NO_3)_3$ was mesopore (2-15 nm) [24].

The initial adsorption rate and half-life time of DBAN by CF-$Fe(NO_3)_3$ were faster than those of CF and CF-$FeCl_3$ due to the larger pore volume of CF-$Fe(NO_3)_3$, which was 1.9 and 1.2 times greater than those of CF and CF-$FeCl_3$, respectively. Moreover, the pore size of CF-$Fe(NO_3)_3$ was 1.3 and 1.8 times larger than that of CF and CF-$FeCl_3$, respectively. This is consistent with previous studies that reported that the adsorption rate of the porous material is related to the porous structure of the sorbent [14, 29]. Therefore, the different adsorption behaviors of CF, CF-$FeCl_3$, and CF-$Fe(NO_3)_3$ may be due to the nature specificity of the structure with direct porous.

Furthermore, adsorption kinetics might be related to intra-pore diffusion. In general, the adsorption process in the aqueous phaseinvolves three successive mass transfer steps including the film or external diffusion, the intraparticle or pore diffusion, and adsorption at the active site of the adsorbent's surface [30]. However, the last step is usually left out of kinetic analyses because it happens quickly. Thus, the rate-limiting step might be determined between film diffusion and intraparticle diffusion.

Hence, the intra-pore diffusion equation was utilized to predict adsorption kinetics. The results qt versus $t_{1/2}$ for DBAN adsorption with CF, CF-$FeCl_3$, and CF-$Fe(NO_3)_3$ are shown in Figure 2. The results showed that various adsorption phases

were involved in the adsorption process. In Figure 2, the influence of boundary diffusion was detected on the first slope, while the influence of pore diffusion was detected on the second slope. According to the intraparticle diffusion model, if intraparticle diffusion is involved in adsorption, the relationship between q_t and $t_{1/2}$ should be linear. Thus, it can be confirmed that intraparticle diffusion was involved in the adsorption process for all adsorbents.

The relationship between q_t and $t_{1/2}$ can be used to indicate the rate-limiting step of intraparticle diffusion. If the linear line passes through the origin, intraparticle diffusion is the rate-limiting step. Whereas if the linear line does not pass through the origin, this indicates that intraparticle diffraction is not the sole rate-limiting step. Other kinetic models also regulate the rate of adsorption [31]. From Figure 2, the linear line between q_t and $t_{1/2}$ does not pass through the origin. Thus, it can be indicated that intraparticle diffraction is not the sole rate-limiting step of the adsorption process for all adsorbents.

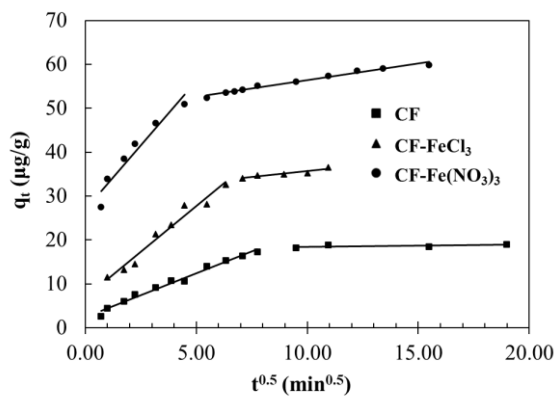

Figure 2 The intraparticle diffusion model of DBAN on CF, CF-$FeCl_3$, and CF-$Fe(NO_3)_3$

Table 1 Kinetic parameters of DCAN adsorption onto CF, CF-$FeCl_3$, and CF-$Fe(NO_3)_3$ using linear driving force and pseudo-second-order model

Materials	$q_{e\ exp}$ (µg/g)	linear driving force model				
		$q_{e\ cal}$ (µg/g)	k_{LDF} (1/s)	k_L (cm/s)	D_p (cm^2/s)	RRSME (µg/g)
CF	17.3	18.8	33.0×10^{-5}	24.7×10^{-5}	55.0×10^{-11}	2.01
CF-$FeCl_3$	34.0	35.8	29.1×10^{-5}	16.1×10^{-5}	48.5×10^{-11}	1.37
CF-$Fe(NO_3)_3$	55.1	58.3	8.40×10^{-5}	2.35×10^{-5}	2.24×10^{-11}	1.27
Materials	$q_{e\ exp}$ (µg/g)	**pseudo-second-order model**				
		$q_{e\ cal}$ (µg/g)	k_2 (g/µg·min)	h (µg/g·min)	$t_{1/2}$ (min)	RRSME (µg/g)
CF	17.3	19.5	0.005	2.0	9.9	<0.2
CF-$FeCl_3$	34.0	37.7	0.004	5.5	6.9	1.75
CF-$Fe(NO_3)_3$	55.1	55.3	0.023	72.0	0.8	3.19

Table 2 Parameters of the intraparticle diffusion model of DBAN adsorbed on CF, CF-$FeCl_3$, and CF-$Fe(NO_3)_3$

Materials	k_{p1} (µg/g /$min^{0.5}$)	C_1 (µg/g)	R_1^2	k_{p2} (µg/g /$min^{0.5}$)	C_2 (µg/g)	R_2^2
CF	2.00	2.43	0.984	0.05	17.98	0.363
CF-$FeCl_3$	4.16	6.89	0.968	0.55	30.23	0.874
CF-$Fe(NO_3)_3$	5.83	26.99	0.930	0.76	48.85	0.981

The estimated parameters of the intraparticle diffusion model are shown in Table 2 which illustrates that the rate constant (k_p) of CF-$Fe(NO_3)_3$ was higher than those of CF and CF-$FeCl_3$. This indicated that the rate of DBAN solution moving through a CF-$Fe(NO_3)_3$ adsorbent was faster than that of CF and CF-$FeCl_3$ adsorbents both through film or external diffusion and intraparticle diffusion. This is well consistent with the study of Panida et al. [14], which reported that the adsorption rate was affected by the pore size of the sorbent, with the intraparticle diffusion rate constants of mesoporous materials were higher than those of microporous materials. In addition, it was found that the slopes of the second linear (k_{p2}) of DBAN adsorbed on CF, CF-$FeCl_3$, and CF-$Fe(NO_3)_3$ were less than the slopes of the first linear (k_{p1}). It can be concluded that intraparticle diffusion should restrict the adsorption rate.

Adsorption kinetic of five HANs species removal using CF-Fe(NO$_3$)$_3$ adsorbent.

Based on the results in Figure 1 and 2, the CF-$Fe(NO_3)_3$ adsorbent was found to provide high efficiency to remove DBAN species. Then, the CF-$Fe(NO_3)_3$ adsorbent was selected and used to investigate the removal efficiency for five HANs species. The results of the adsorption kinetics of five HANs species are shown as the kinetics curve in Figure 3.

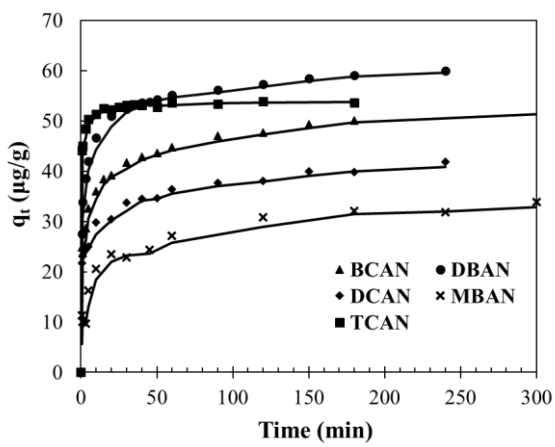

Figure 3 Adsorption kinetic of five HANs on CF-$Fe(NO_3)_3$

The results indicated that the initial rate of adsorption was fast and was significant deceleration before reaching equilibrium. TCAN species exhibit the fastest rate of approaching equilibrium within 30 minutes. The other species, including MBAN, DBAN, BCAN, and DCAN, required 180 minutes to reach equilibrium. The molecular surface characteristics of

various HANs might be impacting the rate of reaching equilibrium. HANs species that had low solubility reached equilibrium faster. The solubility of each HANs species was affecting the rate of reaching equilibrium. The solubility of each species from high to low was MBAN, DBAN, DCAN, and TCAN, respectively [14]. Thus, TCAN, with the lowest solubility, was the fastest to reach equilibrium, followed by the other species. The low solubility of HANs species can be used to indicate the hydrophobicity of the solution. HANs species with low solubility have more hydrophobicity and tend to adsorb on the adsorbent. Thus, the hydrophobicity of the solution also affected the time for reaching equilibrium.

Table 3 shows the kinetic parameters of five HANs adsorption onto CF-Fe$(NO_3)_3$ calculated from the linear driving force and the pseudo-second-order model. The adsorption kinetics model was investigated using the RRSME value. The RRSME is the differential value between the obtained value from the experiment and the calculated value from the equation. The adsorption kinetics model with a lower RRSME value indicated the adsorption kinetics was matched with this model. When comparing the RRSME of the linear driving force and the pseudo-second-order model. It was found that the adsorption kinetics of five HANs onto adsorbents were well matched to the linear driving force model with a lower RRSME value than the pseudo-second-order model.

Among the HANs species, TCAN was mostly adsorbed on CF-Fe$(NO_3)_3$ with the highest K_{LDF} value due to the lowest solubility of TCAN which indicated TCAN was more hydrophobic than other species. The D_p value of five HANs on CF-Fe$(NO_3)_3$ is in the order of TCAN > MBAN > DCAN > BCAN > DBAN, respectively which well corresponds with the adsorption capacities of each HANs species.

Adsorption isotherms

Adsorption kinetic of five HANs species removal using CF-Fe$(NO_3)_3$ adsorbent.

In this study, four distinct adsorption isotherm models, i.e., Linear isotherm, Freundlich isotherm model, Dubinin–Radushkevich isotherm model, and Redlich–Peterson isotherm model, were used to describe the adsorption mechanism of DBAN and synthesized adsorbents. Four isotherm models were applied in this study because all isotherm models were compatible with the low range of equilibrium concentration used in this study (0–125 μg/L).

As shown in Figure 4, the isotherm data shows only a linear function due to the low concentration of DBAN used in this study. So, these phenomena are not appropriate for forecasting the maximal HAN adsorption capacity with a nonlinear isotherm model. From the results, CF-Fe$(NO_3)_3$ shows the highest adsorption capacity of DBAN, followed by CF-$FeCl_3$ and CF, respectively.

Table 3 Kinetic parameters of five HANs adsorption onto CF-Fe$(NO_3)_3$ using linear driving force and pseudo-second-order model

Materials	$q_{e\,exp}$ (μg/g)	linear driving force model				
		$q_{e\,cal}$ (μg/g)	k_{LDF} (1/s)	k_L (cm/s)	D_p (cm^2/s)	RRSME (μg/g)
BCAN	44.7	49.7	14.0×10^{-5}	3.92×10^{-5}	3.73×10^{-11}	2.01
DBAN	55.1	58.3	8.40×10^{-5}	2.35×10^{-5}	2.24×10^{-11}	1.37
DCAN	31.9	35.5	21.0×10^{-5}	5.88×10^{-5}	5.60×10^{-11}	1.27
MBAN	30.8	33.4	21.5×10^{-5}	6.03×10^{-5}	5.74×10^{-11}	1.52
TCAN	53.1	53.4	24.0×10^{-5}	6.71×10^{-5}	6.39×10^{-11}	0.36
Materials	$q_{e\,exp}$ (μg/g)	**pseudo-second-order model**				
		$q_{e\,cal}$ (μg/g)	k_2 (g/μg·min)	h (μg/g·min)	$t_{1/2}$ (min)	RRSME (μg/g)
BCAN	44.7	45.5	0.021	43.5	1.0	4.37
DBAN	55.1	55.3	0.023	72.0	0.8	3.19
DCAN	31.9	32.0	0.030	31.2	1.0	3.45
MBAN	30.8	32.2	0.005	5.7	5.7	3.08
TCAN	53.1	52.9	0.150	419	0.1	<0.2

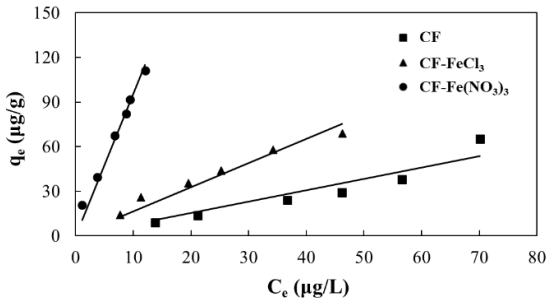

Figure 4 Adsorption isotherm of DBAN on CF, CF-$FeCl_3$, and CF-$Fe(NO_3)_3$

Isotherm parameters for DBAN adsorption on CF, CF-$FeCl_3$, and CF-$Fe(NO_3)_3$ are shown in Table 4. The correlation coefficient (RRSME) of DBAN adsorption on all adsorbents was fitted with the linear and Redlich-Peterson isotherm models, with the range of RRSME at 4.41-6.03 and 4.29-5.96, respectively.

The linear partition coefficient (K_p) was calculated from Eq. (7). The result showed that the K_p values of DBAN adsorption on CF, CF-$FeCl_3$, and CF-$Fe(NO_3)_3$ were 0.77, 1.63, and 9.53 L/g, respectively. The highest K_p values of DBAN adsorption were found in CF-$Fe(NO_3)_3$ following CF-$FeCl_3$ and CF, respectively. It can be concluded that CF-$Fe(NO_3)_3$ has the highest efficiency to adsorb DBAN. When considering the pore structure of all adsorbents, CF-$Fe(NO_3)_3$ had a higher porosity than CF and CF-$FeCl_3$ [24]. Thus, it can be indicated that the pore structure of the adsorbent influenced the K_p value.

The Freundlich isotherm constant value was calculated from Eq. (8). The range of the 1⁄n value for all adsorbents was nearly 1. So, the Freundlich isotherm equation was transformed into a linear equation. Then, the K_F value was calculated as shown in Table 4. The results showed that the K_F values of DBAN adsorption on CF, CF-$FeCl_3$, and CF-$Fe(NO_3)_3$ were 0.49, 4.25, and 7.29 µg/g, respectively. It was the same trend with the linear isotherm, which can indicate that the CF-$Fe(NO_3)_3$ has the highest efficiency to adsorb DBAN.

The R-P isotherm constant value was calculated from Eq. (9). The value of β_R was equal to 0 (0.00018 L/µg) for all adsorbents. So, the R-P isotherm equation was transformed into a linear equation. Then, the K_R value was calculated as shown in Table 4. The results showed that the K_R values of DBAN adsorption on CF, CF-$FeCl_3$, and CF-$Fe(NO_3)_3$ were 0.76, 1.63, and 9.54 L/g, respectively. It was the same trend with the linear isotherm and the Freundlich isotherm which can be indicated that the CF-$Fe(NO_3)_3$ had the highest efficiency to adsorb DBAN.

From the obtained results of the three isotherm models, it can be concluded that CF-$Fe(NO_3)_3$ had a higher efficiency to remove DBAN than other adsorbents. Thus, it can be indicated that the activation of adsorbent with ferric nitrate can increase the efficiency of removing DBAN due to the increased of porosity of the adsorbent.

The D-R isotherm model was used to explain the type of adsorption mechanism by investigating the mean free adsorption energy (E). The mean free adsorption energy was defined as the change of free energy for transferring one mol of adsorbate to the surface of a solid [32]. The obtained E values from the DBAN adsorption on all adsorbents ranged from 0.04 to 0.37 kJ/mol. The E values that were lower than 8 indicate that the adsorption mechanism was mainly physical absorption [33]. So, it can be indicated that physical adsorption occurred for DBAN adsorption on all adsorbents, which is consistent with the adsorption kinetics results.

Adsorption kinetic of five HANs species removal using CF-Fe(NO_3)$_3$ adsorbent.

As shown in Figure 5, all the isotherm data shows a linear function. TCAN species was highly adsorbed by CF-$Fe(NO_3)_3$ and followed by DBAN, BCAN, DCAN, and MBAN, respectively. When considering the solubility of each HANs species, it was found that the adsorption capacity of CF-$Fe(NO_3)_3$ was inversely proportional to the solubility of the five HANs species.

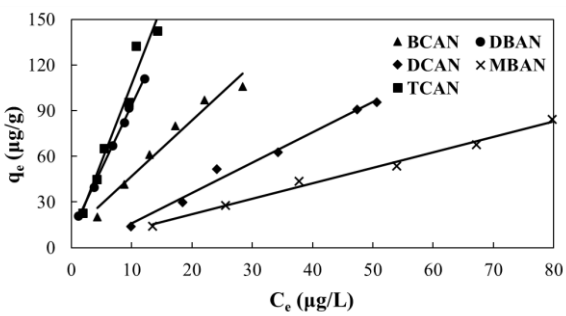

Figure 5 Adsorption isotherm of five HANs on CF-$Fe(NO_3)_3$

Table 5 shows the calculated isotherm parameters for five HANs adsorption on CF-Fe$(NO_3)_3$. The correlation coefficient (RRSME) from low to high was followed by linear ≈ Redlich-Peterson > Freundlich> Dubinin-Radushkevich, respectively. From the obtained results, it was found that the linear models were matched for the adsorption of all the HANs on CF-Fe$(NO_3)_3$ with a low RRSME in the range of 2.18-9.20.

The adsorption of five HANs species was fitted with linear isotherm, Freundlich isotherm, and R-P isotherm. The coefficient of each isotherm was calculated, including K_P, K_F, and K_R, respectively. All the calculated coefficients of each isotherm model showed the same trends for five HANs species. TCAN was found to have the highest coefficient values at 10.75 L/g, 13.59 μg/g, and 10.76 L/g for K_P, K_F, and K_R, respectively. It can be indicated that TCAN was easier to adsorb on the CF-Fe$(NO_3)_3$ than other species due to its characteristics, which have more hydrophobicity than other species. On the other hand, the lowest coefficient values were found for MBAN species at 1.04 L/g, 1.22 μg/g, and 1.04 L/g for K_P, K_F, and K_R, respectively. These results correspond with the characteristics of MBAN, which has the lowest hydrophobicity among all species.

In the D-R isotherm model, the E values for the adsorption of the five HANs species on the CF-Fe$(NO_3)_3$ ranged from 0.06 to 0.37 kJ/mol. Thus, it can be indicated that physical adsorption occurred for all five HANs species adsorption on CF-Fe$(NO_3)_3$. Low adsorption energy for all HANs species could be explained that all HANs species are more easily adsorbed onto the CF-Fe$(NO_3)_3$ adsorbents.

The effect of halogen atoms (Cl and Br) on HANs adsorption isotherm was also evaluated by comparing the adsorption isotherm of five HANs onto CF-Fe$(NO_3)_3$. The results showed the affinity of each HANs on the adsorbent from high to low were following TCAN > DBAN > BCAN > DCAN > MBAN, respectively with the same trends with the K_P value of each HANs species as shown in Table 5. When considering the halogen atoms of each HANs species, it was observed that HANs with a higher number of halogen atoms have higher K_P values where tri-HAN > di-HAN > mono-HAN. In addition, the Br-HAN was provided with a higher K_P than the Cl-HAN. The HANs species with a higher K_P value had a higher adsorption capacity. A high K_P value implies that the adsorbent has a high affinity for HAN adsorption [14].

Table 4 Isotherm parameters of DBAN adsorption on CF, CF-$FeCl_3$, and CF-Fe$(NO_3)_3$

Materials	**Linear isotherm**			**Redlich-Peterson isotherm**			
	K_p (L/g)	RRSME		K_R (L/g)	B (L/μg)	β_R	RRSME
CF	0.77	6.03		0.76	0.000	0.00000	5.96
CF-$FeCl_3$	1.63	4.41		1.63	0.001	0.00018	4.29
CF-Fe$(NO_3)_3$	9.53	4.78		9.54	0.001	0.00018	4.68
Materials	**Freundlich isotherm**			**Dubinin–Radushkevich isotherm**			
	K_F (μg/g)	$1/n$	RRSME	q_{DR} (μg/g)	B (mol^2/KJ^2)	E (KJ/mol)	RRSME
CF	0.49	0.72	27.88	90	35.6×10^{-11}	0.04	8.05
CF-$FeCl_3$	4.25	0.73	1.90	63	2.3×10^{-11}	0.15	6.62
CF-Fe$(NO_3)_3$	7.29	1.12	6.85	116	0.4×10^{-11}	0.37	10.82

Table 5 Isotherm parameters of DBAN adsorption on CF, CF-$FeCl_3$, and CF-$Fe(NO_3)_3$

HANs	Linear isotherm		Redlich-Peterson isotherm			
	K_p (L/g)	RRSME	K_R (L/g)	B (L/μg)	β_R	RRSME
BCAN	4.19	7.32	4.19	0.001	0.00018	7.26
DBAN	9.53	4.78	9.54	0.001	0.00018	4.68
DCAN	1.89	3.77	1.89	0.001	0.00018	3.64
MBAN	1.04	2.18	1.04	0.001	0.00018	1.93
TCAN	10.75	9.20	10.76	0.001	0.00018	9.15

HANs	Freundlich isotherm			Dubinin–Radushkevich isotherm			
	K_F (μg/g)	$1/n$	RRSME	q_{DR} (μg/g)	B (mol^2/KJ^2)	E (KJ/mol)	RRSME
BCAN	2.43	1.35	5.32	113	1.5×10^{-11}	0.18	8.32
DBAN	7.29	1.12	6.85	116	0.4×10^{-11}	0.37	10.82
DCAN	1.53	1.06	3.43	109	7.8×10^{-11}	0.08	7.09
MBAN	1.22	0.96	1.80	84	14.1×10^{-11}	0.06	8.06
TCAN	13.59	0.90	8.46	148	0.4×10^{-11}	0.34	13.45

Conclusion

The adsorption mechanism of HANs by canvas fabric adsorbents was investigated. Three different adsorbents were used in this study including the canvas fabric derived adsorbent (CF), activated canvas fabric derived adsorbent with $FeCl_3$ (CF-$FeCl_3$), and activated canvas fabric derived adsorbent with $Fe(NO_3)_3$ (CF-$Fe(NO_3)_3$). The activated adsorbent with $Fe(NO_3)_3$ increases the removal efficiency when considering adsorption kinetics and isotherms. The CF-$Fe(NO_3)_3$ adsorbent showed a mesopore structure with a larger porosity and the adsorption occurs not only outer the pore layer but also inside the pore surface. The larger pore volume of CF-$Fe(NO_3)_3$ resulted in a faster initial adsorption rate and half-life time of DBAN. In addition, the results of intraparticle diffusion showed that CF-$Fe(NO_3)_3$ was faster to adsorb DBAN than other adsorbents. When considering the adsorption kinetics of five HANs species, TCAN species showed the fastest rate to reach equilibrium within 30 minutes due to the lower solubility of TCAN. Thus, TCAN was highest adsorbed on CF-$Fe(NO_3)_3$ followed by MBAN, DCAN, BCAN, and DBAN, respectively. From the RRSME value of each kinetics model, it can indicate that the adsorption kinetics of five HANs species were fitted with a linear driving force model. Based on the D-R isotherm model, the adsorption mechanism of DBAN on all adsorbents was physical adsorption due to the lower E values. The results of linear, Freundlich, and R-P isotherm indicated that CF-$Fe(NO_3)_3$ had the highest efficiency in removing DBAN than other adsorbents. The results of the adsorption isotherm of five HANs species showed that TCAN was easier to adsorb on the CF-$Fe(NO_3)_3$ than other species due to its lower solubility. On the other hand, MBAN which had higher solubility had lower efficiency to adsorb on CF-$Fe(NO_3)_3$ adsorbent. In addition, TCAN with more halogen atoms (tri-HANs) resulted in a highly adsorbed on adsorbent. All HANs species were adsorbed on CF-$Fe(NO_3)_3$ adsorbent with a physical adsorption mechanism due to the low adsorption energy obtained from the D-R isotherm. The potential of reusing spent adsorbent through an efficient regeneration process will be further investigated based on the obtained results of the adsorbent mechanism. The kinetics and isotherm adsorption mechanisms of canvas fabric derived adsorbent and activated adsorbent with ferric solution were elucidated in this study. The next step of the research will focus on the potential of reusing spent adsorbent through an efficient regeneration process. The obtained results of the adsorbent mechanism revealed that physical adsorption occurred between HANs species and carbon material adsorbent, which were easier to remove from spent adsorbents. Then, the possible techniques for the regeneration process will be further investigated.

Acknowledgement

This research work was partially supported by the Graduate School of Chiang Mai University.

References

[1] Dubey, S., Gusain, D., Sharma, Y. C. and Bux, F. 2020. Chapter 15 - The occurrence of various types of disinfectant by-products (trihalomethanes, haloacetic acids, haloacetonitrile) in drinking water. Disinfection By-products in Drinking Water. Butterworth-Heinemann. 371-391.

[2] Han, J., Zhang, X., Jiang, J. and Li, W. 2021. How Much of the Total Organic Halogen and Developmental Toxicity of Chlorinated Drinking Water Might Be Attributed to Aromatic Halogenated DBPs?. Environmental Science and Technology. 55(9): 5906-5916.

[3] Cheng, J. B., Zhao, H. B., Zhang, A. N., Wang, Y. Q. and Wang, Y. Z. 2022. Porous carbon/Fe composites from waste fabric for high-efficiency electromagnetic wave absorption. Journal of Materials Science & Technology. 126: 266-274.

[4] Richardson, S. D. 2011. Disinfection By-Products: Formation and Occurrence in Drinking Water. Encyclopedia of Environmental Health. 110-136.

[5] Krasner, S. W., Weinberg, H. S., Richardson, S. D., Pastor, S. J., Chin, R., Sclimenti, M. J., Onstad, G. D. and Thruston, A. D. 2006. The occurrence of a new generation of disinfection by-products. Environmental Science & Technology. 40: 7175-7185.

[6] WHO. 2017. Guidelines for drinking-water quality: fourth edition incorporating the first addendum.

[7] Allen, J. M., Plewa, M. J., Wagner, E.D., Wei, X., Bokenkamp, K., Hur, K., Jia, A., Liberatore, H. K., Lee, C. F. T., Shirkhani, R. And Krasner, S. W. 2022. Drivers of Disinfection Byproduct Cytotoxicity in U.S. Drinking Water: Should Other DBPs Be Considered for Regulation?. Environmental Science and Technology. 56(1): 392-402.

[8] Jayawardana, T.K., Hossain, M. F., Patel, D. and Kimura, S. Y. 2023. Haloacetonitrile stability in cell culture media used in vitro toxicological studies. Chemosphere. 313: 137568.

[9] Ma, X., Cheng, J., Zhang, P., Wu, Y., Deng, J., Dong, F., Li, X. and Dietrich, A. M. 2024. Impact of boiling on chemical and physical processes for reduction of halomethanes, haloacetonitriles, and haloacetic acids in drinking water. Science of The Total Environment. 906: 167657.

[10] Shi, W., Wang, L. and Chen, B. 2017. Kinetics, mechanisms, and influencing factors on the treatment of haloacetonitriles (HANs) in water by two household heating devices. Chemosphere. 172: 278-285.

[11] Chang, X., Yao, X., Ding, N., Yin, X., Zheng, Q., Lu, S., Shuai, D. and Sun, Y. 2019. Photocatalytic degradation of trihalomethanes and haloacetonitriles on graphitic carbon nitride under visible light irradiation. Science of The Total Environment. 682: 200-207.

[12] Zhang, X., Yao, J., Zhao, Z. and Liu, J. 2019. Degradation of haloacetonitriles with UV/peroxymonosulfate process: Degradation pathway and the role of hydroxyl radicals. Chemical Engineering Journal. 364: 1-10.

[13] Zhang, D., Dong, S., Zhang, A., Chen, L., Yu, Z., Wang, Q. and Chu, W. 2021. Catalytic hydrolysis: A novel role of zero-valent iron in haloacetonitrile degradation and transformation in unbuffered systems. Science of The Total Environment. 801: 149537.

[14] Prarat, P., Ngamcharussrivichai, C., Khaodhiar, S. and Punyapalakul, P. 2019. Adsorption of single and mixed haloacetonitriles on silica-based porous materials: Mechanisms and effects of porous structures. Journal of Environmental Sciences. 79: 346-360.

[15] Prarat, P., Ngamcharussrivichai, C., Khaodhiar, S. and Punyapalakul, P. 2013. Removal of haloacetonitriles in aqueous solution through adsolubilization process by polymerizable surfactant-modified mesoporous silica. Journal of Hazardous Materials. 244-245: 151-159.

[16] Din, M. I., Ashraf, S. and Intisar, A. 2017. Comparative Study of Different Activation Treatments for the Preparation of Activated Carbon: A Mini-Review. Science Progress. 100(3): 299-312.

[17] Qian, H., Lin, Y. L., Xu, B., Wang, L. P., Gao, Z. C. and Gao, N. Y. 2018. Adsorption of haloforms onto GACs: Effects of adsorbent properties and adsorption mechanisms. Chemical Engineering Journal. 349: 849-859.

[18] Nakamura, T., Kawasaki, N., Araki, M., Yoshimura, K. and Tanada, S. Part A, 2001. TRIHALOMETHANE REMOVAL BY ACTIVATED CARBON FIBER. Journal of Environmental Science and Health. 36(7): 1303-1310.

[19] Numee, P., Sangtawesin, T., Yilmaz, M. and Kanjana, K. 2024. Activated carbon derived from radiation-processed durian shell for energy storage application. Carbon Resources Conversion. 7(2): 100192.

[20] Kuok, K. K., Chiu, P. C., Rahman, M. R., Chin, M. Y. and Bin Bakri, M. K. 2024. Sustainable bamboo and coconut shell activated carbon for purifying river water on Borneo Island. Waste Management Bulletin. 2(1): 39-48.

[21] Xu, Z., Tian, D., Sun, Z., Zhang. D/. Zhou, Y., Chen, W. And Deng, H. 2019. Highly porous activated carbon synthesized by pyrolysis of polyester fabric wastes with different iron salts: Pore development and adsorption behavior. Colloids and Surfaces A: Physicochemical and Engineering Aspects. 565: 180-187.

[22] Dridi-Dhaouadi, S., Douissa-Lazreg, B. N. and M'Henni, M. F. 2011. Removal of lead and yellow 44 acid dye in single and binary component systems by raw Posidonia oceanica and the cellulose extracted from the raw biomass. Environmental technology. 32(3-2): 325-340.

[23] Sandin, G. and Peters, G.M. 2018. Environmental impact of textile reuse and recycling - A review. Journal of Cleaner Production. 184: 353-365.

[24] Yimyam, K., Wongrueng, A. and Rakruam, P. 2023. Haloacetonitriles adsorption using a low-cost adsorbent derived from canvas fabric. Environmental Research. 234: 116539.

[25] Ho, Y. S. and McKay, G. 1998. Sorption of dye from aqueous solution by peat. Chemical Engineering Journal. 70(2): 115-124.

[26] Weber Jr, W. and Morris, J. 1963. Kinetics of Adsorption on Carbon from Solution. Journal of Scientific and Engineering Division.

[27] Rodrigues, A. E. and Silva, C. M. 2016. What's wrong with Lager green pseudo first order model for adsorption kinetics?. Chemical Engineering Journal. 306: 1138-1142.

[28] Wu, F. C., Tseng, R. L., Huang, S. C. and Juang, R. S. 2009. Characteristics of pseudo-second-order kinetic model for liquid-phase adsorption: A mini-review. Chemical Engineering Journal. 151(1): 1-9.

[29] Ruiz, B., Cabrita, I., Mestre, A. S., Parra, J. B., Pires, J., Carvalho, A. P. and Ania, C. O. 2010. Surface heterogeneity effects of activated carbons on the kinetics of paracetamol removal from aqueous solution. Applied Surface Science. 256(17): 5171-5175.

[30] Liu, Q. S., Zheng, T., Wang, P., Jiang, J. P. and Li, N. 2010. Adsorption isotherm, kinetic and mechanism studies of some substituted phenols on activated carbon fibers. Chemical Engineering Journal. 157(2): 348-356.

[31] Ozcan, A., Ozcan, A. and Gok, O. 2007. Adsorption kinetics and isotherms of anionic dye of reactive blue 19 from aqueous solutions onto DTMA-sepiolite. Hazardous Materials and Wastewater-Treatment, Removal and Analysis. Nova Science Publishers. New York.

[32] Zhan, Y., Lin, J. and Zhu, Z. 2011. Removal of nitrate from aqueous solution using cetylpyridinium bromide (CPB) modified zeolite as adsorbent. Journal of Hazardous Materials. 186(2): 1972-1978.

[33] Abin-Bazaine, A., Trujillo, A. C. and Olmos-Marquez, M. 2022. Adsorption Isotherms: Enlightenment of the Phenomenon of Adsorption. Wastewater Treatment. Intechopen: 104260.

Thai Environmental Engineering Journal Vol. 38 No. 2 (2024) : 91-100
www.eeat.or.th

Performance Assessment of the Onsite Wastewater Treatment System at High-rise Condominium in Bangkok: A Case Study

Nicharee Sian-oon[1], Tomohiro Okadera[2] and Wilasinee Yoochatchaval[3*]

[1]Department of Environmental Engineering, Faculty of Engineering,
Kasetsart University, Bangkok 10900, Thailand
[2]National Institute for Environmental Studies, 16-2 Onogawa,
Tsukuba, Ibaraki 305-8506, Japan
[3*]Department of Environmental Engineering, Faculty of Engineering,
Kasetsart University, Bangkok 10900, Thailand
[*]E-mail : fengwny@ku.ac.th

Article History; *Received: 10 June 2024, Accepted: 15 August 2024, Published: 30 August 2024*

Abstract

Condominiums in Bangkok increase annually to accommodate the growing population. The wastewater generated from residents' activities could potentially impact natural water quality. This study aims to assess the efficiency of onsite wastewater treatment from the high-rise condominium in Bangkok and investigate the presence of microplastic contamination in discharged wastewater. The revealed removal efficiencies of SS, VSS, BOD, COD, NH_4-N, and TN at 82.75%, 81.55%, 94.80%, 85.60%, 75.0%, and 21.4%, respectively. The *E. coli* could be treated at $1.44\log_{10}$. The effluent's pH, SS, and BOD values met the wastewater effluent standards according to the notification of the Ministry of Natural Resources and Environment on effluent standards from buildings of certain types and size. The presence of microplastics in wastewater originating from the high-rise condominium building is detected in both influent and effluent, at quantities of 4 pieces/L and 2 pieces/L, respectively. Fiber-shaped microplastics were found the most, followed by fragments, films, and granules, in that order. The random sampling of microplastics for analysis to identify the polymer type revealed the presence of Polyethylene terephthalate (PET), Polypropylene (PP), Low Density Polyethylene (LDPE), and detected Polydimethylsiloxane (PDMS).

Keywords : Bangkok; condominium; onsite treatment; process performance; treatment efficiency; microplastic

Introduction

Bangkok has witnessed a significant surge in condominium construction. From 2017 to June 2023, the number of condominium registrations has increased, with 506 projects, 1,050 buildings, and 223,815 units being registered during this period [1]. Government regulations mandate on-site wastewater treatment facilities for condominiums to address environmental concerns [2].

The growing number of condominiums serves as a significant source of wastewater discharge that undergoes treatment through onsite wastewater treatment systems (OWTSs) before being discharged into the aquatic environment, specifically into canals. Thus, the efficiency of OWTSs plays a pivotal role in relation to water quality in canals. Canal water quality monitoring in Bangkok from 2010 to 2021 shows a rising trend in Biochemical Oxygen Demand (BOD) concentration [3], indicating a deteriorating water quality trend. This study focuses on OWTS in Bangkok condominiums, which is considered as one of the significant sources of wastewater generation. The

inadequate performance of the OWTS may result in the release of high-strength wastewater into the aquatic ecosystem, consequently deteriorating the water quality within the environment.

Even though OWTS effectively treat wastewater to meet regulatory standards, other pollutants may still be present in wastewater. Recently, plastic wastes measuring less than 5 mm in length, which are commonly known as 'microplastics (MPs)' have garnered considerable attention as an emerging threat, with consequential implications in terms of ecotoxicology and ecology for water ecosystems [4, 5]. The presence of microplastics in aquatic environments can be investigated by analyzing effluent obtained from wastewater treatment plants (WWTPs) [6], which serve as crucial receptors of MPs before releasing them into natural water bodies [7].

This study aims to investigate the source of wastewater discharge, with a specific focus on assessing the efficiency of high-rise condominium's OWTS and examining the release of MPs from OWTS into the surrounding environment.

Methodology

Sampling site

The sampling site selected for this study was an activated sludge OWTS installed at a high-rise condominium "A" in On-nuch district, Bangkok, Thailand. Out of the total 987 units in the building, 936 units were occupied at the time of the study. The location of the sampling site is shown in Figure 1.

The wastewater treatment system has a capacity of 615 m^3/day. The flow diagram of wastewater treatment plant shown in Figure 2. Water samples were collected at 2 sampling points to analyze water quality and microplastic contamination in wastewater. The first sampling point was the influent from septic tank (No.1), the second sampling point was the effluent from clarifier tank (No.2).

Water quality characterization analysis

The sampling process for water quality characterization analysis took place on a weekly basis, spanning from January 2023 to June 2023. The pH measurement was carried out by using pH meter. Concentrations of suspended solids (SS) and volatile suspended solids (VSS) were determined using a glass fiber filter (GB140; pore size 0.4 μm, Advantec Co. Ltd., Japan). The BOD with additional allylthiourea (ATU) were determined according to the standard method [8]. The COD was analyzed using a HACH DR900 spectrophotometer (Hach Co, USA). Persulfate Digestion Method were used for analyzing the total nitrogen (TN) concentration. Ammonia, Nitrite and Nitrate (NH_4-N, NO_2^--N and NO_3^--N) concentrations were analyzed by a spectrophotometer (DR1900, Hach Co, USA). The *Escherichia coli.* (*E. Coli*) concentration in wastewater was analyzed using a Nissui Compact Dry EC plate (Nissui, Japan).

Figure 1 The location of high-rise condominium A

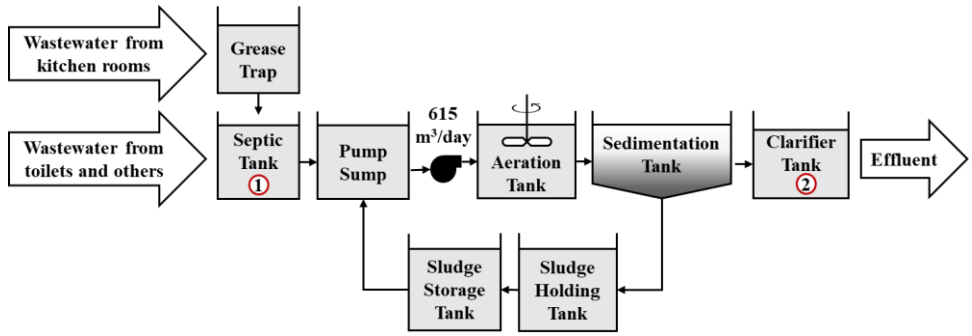

Figure 2 Flow diagram of a high-rise condominium A's onsite WWTP (Completely Mix)

Microplastic analysis

The MP sample collection was conducted on four occasions: twice during the dry season (late January and late March) and twice during the wet season (mid-May and mid-June) of 2023. A rotary pump with a 12 V/DC 8 A power supply was used for the sampling process. The water was pumped through a 0.3 mm (No. 50) stainless steel sieve. Analysis samples were obtained from 50 liters of influent wastewater and 100 liters of effluent wastewater, with a total of 5 replicates per sample. After collection, the residue retained on the sieve was carefully transferred into individual glass jars and subsequently stored at 4 ºC to maintain the integrity of the samples for subsequent laboratory analysis. The analysis of MPs in wastewater was adapted from a method developed by National Oceanic and Atmospheric Administration (NOAA) [9]. The number of MPs present and MP shapes were analyzed by using a stereomicroscope (Olympus, SZ61TR) at a magnification of 45X. The polymer types of MPs were identified using a Fourier transform-infrared spectrophotometry (FT-IR, Bruker Alpha II) in attenuated total reflectance (ATR) mode.

Results and Discussions

Wastewater characteristics and removal performance

Wastewater characteristics and removal performance of high-rise condominium A's OWTS are shown in Table 2. In accordance with wastewater effluent standards for buildings in Thailand, the pH values, SS concentration, and BOD concentration of OWTS effluent met the required quality standards. The pH values of wastewater in the OWTS were near neutral, ranging within the suitable range for the growth of bacteria (between 6.5 and 7.5) in the biological treatment process [11].

The efficiency of OWTS in removing SS, VSS, BOD, and COD in wastewater was relatively high (>80%) and the NH_4-N removal rate was 75%, the removal performance of condominium A's OWTS was similar to the removal performance of mini-sewage treatment plants with activated sludge that operating normally in the study of Marzac et al. [10]. Conversely, Micek et al. [12] found that household WWTPs with activated sludge achieved removal efficiencies of 17% and 48% for TSS, these low efficiencies are due to the significant proportion of TSS (>60%) was removed in the preliminary settling tanks (septic tanks), in addition to the mechanical treatment occurring in preliminary settling tanks, the wastewater retention time has also improved the sedimentation process of solids in each stage.

Over the course of a 20-week monitoring period, the BOD concentration in the effluent did not surpass the building effluent quality standard, which dictates that it must not exceed 20 mg/L [2] as shown in Figure 3. Throughout this duration, the BOD treatment exhibited an average efficiency of 94.8±3.21%. In the research study investigating the efficiency of two household WWTPs with activated sludge conducted by Micek et al. [12], it was found that the BOD removal efficiency was 83% and 66%. In addition, Rodrigues Mesquita et al. [13] also found effective removal of high BOD levels in three decentralized WWTPs consisting of septic tanks and anaerobic filters, with average annual efficiencies of BOD removal at 78%, 80%, and 93%. The higher BOD removal efficiency (97%) was found in the study on the use of a low-cost ceramic filter bioreactor (CFBR) for

treating effluent from septic tanks in small communities in Saudi Arabia, conducted by Alresheedi et al. [14].

In general, untreated wastewater typically has a BOD/COD ratio ranging from 0.3 to 0.8 and treated wastewater has a BOD/COD ratio ranging from 0.1 to 0.3. If untreated wastewater has a BOD/COD ratio greater than or equal to 0.5, the wastewater is considered easily treatable by biological treatment, if the ratio is below approximately 0.3, it suggests that the wastewater might contain some toxic substances or may be required the acclimated microorganisms in its stabilization [11]. The influent wastewater entering the OWTS has a BOD/COD ratio of 0.32±0.12, while the effluent wastewater from the OWTS has a BOD/COD ratio of 0.13±0.10. Although the BOD/COD of the influent wastewater was not less than 0.3, but the biological degradation process of the activated sludge system in Condominium A's OWTS may proceed slowly. Therefore, it might be necessary to consider adding suitable bacterial strains to support the biological treatment [15].

The conventional process for nitrogen removal from wastewater includes nitrification followed by denitrification process [16]. The influent nitrogen primarily exists as soluble ammonia. In the process of nitrification, ammonia nitrogen is oxidized to nitrite nitrogen, which is relatively unstable, and then nitrite nitrogen is further oxidized to nitrate nitrogen. This process relies on nitrifying bacteria and occurs under conditions with oxygen [11, 17]. From the concentration of NH_4-N, NO_2^--N, and NO_3^--N in the influent and effluent in Table 1, The decrease in NH_4-N concentrations, along with the increase in NO_2^--N, and NO_3^--N concentrations in wastewater demonstrates that the nitrification process proceeded properly within the OWTS of condominium A.

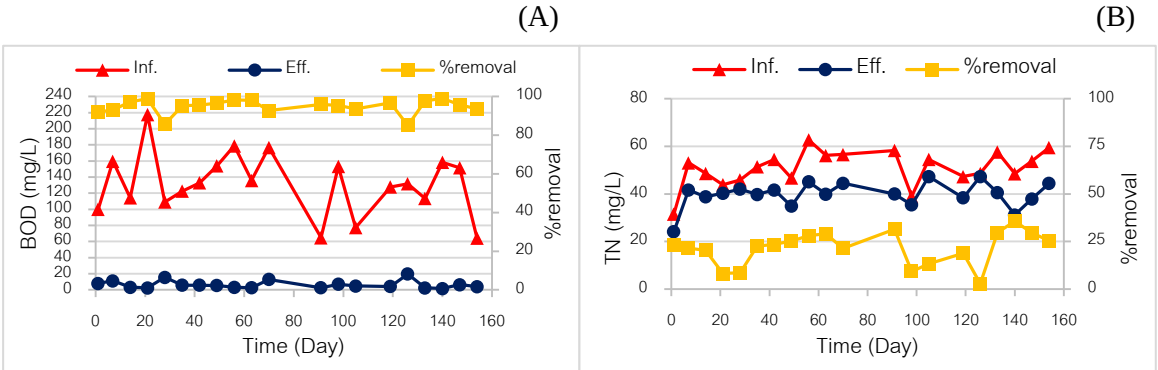

Figure 3 BOD removal performance (A); TN removal performance (B)

Table 1 Laboratory study results of wastewater characteristics

No.	Parameter	STD*	Sample**		Removal rate
			Influent	Effluent	
1	pH	5 - 9	6.66±0.29	6.71±0.21	
2	SS (mg/L)	30	180.84±83.78	24.23±20.01	82.8±15.59
3	VSS (mg/L)	-	151.41±72.03	21.42±17.63	81.5±16.59
4	BOD (mg/L)	20	132.25±38.87	6.48±4.84	94.8±3.81
5	COD (mg/L)	-	437.07±127.51	58.38±32.89	85.6±8.58
6	NH_4-N (mg/L)	-	51.26±15.29	13.10±10.65	75.0±19.61
7	NO_2^--N (mg/L)	-	0.03±0.04	5.30±4.88	
8	NO_3^--N (mg/L)	-	3.74±4.67	17.80±14.51	
9	T-N (mg/L)	-	50.92± 7.44	39.76±5.46	21.4±8.85
10	*E. coli* (CFU/mL)	-	$5.39\times10^4\pm5.97\times10^4$	$4.70\times10^3\pm8.04\times10^3$	$1.44\log_{10}$

* STD= water quality standards of building effluent in Thailand [2]

**20 samples of influent and 20 samples of effluent were analyzed for all parameters

The efficiency of TN removal by the OWTS reached a maximum of 35.67% throughout the sampling period as shown in Figure 3. The TN removal performance of the OWTS in condominium A is relatively low, similar to the research conducted by Micek et al. [12], which found that the efficiency of TN removal in two household WWTPs utilizing activated sludge systems was at 21% and 34%, resulting in high concentrations of TN, NO_2^--N, and NO_3^--N in the effluent due to the insufficient capability of WWTPs with activated sludge to create suitable conditions for the denitrification process.

The average efficiency of *E. coli* elimination by the onsite treatment system in condominium A was $1.44\log_{10}$. Throughout the sampling period, the efficiency of *E. coli* elimination by the onsite treatment system ranged from $0.22\log_{10}$ to $3.23\log_{10}$. The modification of septic tanks with anaerobic and aerobic chambers for onsite wastewater treatment provided by Abbassi et al. [18], included two modified septic tanks (MST) operated in different configurations: suspended growth biological treatment system (MST-S) and attached growth biological treatment system (MST-A), the *E. coli* removal in MST-S achieved a $2\log_{10}$ reduction, which is higher than in MST-A, where the efficiency of *E. coli* removal was approximately $1\log_{10}$, the higher *E. coli* removal in MST-S may be attributed to the formation of bioflocs, which can aggregate *E. coli* and settle them out in the sedimentation tank. However, the concentration of *E. coli* in the effluent from MST remains relatively high, ranging from 10^3 to 10^6 MPN/100mL, which may require further tertiary treatment utilization. According to the study provided by Takemura et al. [19], the down-flow hanging sponge (DHS) reactor has been utilized as a post-treatment process for sewage treatment systems operating under short hydraulic retention times (HRT) of 1 to 3 hours, the DHS reactor could reduce the concentration of *E. coli* from an order of 10^4 CFU/mL in the influent to a range of 10^1 to 10^3 CFU/mL of *E.coli* concentration in the effluent, and the removal of *E. coli* was higher than $2\log_{10}$. The integration of tertiary treatment within the OWTS of condominium A may potentially serve as a viable strategy for mitigating the concentration of *E. coli* in the effluent.

Microplastics contamination

The microplastics contamination in wastewater from high-rise condominium A is shown in Table 2. From the collection of MP samples in the influent and effluent of the OWTS of high-rise condominium A the presence of MP contamination was detected in the wastewater generated by the condominium. The concentration of MPs in the effluent water was lower than the MPs concentration in the influent water in all sampling events. This demonstrates a reduction in MPs in the wastewater after treatment by the OWTS. Rajsiri and Leungprasert [20] reported that the amount of microplastics in untreated wastewater from two high-rise condominiums near Bang Khen canal was approximately 1.48±0.06 pieces/L and 1.80±0.19 pieces/L during the dry season from December 2021 to March 2022, which differs from the concentration of microplastics detected in the untreated wastewater generated from the high-rise condominium in this study. This might be due to the varying activities of residents in different areas.

Table 2 MPs concentration in wastewater from OWTS during dry season and wet season in 2023

MPs (pieces/L)	Dry season		Wet season	
	January	**March**	**May**	**June**
Influent	4±0.70	5±1.15	4±0.69	3±1.23
Effluent	2±0.19	2±0.67	2±0.49	1±0.25

Remark: Each sample was analyzed with a total of 5 replicates.

The MPs in the effluent from condominium A's OWTS are eventually discharged into the environment. According to the analysis of MPs contamination in the effluent of condominium A's OWTS during the dry season and wet season, the average quantity of MPs in the effluent was 2±0.53 pieces/L and 1±0.51 pieces/L, respectively. The t-test results indicated that the average quantity of MPs in the effluent during the dry season was significantly higher than the average quantity observed in the influent. Furthermore, the abundance of MPs in the effluent of OWTS significantly differs between the dry and wet seasons ($p < 0.05$). These results are consistent with the findings of Kittipongvises et al. [21], which reported that the presence of microplastics in wastewater from the wastewater treatment plant in Nonthaburi, Thailand, was lower during the wet season compared to the dry season in both 2019 and 2020 due to the dilution caused by rainfall during the wet season. The study conducted by Flores-Munguía et al. [22] presented the counterexample, which found that the quantity of MPs in wastewater from three WWTPs in Mexico were higher during the wet season compared to the dry season and the MP removal efficiencies of WWTPs were decreased during the wet season. The high concentrations of MPs in wastewater during the wet season might result from the urban surface runoff carrying microplastics into the water cycle and the poor settleability of the MP particles due to the higher flow velocity during rainfall events [23]. In addition, heavy rainfall may induce the resuspension of microplastics in WWTP [24], resulting in a higher quantity of MPs in wastewater samples during the wet season. In this study, the presence of MPs in wastewater samples during each season may be related to the activities of resident in the condominium, particularly those related to laundering items other than clothing (such as blankets, quilt, curtains, and various fabric covers), which are often less frequent during the rainy season, possibly contributing to a lower presence of microplastic fibers released during this season. Consequently, the quantity of microplastics detected during the rainy season may be reduced compared to other seasons.

Although the analysis of MP samples has shown a decrease in the quantity of MPs in wastewater generated from the condominium after being treated by OWTS, there remains a high level of MPs in the effluent released into the environment. The discharge rate of wastewater from the OWTS of high-rise condominium A is 280.17 m^3/h. It is estimated that during the dry season, the average release of MP items into the environment per day is 13,448,160 pieces. During the wet season, an average of 6,724,080 pieces of MP are released into the environment per day. In the study conducted by Hidayaturrahman and Lee [25] which investigated the quantity of MPs in wastewater from three centralize full-scale WWTPs in South Korea, it was observed that all three WWTPs exhibited high efficiency in microplastic removal (>98%). However, despite their high removal efficiency, there was still a release of MPs averaging 47.24 billion pieces/L with an average flow rate of 172,211.3 m^3/day. Another example of a study that aligns with the finding was reported by Magni et al. [26], who found that the WWTP was not completely remove MPs from the wastewater, approximately 160,000,000 pieces of MPs were released into freshwater daily by the selected WWTP located in Italy.

In this study, it can be observed that the quantity of MPs released into the environment by OWTS of condominium A was lower than the quantity of MPs released by Centralized WWTPs. This difference may depend on the flow rate of wastewater within each wastewater treatment system, the characteristics of the wastewater sources (such as residential areas, rural regions, and industrial sources), and the distinct treatment processes employed by each wastewater treatment systems.

Shape of microplastics

The MP in this study were categorized into four shapes: fiber, film, fragment, and granule. Figure 4 shows the MP shapes found in this study. The most common shape of MPs found in the wastewater generated from high-rise condominium A was fiber. The analysis of MP samples collected from OWTS revealed that fiber was the predominant shape observed in the influent, accounting for 96.17% of total

MPs detected in the influent. Meanwhile, fragments, films, and granules were found in proportions of 3.01%, 0.74%, and 0.08%, respectively. The proportions of MP shapes found in the effluent were similar to the MP shapes found in the influent. Fibers accounted for 93.17% of the MPs detected in the influent, while fragments, films, and granules were found to be 4.90%, 1.84%, and 0.08% in the effluent, respectively. The highest proportion of fibers may be due to the shedding of synthetic textile fibers into wastewater during laundry [27, 28]. While granules, which is the spherical shape MP that may originate from breakage during production processes or be microbeads, which are primary microplastics produced for use in personal care products [29] have rarely been found in this study, align with Thailand's law effective since January 1, B.E. 2563. This law was introduced through Notification of the Ministry of Public Health (No.2) B.E. 2562, which banned the manufacture, import, or sale of cosmetics containing microplastic components [30].

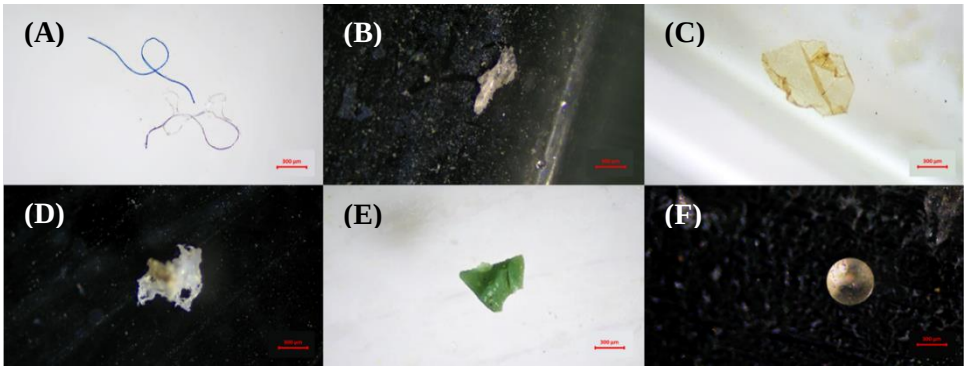

Figure 4 Shapes of microplastic (from influent wastewater) captured from stereomicroscope (Olympus, SZ61TR): Fiber (A); Film (B, C); Fragment (D, E); Granule (F)

Polymer of microplastics

From a random sample of 12 pieces of MPs for analyzed using Fourier transform-infrared spectrophotometry, the identified types of MP polymers were Polyethylene terephthalate (PET), Polypropylene (PP), and Low Density Polyethylene (LDPE) in quantities of 7, 2, and 2 pieces respectively, consistent with the findings of Rajsiri and Leungprasert [20], which indicated that PE, PP, and PET were the polymer types most commonly found in the highest proportions in domestic wastewater. Furthermore, this study also found 1 piece of the MP samples was Polydimethylsiloxane (PDMS), which is classified as a silicon elastomer polymer commonly used in various fields such as microfluidic systems, medical devices, electronic components, coatings, and may be found in daily life products such as plastic bags and synthetic fibers [31]. Similarly, Me Maw et al. [32] also detected the PDMS microplastic in wastewater from a WWTP located at a university in Thailand. However, PDMS has been rarely reported due to its minimal presence in the environment [33].

Conclusion

The performance of OWTS from the high-rise condominium building was relatively good with a removal rate for SS, VSS, BOD, COD, and NH_4-N at 82.75%, 81.55%, 94.80%, 85.60%, and 75.0% respectively. The *E. coli* could be treat at 1.44$\log_{10}$. However, the total nitrogen removal rate was low with 21.4%. The nitrogen content in wastewater released into aquatic ecosystems becomes nutrients for phytoplankton. High levels of nutrients accelerate alga blooming, increasing the amount of algae covering the water surface. Consequently, the dissolved oxygen levels in the water decrease, leading to the decay of aquatic ecosystems. To achieve higher nitrogen removal performance, adding a treatment unit specifically designed for nitrogen removal could be suitable.

The presence of MPs in wastewater generated from the high-rise condominium building was detected in both influent and effluent of OWTS. The amount of MPs in wastewater decreased after being treated by the OWTS. Nevertheless, a significant amount of MPs in wastewater are still released in to the environment daily, even when treated by the OWTS. Fiber-shaped MPs were the most found, followed by fragments, films, and granules, respectively. Although there has been a law banning the manufacture, import, or sale of cosmetics containing MP components in Thailand that has led to a rare presence of granule-shaped MPs, but other shapes of MPs are still generally present. To reduce the amount of MPs in domestic wastewater that could be released into the environment, it might be achieved through legislation to reduce the production and sale of plastic products, especially synthetic fabrics, which are the origin of MP fibers that were commonly found in the highest proportions in wastewater. Additionally, studies and standards established for wastewater treatment systems should include considerations the effective removal of microplastics from wastewater before discharge into the environment, minimizing environmental impact.

The polymer type of MPs in wastewater was PET, PP, and LDPE, which are commonly polymers found in domestic wastewater. Additionally, another polymer type detected was PDMS.

Acknowledgement

The original data were supported by National Institute for Environmental Studies, Japan.

References

[1] Real Estate Business Promotion Bureau. 2023. Statistics of Condominium Registrations Nationwide from 2009 to 2023. https://spapp.dol.go.th/FileEstate.aspx?ESID2=155, 12 July 2023. [in Thai]

[2] Royal Thai Government Gazette. 2005. Vol 122 Sect 125d, pp.4-10. [in Thai]

[3] Water Quality Management Office. 2022. Average canal water quality information (1997-present). https://wqmo.blogspot.com/p/blog-page_28.html, 1 November 2023. [in Thai]

[4] Mrowiec, B. 2017. Plastic pollutants in water environment. Environmental Protection and Natural Resources 28(4): 51-55.

[5] Bui, X.T., Vo, T.D.H., Nguyen, P.T., Nguyen, V.T., Dao, T.S. and Nguyen, P.D. 2020. Microplastics pollution in wastewater: Characteristics, occurrence and removal technologies. Environ. Technol. Innov. 19: 101013.

[6] Blair, R.M., Waldron, S., Phoenix, V. and Gauchotte-Lindsay, C. 2017. Micro- and Nanoplastic Pollution of Freshwater and Wastewater Treatment Systems. Springer. Sci. Rev. 5: 19-30.

[7] Xu, Z., Bai, X. and Ye, Z. 2021. Removal and generation of microplastics in wastewater treatment plants: A review. J. Clean. Prod. 291: 125982.

[8] American Public Health Association. 2017. Standard Methods for the Examination of Water and Wastewater, 23rd ed. Washington, D.C., USA.

[9] Masura, J., Baker, J., Foster, G. and Arthur, C. 2015. Laboratory Methods for the Analysis of Microplastics in the Marine Environment: Recommendations for Quantifying Synthetic Particles in Waters and Sediments. NOAA Marine Debris Division. Silver Spring, MD, USA.

[10] Marzec, M. and Jó´zwiakowski, K. 2007. Operational and environmental problems of the functioning of mini-sewage treatment plants with activated sludge. Pol. J. Environ. Stud. 16: 525-529.

[11] Tchobanoglous, G., Burton, F.L. and Stensel, H.D. 2003. Wastewater Engineering: Treatment and Reuse, 4th ed. McGraw-Hill, Boston, NY, USA.

[12] Micek, A., Jóźwiakowski, K., Marzec, M., Listosz, A. and Grabowski, T. 2021. Efficiency and Technological Reliability of Contaminant Removal in Household

WWTPs with Activated Sludge. Appl. Sci. 11: 1889.

[13] Rodrigues Mesquita, T. C., Pereira Rosa, A., de Oliveira Santos, T. F., Carraro Borges, A., Calijuri, M. L. and de Paula Souza, F. M. 2021. Decentralized management of sewage using septic tanks and anaerobic filters and its potential to comply with required standards in a developing country: a case study in Brazil. Environ Sci Pollut Res Int. 28(36): 50001-50016.

[14] Alresheedi, M. T., Albuaymi, A. M., AlSaleem, S. S., Haider, H., Shafiquzzaman, M., AlHarbi, A. and Ahsan, A. 2023. A. Low-cost ceramic filter bioreactor for treatment and reuse of residential septic tank effluent: A decentralized approach for small communities. Environ. Technol. Innov. 31: 103213.

[15] Młyński, D., Młyńska, A., Chmielowski, K. and Pawełek, J. 2020. Investigation of the Wastewater Treatment Plant Processes Efficiency Using Statistical Tools. Sustainability 12(24): 10522.

[16] Rahimi, S., Modin, O. and Mijakovic, I. 2020. Technologies for biological removal and recovery of nitrogen from wastewater. Biotechnol Adv. 43: 107570.

[17] Ratanatamskula, C., Suksusieng, N. and Yamamoto, K. 2014. prototype IT/BF–MBR (inclined tube/biofilm-membrane bioreactor) for high-rise building wastewater recycling. Desalination Water Treat. 52: 719-726.

[18] Abbassi, B. E., Abuharb, R., Ammary, B., Almanaseer, N. and Kinsley, C. 2018. Modified Septic Tank: Innovative Onsite Wastewater Treatment System. Water. 10(5): 578.

[19] Takemura, Y., Yoochatchaval, W., Danshita, T., Miyaoka, Y., Aoki, M., Tran, P. T., Tomioka, N. and Syutsubo, K. 2022. A pilot-scale study of a down-flow hanging sponge reactor as a post-treatment for domestic wastewater treatment system at short hydraulic retention times. J. Water Process Eng. 50: 103313.

[20] Rajsiri, K. and Leungprasert, S. 2022. Investigation of Microplastics Contaminationin Domestic Wastewater. Thai Environmental Engineering Journal 36(3): 11-18.

[21] Kittipongvises, S., Phetrak, A., Hongprasith, N. and Lohwacharin, J. 2022. Unravelling capability of municipal wastewater treatment plant in Thailand for microplastics: Effects of seasonality on detection, fate and transport. J. Environ. Manage. 302: 113990.

[22] Flores-Munguía, E. J., Rosas-Acevedo, J. L., Ramírez-Hernández, A., Aparicio-Saguilan, A., Brito-Carmona, R. M. and Violante-González J. 2023. Release of Microplastics from Urban Wastewater Treatment Plants to Aquatic Ecosystems in Acapulco, Mexico. Water. 15(20): 3643.

[23] Wolff, S., Kerpen, J., Prediger, J., Barkmann, L. and Müller, L. 2018. Determination of the microplastics emission in the effluent of a municipal waste water treatment plant using Raman microspectroscopy. Water Res X. 2: 100014.

[24] Kim, M. J., Na, S. H., Batool, R., Byun, I. S. and Kim, E. J. 2022. Seasonal variation and spatial distribution of microplastics in tertiary wastewater treatment plant in South Korea. J Hazard Mater. 438: 129474.

[25] Hidayaturrahman, H. and Lee, T. G. 2019. A study on characteristics of microplastic in wastewater of South Korea: Identification, quantification, and fate of microplastics during treatment process. Mar Pollut Bull. 146: 696-702.

[26] Magni, S., Binelli, A., Pittura, L., Avio, C. G., Della Torre, C., Parenti, C. C., Gorbi, S. and Regoli, F. 2019. The fate of microplastics in an Italian Wastewater Treatment Plant. Sci. Total Environ. 652: 602-610.

[27] Sun, J., Dai, X., Wang, Q., van Loosdrecht, M. C. M., and Ni, B. J. 2019. Microplastics in wastewater treatment plants: Detection, occurrence and removal. Water Res. 152: 21-37.

[28] Tang, N., Liu, X. and Xing, W. 2020. Microplastics in wastewater treatment plants of Wuhan, Central China: Abundance, removal, and potential source in household wastewater. Sci Total Environ.745: 141026.

[29] Rochman, C.M., Brookson, C., Bikker, J., Djuric, N., Earn, A., Bucci, K., Athey, S., Huntington, A., McIlwraith, H., Munno, K. De Frond, H., Kolomijeca, A., Erdle, L., Grbic, J., Bayoumi, M., Borrelle, S. B., Wu, T., Santoro, S., Werbowski, L. M., Zhu, X., Giles, R. K., Hamilton, B. M., Thaysen, C., Kaura, A., Klasios, N., Ead, L., Kim, J., Sherlock, C., Ho, A. and Hung, C. 2019. Rethinking microplastics as a diverse contaminant suite. Environ Toxicol Chem. 38(4):703-711.

[30] Royal Thai Government Gazette. 2019. Vol 136 Special part 312g, p.4. [in Thai]

[31] Ariati, R., Sales, F., Souza, A., Lima, R.A. and Ribeiro, J. 2021. Polydimethylsiloxane Composites Characterization and Its Applications: A Review. Polymers 13(23): 4258.

[32] Me Maw, M., Kitpati Boontanon, S., Jindal, R., Boontanon, N., and Fujii, S. 2022. Occurrence and Removal of Microplastics in Activated Sludge Treatment Systems: A Case Study of a Wastewater Treatment Plant in Thailand. Engineering Access. 8(1): 106-111.

[33] Hu, K., Yang, Y., Zuo, J., Tian, W., Wang, Y., Duan, X. and Wang, S. 2022. Emerging microplastics in the environment: Properties, distributions, and impacts. Chemosphere 297: 134118.

Thai Environmental Engineering Journal

Aims and Scope

Thai Environmental Engineering Journal is published 3 times a year by Environmental Engineering Association of Thailand in aims of provide an interdisciplinary platform for the disseminating recent research work in Environmental field. The journal's scope includes:

- Treatment Processes for Water and Wastewater
- Air Pollution and Control
- Solids and Hazardous Wastes Management
- Site Remediation Technology
- Water Resource Management; Surface water and Groundwater
- Environmental Management Protection and Conservation
- Impact Assessment of Pollution and Pollutants
- All areas of Environmental Engineering and Sciences

Frequency; 3 issues per year, every four months at April, August and December

Information for Authors

Manuscript submitted for publication should be of high academic merit and have never before, in whole or in part, been published elsewhere and will not be published elsewhere, except in abstract form. Manuscripts, parts of which have been previously published in conference proceeding, may be accepted if they contain additional material not previously published and not currently under consideration for publication elsewhere.

Submission of Manuscripts

All manuscripts should be submitted in https://www.tci-thaijo.org/index.php/teej/index

Manuscript Format and Style

Text format

Manuscript should be prepared using a text processing software such as Microsoft Word for windows. A4 size paper is conventionally accepted. Margins set up (in Page set up Menu) are outlined as follow.

Top Margin 3.0 cm., Bottom Margin 3.0 cm.

Left margin 2.5 cm., Right Margin 2.5 cm.

Title, author co-authors, address of correspondence and abstract are included in the first section while the remainder of paper is to appear in the second section. The total pages including figures, tables and references should not exceed 10 pages.

Font, font size & typeface

Times New Roman font type is required for Thai text and English text. Font size [Pica] for various text function are tabulated as follow.

Text functions	Font = Times New Roman	
	Pica Size**	Typeface
Title [English]	16 [CT]	Bold
Author & Co-authors	11 [CT]	Bold
Address of correspondence	11 [CT]	Normal
Abstract heading	12 [LRJ]	Bold
Abstract & Main Texts	11 [LJ]	Normal
Section Heading & Number*	12 [LJ]	Bold
Subsection Heading & Number	11 [LJ]	Bold

* Including "Abstract" "Acknowledgement" and "References"

** CT = Centre Text, LJ = Left Justified, LRJ = Left & Right Justified

Title

All titles of manuscript should be short and precise; long title should be condensed whenever possible (not more than 42 characters). Title should be printed with every first letter of every word capitalized, excluding prepositions and articles. Directly below the title, author should print their full names (first name then family name), address and institution. E-mail of corresponding author and between 3-5 key words should also be provided.

Abstract

Abstract should be provided on separate sheets and be not more than 300 words. International contributor who are unable to provide an abstract in Thai may submit an English abstract alone.

Style Guidelines

Units of measurement should be indicated in SI units throughout.

Tables

Tables and figures should be numbered with Arabic numerals, in order in which they are cited in the text. The table's titular heading should concisely detail the content of the table and include units of measure for all numerical data.

Format of Research Paper

The format of research paper is listed as follows:

1) Title
2) Author
3) Abstract
4) Introduction
5) Materials and Methods
6) Results and Discussion
7) Conclusions
8) References

References

The references section at the end of the manuscript should list all and only the references cited in the text in numberical order, with references given in Thai first and those in English following. In this section, the names of all authors should be provided if more than six, or the first three followed by *et. al.*

Reference to a journal article:

List all authors when six or fewer; when seven or more list only the first three (3) and add *et. al.* Titles of articles from academic journals should be listed in full and begin with a capital letter.

[1] Inthorn, D., Sidtitoon, N., Silapanuntakul, S. and Incharoensakdi, A. 2002. Sorption of mercury, cadmium and lead in aqueous solution by the use of microalgae. Science Asia. 28(3): 253-261.

Reference to article or abstract in a conference proceedings:

[1] Inthorn, D., Singhakarn, C. and Khan, E. Decolorization of reactive dyes by pre-treated Flute reed (phargmites karka (Retz)). At 34th Mid-Atlantic Industrial & Hazardous Conference, Annual Mid Atlantic Industrial and Hazardous Waste Conference at Rugers University, New Jersey, USA on September 20-21, 2002.

Reference to a book:

[1] Polprasert, C. 1996. Organic Waste Recycles. John Wiley & Sons Inc., New York.

Reference to article in a conference proceedings:

[1] Inthorn, D. Heavy metal removal. In: Kojima, H. and Lee, Y.K. Photosynthetic Microorganisms in Environmental Biotechnology, Springer-Verlag, 2001; 111-135.

Reference to an electronic data source:

Use the above format and supply the complete URL as well as the access date.

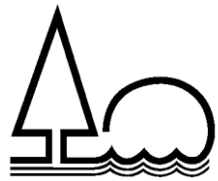

Subscription Form
Thai Environmental Engineering Journal

Date_____

Name_____

Address_____

_____

_____

_____

_____

Tel:_____ Fax:_____E-mail:_____

A subscription to the Thai Environmental Engineering Journal is request for_____year
(1,000 Baht/year for 3 Volume)

Signature_____

(_____)

Payment by "Environmental Engineering Association of Thailand"

- ❍ Bank Transfer: Savings Account No. 053-1-24040-3, Bank of Ayudhya Plc., Klong Prapa Branch
- ❍ Bank Transfer: Savings Account No. 056-2-32298-0, Siam Commercial Bank Plc., Aree Sampan Branch

Environmental Engineering Association of Thailand
122/4 Soi Rawadee, Rama VI Rd., Phayathai,
Phayathai, Bangkok 10400
Tel: +66 (0) 2617-1530-1 Fax: +66 (0) 2279-9720
E-mail: teej@eeat.or.th Website: http://www.eeat.or.th

THAI
ENVIRONMENTAL ENGINEERING JOURNAL
Environmental Engineering Association of Thailand (EEAT)

ISSN (PRINT) : 1686 - 2961
ISSN (ONLINE) : 2673 - 0359

Vol. 38 No. 2 May – August 2024